ACROPOLIS
European NoE on Cognitive Communications

SEVENTH FRAMEWORK PROGRAMME

Advanced coexistence technologies for radio optimisation in licensed and unlicensed spectrum

(ACROPOLIS)

Document Number D14.3

Assessment of interference in cognitive radio-based networks

Contractual date of delivery to the CEC:	30/01/2013
Actual date of delivery to the CEC:	15/01/2013, revised 04/07/2014
Project Number and Acronym:	257626 - ACROPOLIS
Editor:	L. Goratti (JRC), G. Baldini (JRC)
Authors:	L. Goratti (JRC), G. Baldini (JRC), P. Chawdhry (JRC), O. Holland (KCL), A. Bantouna (UPRC), S. Bovelli (EADS)
Participants:	UPRC, KCL, JRC, EADS
Workpackage:	WP14
Security:	PU
Nature:	Report
Version:	1.1
Total Number of Pages:	84

Abstract:

A survey of interference issues in spectrum sharing is presented, particularly on aggregate interference. It is shown that the distribution of aggregate interference power can be modelled with a family of heavy tail 'stable distributions'. The report also reviews some of the landmark practical work in Europe for CEPT and OFCOM based on measurements in the context of spectrum sharing in the television white space. The need to protect incumbents from harmful interference from white space devices has led to setting the protection ratios for DVB-T receivers of digital terrestrial television users and the wireless microphones of the PMSE community. These protection ratios will form the basis of regulatory limits in future while considering the allowable use of white space technologies by secondary users while minimising risk of interference to primary users.

Keywords: Aggregate interference, cognitive radio, white spaces, commons, stochastic geometry, simulation tools.

Document Revision History

Version	Date	Author	Summary of main changes
0.1	07.06.2011	JRC	Initial structure of the document, ToC developed
0.2	31.08.2011	JRC	New structure
0.3	19.10.2012	JRC, EADS, KCL, UPRC	Update structure and work sharing
0.4	09/12/2012	JRC	Update structure and contributions
0.5	12/12/2012	JRC	Update to the sections
0.6	14/12/2012	JRC	Abstract and executive summary added
0.7	16/12/2012	KCL	Document update and contributions
0.8	18/12/2012	JRC,UPRC	Document update and contributions
0.9	10/01/2013	JRC	Document update
0.91	14/01/2013	JRC, KCL, UPRC, EADS	Document update and contributions
0.92	18.01.2013	JRC	Editorial updates
1.0	18.01.2013	JRC, KCL, UPRC, EADS	Final revision after review by Executive Committee
1.1	03.07.2014	JRC, KCL	Revised after comments from Project Final Review

Executive Summary

With exponential growth in wireless communication technologies, there is increasing pressure on the regulators to adopt modern spectrum management techniques where spectrum sharing is a key paradigm. However, spectrum sharing (over frequencies, time and space) increases the risk of harmful interference the prevention of which is a major task of the regulators. This report addresses the key issues of interference in the presence of secondary users.

Since the early 2000's the concept of cognitive radio, aimed to enable efficient use of the spectrum, has gained currency in the academia and industry. Today cognitive radio is seen as a key enabling technology for spectrum sharing. The first and second digital divided that has followed the switch-over from analogue to digital TV, promises to release valuable portions of spectrum in the UHF band, some of which may be available for spectrum sharing.

Spectrum regulatory authorities are now devising regulatory framework for spectrum sharing. However, the problem of interference in spectrum sharing is a major challenge, and especially the issue of aggregate interference given the proliferation of wireless services and devices and the fact that regulatory concepts such as TV White Space access (e.g., channel availabilities) are generally only assessed based on the assumption of a single interferer.

This report is devoted to a review of the most advanced analytical and simulation techniques that can be used to model aggregate interference, as well as measurement campaigns by the regulators on protection of the incumbents from interference in the TV white spaces.

Chapter 2 reviews opportunistic spectrum access which creates the opening of underutilized portions of the licensed spectrum for reuse, provided that the transmissions of secondary radios do not cause harmful interference to primary users (PUs). For secondary users to accurately detect and access the idle spectrum, CR has been proposed as the enabling technology for spectrum sharing.

Spectrum sharing is however challenging due to the uncertainty associated with the aggregate interference in a wireless network. Such uncertainty can be resulted from the unknown number and location of interferers and unknown location of the primary signals as well as channel fading, shadowing, and other environment-dependent conditions. Therefore, it is crucial to incorporate such uncertainty in the statistical model of the aggregate interference in order to quantify its effect on the primary network system performance. A unifying framework for characterizing the network interference is found useful in investigating a variety of issues involving the aggregate interfering power generated asynchronously in a wireless environment subject to path-loss, shadowing, and multipath fading.

Chapter 3 considers operational scenarios selected for the characterization of the aggregate interference which are closely connected with the different forms of spectrum-sharing that are currently being considered. Spectrum sharing can be distinguished on the basis of three principal parameters: time, frequency and space.

Chapter 4 is the theoretical heart of the report. It presents an overview of some fundamental aspects of modelling the aggregate interference in wireless systems which

plays a major role in the management and optimization of wireless networks since aggregate interference in a shared wireless channel has a number of implications on network performance.

Depending on the radio technology used, narrowband or ultra wideband, the type of environment where the network has to operate (urban or rural), network performance may vary quite dramatically. In a realistic environment, the location of the wireless devices with respect to the receiver, the time of arrival of the received packets and the different levels of received power affect the performance of a wireless link.

The capture model, where a transmitted packet is received correctly by the intended receiver despite collisions with concurrent transmissions, has been successfully applied to model realistic performance of packet switched radio networks under various transmission schemes and propagation effects.

Stochastic geometry provides excellent means to devise the performance of packet switched radio networks in which devices generate harmful interference affecting each other's behaviour. The core contribution of this approach consists of modelling the nodes of a wireless network as a point process (PP). The section reviews how stochastic geometry is helpful for modelling the behaviour of a wireless network where the aggregate interference assumes the key role.

The assumption of the Poisson distribution of the devices over space and the Gaussian modelling of the distribution of the aggregate interference power provided already a good insight of the network behaviour. This has represented a fundamental step that bridged together the systemic approach with the physics of the radio signal propagation.

Modelling the distribution of the aggregate interference power is considered. In particular, the distribution of the aggregate interference power generated by a Poisson field of interferers belongs to the family of stable distributions. Stable distributions assume an important role when modelling the distribution of the aggregate interference power generated by an infinite number of nodes distributed over space according to a PPP.

The computation of the distribution of the aggregate interference power is particularly important when typical propagation effects such as fading and shadowing are superimposed on top of the link distance loss. Three cases are considered: Rayleigh fading, Nakagami-*m* fading and shadowing.

A reference scenario explains how the distribution of the aggregate interference power is calculated. It shows that nodes are distributed over space according to a point process with respect to the common receiver which is placed at the origin of the reference system. Despite the number of nodes can be high, what really matters is the number of active transmitters. The transmission of each device can arrive from different distances and encounter different levels of fading and shadowing.

Existing literature shows different approaches to the way the aggregate interfering process is modelled. When the interferers are distributed according to a PPP, the distribution of the aggregate interference power belongs to the family of stable distributions with location parameter δ=0 and with the other parameters that depend on the characteristics of the radio signal, the fading and the shadowing. These approaches are based on *i*) the theory of shot noise and elements of stochastic geometry; *ii*) modelling based on the LePage series representation of the aggregate interference and *iii*) an approach relying more on standard probability theory. The derivation of the distribution of the aggregate interference is helpful for determining the probability of detecting the transmission of a PU from the point of view of a CR network.

Chapter 5 is dedicated to review some of the simulation tools that can be used to quantify the aggregate interference power generated by cognitive radio networks over a primary link. A number of simulators are nowadays available including licensed and unlicensed software tools. Licensed software include Matlab and Opnet for example. Unlicensed tools include ns-2, ns-3, OMNET++ and SEAMCAT. All of them have pros and cons however, SEAMCAT is the official tool used by ECC/CEPT to carry out compatibility studies for regulatory proposals in Europe. The other mentioned simulators find applications in modelling many different aspects of the behaviour of wireless and wired networks.

Based on Monte-Carlo simulation method, SEAMCAT allows simulating different interference scenarios with the purpose of addressing compatibility studies between different radio technologies operating in the same or adjacent frequency bands. It is used for co-existence studies in terms of the determining the transmitter/receiver mask, unwanted emissions (spurious out-of-band), blocking/selectivity, etc. For studies on spectrum sharing, SEAMCAT can be used for Monte-Carlo simulations of the interference produced by CR devices operating in TV White Spaces when the interference is measured at the location of the victim receiver (DVB-T or PMSE).

Chapter 6 gives a summary of the main results on the aggregate interference power generated by CR devices.

Chapter 7 considers practical issues in the deployment of cognitive radio, such as standardization, regulation and measurement of interference and protection ratios. Technical standards are set to follow the regulations, including emission requirements, interaction with a geolocation database in the case of TV White Space, etc. A good example of this is the IEEE 802.22 standard which interacts closely with the regulatory trend.

Following the decision in the US by the FCC to open up significant parts of the TV white spaces for shared use, spectrum regulators in other parts of the world are considering similar initiatives. The FCC selected a value of the maximum transmit power for devices operating in the White Spaces in unlicensed fashion. The FCC also defined the so called *erosion margin*, which quantifies how much the TV service can degrade and thus the tolerable amount of interference that CR devices can inject in TV bands. A zero erosion margin would imply zero white spaces. This margin is particularly important as it allows determining how far the CR devices (referred to as White Spaces Devices) have to be from television receivers, taking into account in-band interference and the interference caused by transmissions on adjacent channels.

In the European context, the CEPT/ECC produced its landmark report ECC159 which addresses the technical and operational requirements for the use of cognitive radio in TV white space in 470-790 MHz band. The report considers the use of sensing and geolocation-based approaches to minimise risk of harmful interference to the incumbents. The following incumbent protection cases are considered: digital terrestrial television broadcasting, Programme Making and Special Events (PMSE), radio astronomy (RAS), aeronautical radio navigation (ARNS), mobile/fixed services in bands adjacent to the band 470-790 MHz.

At the national level, the UK's OFCOM authorised in 2011 the Cambridge Trials on TV White Space by a consortium of stakeholders to carry out field tests on the provision of services such as rural broadband and to carry out measurements of several aspects, including:

- Protection of wireless microphones by the PMSE community
- Performance of TV white space base station for mobile and fixed broadband applications
- Measurements on DVB-T protection ratios in the presence of interference from white space devices.

In order to protect PMSE, relevant EIRP restrictions need to be applied on WSDs operating in the geographic cells around the PMSE events. The protection approach is to limit the interference at the PMSE receiver such that the sensitivity of the equipment is not degraded beyond an acceptable margin. To achieve this, the interference from WSD, weighted by the receiver ACS value should be in the range below the receiver's noise floor.

The tests in the Cambridge Trial indicated that protection ratio values for both the high and low power wanted signals are different; the worse adjacent channel protection ratio for the -30dBm wanted signal is as a result of the receiver being overloaded (both wanted and interfering signal powers are large in this case). It was found that the adjacent channel (+-10MHz) minimum protection ratio is better than 55dBm for the non-overloaded case, irrespective of the waveform used. The worst co-channel protection ratio is around 6dB.

In the presence of cognitive radio, specifically of the white space devices in the UHF band, protection of Digital Terrestrial Television (DTT) receivers is required to ensure the quality of DVB-T reception is free from unwanted interference from WSD signals in the adjacent UHF bands.

Tests were carried out by BBC on a range of candidate technologies and assessed DVB-T receiver performance in the UK context [132]. Fourteen popular models of commercially available receivers were tested representing integrated digital television (IDTV), set top boxes (STBs) and programmable video recorders (PVRs). The interference from WSDs was generated through a vector signal generator to replay a waveform recorded from candidate WSD radio technology.

The results of these tests show a considerable variation in performance of DTT receives. Whereas high-end receivers appeared to be fairly resilient to interference from WSD signals, other receivers were found to be vulnerable to the WSD waveforms used in the tests. Broadcast-like signals (e.g. LTE base station at 100% traffic) were dealt with by the receivers without interference. However, burst-like signals (e.g. low traffic CPE signals) result in up to a 30dB degradation in protection ratios.

As a consequence of the BBC tests, they recommend the use of a highly conservative protection ratio values in the UK in order to protect the majority of existing consumer grade DVB-T receivers (largely in the form of low cost set-top boxes used to adapt old analogue TV receivers to DTT reception). The authors concluded that the geolocation database approach to TVWS was feasible provided that the database could take into consideration the various WS technologies and the predicted field strength at the DTT receiver location.

Table of Contents

1. Introduction

Radio waves are present throughout our environment to provide a number of wireless services like radio, TV, cellular communications, wireless internet, radar, SATNAV, among others. As shown in Figure 1-1, what initially looked like a vast expanse of radio spectrum today looks instead very crowded. During the past decade, there has been an explosive growth in mobile/wireless communications and other systems that are sharing the spectrum. Current estimations predict that there will be more than 4.2 billion mobile subscribers worldwide, which means 1 billion of new subscribers in only 3 years. In addition, almost all mobile network operators are now offering data services in order to create new sources of revenue.

The perspective of wireless communications is to maintain the promise of ubiquitous connectivity, thanks to a variety of wireless systems such as Wi-Fi, WiMAX, and the third and fourth generations of cellular networks. On the other hand, mobile subscribers can use a variety of devices, ranging from smartphones to laptops. The surge in mobile and wireless access will become important in any kind of environment. This includes rural areas, where the endeavour of enabling broadband access (likely through wireless means and one future option) will load the spectrum, and inside cities, where the high density of users and their associated activities trigger the demand for high data rates. Such high proliferation of wireless services over a finite spectrum will lead to its shortage in the near future.

A possible solution that could aid circumventing the shortage of radio spectrum is cognitive radio (CR). First conceived in [1], CR is a very broad concept in which wireless devices might be able to learn from experience and finely tune their transmission parameters based on the scenario where they operate to allow spectrum access in a more flexible way with respect to what is in force today. In a few words, CR should be able to empower wireless devices with the feature to access the spectrum whenever there is a resource underutilized or not used at all. Although CR constitutes a very appealing concept, it is clear that the proliferation of wireless devices trying to access the spectrum whenever they need, and the opportunistic spectrum access capabilities which CR might facilitate, could easily cause harmful interferences to license owners in various spectrum bands.

This deliverable focuses first on the identification of the relevant operational scenarios for the sake of modelling interference. Afterwards it provides the detailed analysis of the aggregate interference in wireless networks, tailored to the specific case of CR devices affecting the performance of primary (licensed) transmissions. In addition, in the attempt to make a self-contained document, not only is presented a thorough but non-exhaustive analysis of the aggregate interference but also a short tutorial on the stochastic geometry that is the foundation of such techniques. Simulation tools are also reviewed for the sake of completeness.

The problem of modelling aggregate interference in wireless networks is not new, and it has been addressed in many different ways throughout the literature of mobile and wireless communications. Consequently, it is worth mentioning that several techniques have been developed to mitigate this problem. In essence, interference, and the better management there, is the key reason why many multiple access techniques are developed. For instance, a survey on state-of-the-art coding techniques that can be used to relieve the problem of interference is presented in [2]. Some of these techniques propose the use of low density parity-check codes (LDPC), encoded multiple access channels, and dirty paper coding. Furthermore, two forms of network coding are considered, namely, decode-and-forward and physical-layer network coding.

The remainder of this deliverable is organized as follows. Section 2 provides introductory content for the concept of aggregate interference. Section 3 illustrates the scenarios investigated in this deliverable for addressing interference in cognitive radio networks. Section 4 is the core of the deliverable as it provides the detailed analysis of aggregate interference in order to better model and understand its characteristics. Section 5 reviews existing simulation tools that are useful for estimating the impact on primary services of aggregate interference generated by CR networks. Section 6 is used to make a comparison between analytical and simulation models for interference assessment. Section 7 approaches the problem of interference from the perspective of standardization, estimating availability of White Spaces and measurements. In Section 8 conclusions are drawn and in Section 0 a short tutorial on stochastic geometry is provided for completeness.

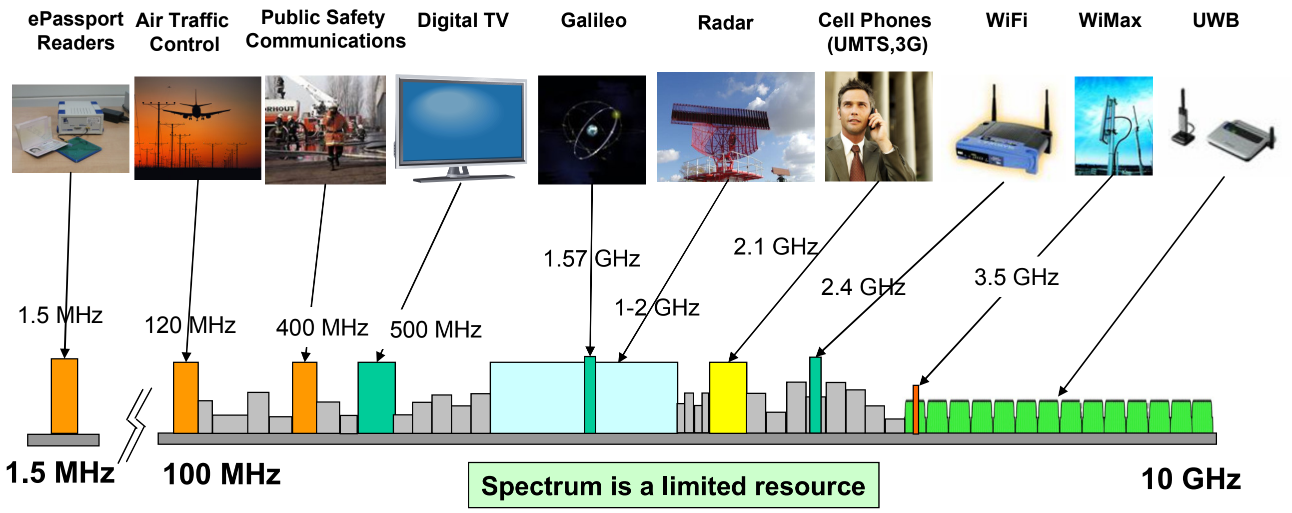

Figure 1-1: Radio Frequency Spectrum and Wireless Services.

2. Wireless interference in Cognitive Radio networks

With the emergence of new wireless applications and devices, there is a dramatic increase in the demand for radio spectrum. Due to the scarcity and the under-utilization of assigned spectrum, government regulatory bodies such as the U.S. Federal Communications Commission (FCC) have started to review their spectrum allocation policies [3][4]. Conventional rigid spectrum allocation forbids flexible spectrum usage that severely hinders efficient utilization of scarce spectrum since bandwidth demands vary along time and space dimensions. Therefore, opportunistic spectrum access together with a CR technology has become a promising solution to resolve this problem [6]-[9].

Opportunistic spectrum access creates the opening of underutilized portions of the licensed spectrum for reuse, provided that the transmissions of secondary radios do not cause harmful interference to primary users (PUs). For secondary users to accurately detect and access the idle spectrum, CR has been proposed as the enabling technology [6][7][9]. For example, if a communication channel is active between the primary and secondary networks, the busy channel assessment can be based on the detection of a preamble shared between the primary and secondary networks or on the energy sensing of the primary network radio signals [10]-[12]. Moreover, the CR network can implement a detect-and-avoid protocol where the transmission power levels of the CR devices are set based on the sensed power of the primary network signals.

Spectrum sharing is however challenging due to the uncertainty associated with the aggregate interference in the network. Such uncertainty can be resulted from the unknown number and location of interferers and unknown location of the primary signals as well as channel fading, shadowing, and other uncertain environment-dependent conditions [13][14]. Therefore, it is crucial to incorporate such uncertainty in the statistical model of the aggregate interference in order to quantify its effect on the primary network system performance. A unifying framework for characterizing the network interference was proposed to investigate a variety of issues involving the aggregate interfering power generated asynchronously in a wireless environment subject to path-loss, shadowing, and multipath fading [15][16]. The original motivation for this work was to quantify the aggregate network emission of randomly located ultra-wide bandwidth (UWB) radios [17]–[19] in terms of their spatial density [20]–[22]. This framework has also been used to study coexistence issues in heterogeneous wireless networks [23]–[27].

A common theme to almost all the papers cited herein is the use of a Poisson point process [28] for positions of the emitting nodes. The Poisson point process has been widely used in diverse fields such as astronomy [29][30], positron emission tomography [31], cell biology [32], optical communications [33]–[36] and wireless communications [30] [37]–[42]. More recently, the Poisson model has been applied to the modelling of the spatial node distributions in a variety of wireless networks such as random access, ad-hoc, relay, cognitive radio, or Femtocell networks [43]–[53].

To address the coexistence problem arisen by secondary cognitive networks, it is of great importance to accurately model the aggregate interference generated by multiple active secondary users in the network. In [50], the moment expression for the aggregate interference generated by Poisson nodes in an arbitrary area was derived assuming the typical unbounded path-loss model. However, the unbounded path-loss model results in significant deviations from realistic performance [51]. For cognitive radio networks, the log-normal distribution was proposed to model the sum of all interferers' powers [47]. This log-normal approximation was also used for the aggregate interference at primary users without accounting for the channel uncertainty due to fading [48]. The optimal power control strategies for secondary users were determined in [49] based on the Poisson model of the primary network.

In [53] and [55], a novel model has been developed in order to represent the aggregate interference of a cognitive network, accounting for the sensing procedure, secondary spatial reuse protocol, spatial density of the secondary users and environment-dependent conditions such as path loss, shadowing, and channel fading. This framework allows modelling the cognitive network interference generated by secondary users in a limited or finite region, taking into account the shape of the region and the position of the primary user. The model allows using secondary spatial reuse protocols characterized by multiple thresholds. In this framework, the characteristic function (CF) of the cognitive network interference is defined. From the CF the cumulants of the cognitive network interference are derived and the cognitive network interference is modelled as truncated-stable random variables. The proposed model is flexible enough to account for the power control of both primary and secondary network. The models allows for the division in sectors of the spatial region in order to account for the presence of obstacles or for non-homogeneous distributions of the nodes.

The analytical model in [54] is suitable for providing an accurate map of the aggregate interfere generated by a network of secondary users. Therefore, it can be used to assess the interference problem in cellular networks when Femtocells are active. For both downlink and uplink of the macro-cell system the effect of the Femtocell interference can be accurately calculated in any kind of scenario accounting also for the presence of buildings (i.e., sub-regions where the digital TV signal may be blocked blocked). Moreover, it was shown how the model is suitable also to address the hidden terminal problem in the scenario of White Spaces [56].

More realistically, the interferers are usually scattered in clusters. The clustering of nodes may be due to geographical reasons: nodes inside a building or groups moving in a coordinated fashion. The clustering may also be "artificially" induced by medium access control (MAC) protocols. In [57], the authors evaluate the Laplace transform of the interference and upper and lower bounds are obtained for the complementary cumulative distribution function (CCDF) of the interference. These bounds allow concluding that the interference follows a heavy-tailed distribution that depends on the path-loss. When the path-loss function has no singularity at the origin (i.e., remains bounded), the distribution of interference depends heavily on the fading distribution. In [58], the aggregate interference is modelled accounting for the clustered spatial distribution of the nodes. In particular the authors analyse the case of Poisson-Poisson distribution where the number of clusters and the number of nodes per cluster are both Poisson distributed. Both models for aggregate interference generated by clustered networks do not consider the effect of the spectrum sensing on the activity of the secondary nodes.

3. Operational scenarios for interference in cognitive radio systems

The operational scenarios selected for the characterization of the aggregate interference are tightly connected with the different forms of spectrum-sharing that are currently under definition. It is important to emphasize that sharing can be distinguished on the basis of three principal parameters: time, frequency and space.

In [59], it is argued that spectrum sharing can be categorized depending on whether it is based on *coexistence* or *cooperation*. In the first place, different networks of devices do not exchange any explicit signalling and at most detect each other's presence. In the second case even devices under different administrative control must cooperate to avoid mutual interferences. The cooperative approach is particularly sensitive to the hidden terminal problem where devices might not be aware of the presence of primary transmissions and thus adopt harmful behaviours.

The second way of categorizing spectrum sharing is based on whether it is done among equals or it is primary-secondary sharing. In the first case all devices have the same equal rights to access the spectrum. In the second, and most celebrated case, some systems have the right to access the spectrum[1] (referred to as primary user - PU), whereas the secondary devices (i.e., CR devices) are not allowed to cause harmful interference to the PU. On top of this distinction, wireless devices are categorized as *unlicensed* or *licensed*. In particular, a licensed system must get the permission from the regulator to operate within a portion of the frequency spectrum. On the other hand, for the case of sharing among equals, referred to as *commons*, in the specific case of unlicensed operations, Wi-Fi is probably the best example. In [60], an exhaustive taxonomy of these aspects is provided and a short summary is shown below:

1. *Command and control*: in this case the regulatory body lays down the detailed rules for spectrum usage that is assigned to an entity for nearly eternal use (e.g., military).
2. *Exclusive-use*: in this case the owner of the spectrum band is licensed to have exclusive access rights.
3. *Shared-use of primary licensed spectrum*: in this case the spectrum owned by a licensee is shared by a non-license holder. As mentioned above, the PU is not aware of the existence of the secondary system, which therefore must ensure minimal interference in order to coexist. More specifically, there exist two possible models, namely *spectrum underlay* (based on coexistence, UWB is a typical example) and *spectrum overlay* (this case is well represented by TV White Spaces).
4. *Commons*: as mentioned above, in this model no system can claim exclusive right of using the shared spectrum. This is clearly the case of Wi-FI or other wireless technologies operating in the ISM band. The extreme of this form of spectrum sharing can be found when devices are all trying to maximize their performance greedily, thus causing the so called "*tragedy of the commons*".

More recently new ways of sharing the spectrum have been proposed. This is the case of the authorized shared access (ASA) that was firstly introduced by Qualcomm [61]. ASA

[1] Licensees pay a fee for exclusive use of assigned frequency bands with rules laid down by regulatory entities.

(sometimes referred to also as licensed spectrum access - LSA) was born as a solution to the problems inherent to previous forms of spectrum sharing models. The first consideration is that spectrum re-farming and setting up all the rules for licensee's protection (e.g., time to clear the frequency bands) take long time and it might not always end with satisfactory solutions. In essence, ASA prescribes forms of subletting spectrum done by licenses in favour of lessees in such a way that secondary devices can receive grant to access a portion of the licensed spectrum though some form of spectrum pricing.

In order to leverage new market opportunities that shall arise from more dynamic use of the spectrum, it is fundamental studying detrimental effects that may arise after the adoption of specific spectrum-sharing models. The most significant aspect is related to the prediction of in-band and out-of-band aggregate interference. Aggregate interference is therefore seen as one of the pitfalls that could hinder a more dynamic use of spectrum. Relying on the definition of the possible forms of spectrum sharing[2], the scenarios considered in this deliverable that are used to characterize the aggregate interference are:

1) Opportunistic secondary spectrum access in the context where there is no explicit agreement of the primary (e.g., as allowed by a higher authority such as the regulator, under very strict rules). TV White Spaces, shared-use of primary licensed TV spectrum in overlay mode from the standpoint of the TV service, is the prominent example of this.
2) Hierarchical sharing where equipment transmitting at both access levels is under the ownership of the same entity. Some visions for "cognitive" or "opportunistic" Femtocells are examples of this.
3) Hierarchical access where the primary explicitly agrees with one or more entities to allow opportunistic access to its spectrum by those entities. This is case for ASA/LSA and some other variants or alternative models.
4) Shared use of licensed spectrum in underlay mode. This is the case for UWB, or some "interference-limited" opportunistic access techniques – depending on the definition of "underlay".
5) Spectrum commons and related models. Interference among secondary systems or among equal systems in unlicensed spectrum.

3.1 Opportunistic Secondary Spectrum Access: TV White Spaces

Currently, the concept of "White Spaces" can be defined in many different ways, as is apparent through investigation of definitions in different regions of the world. The FCC in the USA, for example, denotes as White Spaces portions of the frequency spectrum left unused by the digital TV broadcasting service [62]. In Europe, the Electronic Communications Committee (ECC) [63] of the Conference of European Postal and Telecommunications Administrations (CEPT), defines "White Space" as: *a label indicating a part of the spectrum, which is available for a radio communication application (service, system) at a given time in a given geographical area on a non-interfering / non-protected basis with regard to other services with a higher priority on a national basis*.

[2] It should be noted that this field currently in constant evolution, as well as the associated definitions that are applicable.

In Europe, White Spaces are within the frequency range 470 – 790 MHz, and in order to enable CR systems to operate there protection of the following services must be guaranteed:

1. Broadcasting services, such digital TV,
2. Program making and special event (PMSE) services and equipment, such as wireless microphones,
3. Radio astronomy,
4. Aeronautical radio navigation.

The necessary condition for CR networks to become operative is to be aware of which portions of the spectrum can be used for communications and which one are used by the primary service. This is clearly a critical point and without efficient mechanisms to identify which portions of the spectrum can be used, CR devices can become source of harmful interference with respect to the primary radio service. In order to respond to this need several techniques have been proposed: spectrum sensing, geo-location database and beacons. All the different techniques present pros and cons. For example, spectrum sensing techniques should be as good as to guarantee that CR devices are able to sense radio signals as low as -114 dBm [63]. At the current stage of consumer electronics this could be difficult although likely to happen in the next few years. In alternative to spectrum sensing, or at least, to give more reliability to the entire process, the use of a geo-location database was proposed. This way of approaching the problem, could suit particularly well the case of TV White Spaces, where the rate of change of frequency occupation can be considered static for months or years. The main problem of this approach is mainly the definition of the information that the database should unveil to the CR devices and whether databases should be developed by different organizations, that is private or public. The use of beacons might represent a third way of raising spectrum awareness, as the primary user transmits them in order to clearly sign that is using that specific frequency channel, similar to the concept of a lighthouse. The main problem of this technique is the cost of the hardware. In addition to all these challenges, CR devices have to be able to detect that a channel is again used by the primary service, although the secondary network is performing data exchange, and within a minimum amount of time they should evacuate that channel.

Despite that spectrum sensing was initially considered as “the way” to be pursued in order to discover frequency availability/unavailability, the sensing process is severely affected by the problem of the hidden terminal. In case of CR systems the hidden terminal problem has to be understood from a slight different perspective with respect to the problem traditionally addressed in the field of ad-hoc networks. In fact, this has to be intended as the impossibility of a CR device to detect the transmission of the primary user at a given time and geographical location. Therefore, the CR device would transmit and in case it is close to one receiver of the primary transmission it shall cause harmful interference. With regard to this, a possibility to relieve the problem it is given by the collaborative/cooperative spectrum sensing approach. In this way, the incorrect information of an individual device can be identified and if the conditions are not too adversarial phased out. Clearly, a urban or countryside scenario greatly change the conditions as the received signal has higher chances to be susceptible of multi-path fading and blocking in the first case.

As TV White Spaces are quite well investigated by the scientific literature of CR networks, it is worth mentioning something on PMSE device, with particular emphasis on the wireless microphones. Typical applications of these devices are special event like the Olympic Games and concerts. Wireless microphones are meant to provide high quality audio (i.e., maximum 4 ms latency and a very high dynamic range of up to 117 dB). From the perspective of the regulatory, it is worth mentioning the UK model in which until January 1st 2012, the TV channel #69 is the only one dedicated to the wireless microphones nationwide on a shared license basis. From January 1st 2012 onwards only the TV channel #38 remains available in a similar fashion, whilst the others are regulated depending on date/time/space of a specific need. The typical scenario of a concert in which potentially thousands of CR devices may be allowed to operate in the TV White Space, makes clear that the PMSE devices have to be properly protected. The techniques mentioned above to raise spectrum awareness are still applicable to this case. Owed to the large number of interferers, the study of the aggregate interference for the case of PMSE devices can rely on the well-established characterization of the interference by means of the spatial deployments of nodes according to a homogeneous Poisson point process. These concepts will be however clarified in Section 4.

3.2 Hierarchical Sharing with Equipment Under a Single Entity: Femtocells and Related Examples

3.2.1 Scenario 1: Ad-hoc deployment

According to recent studies [64], 50% of phone calls and 70% of data services will take place indoors in the upcoming years. The aim of this section is to review some of the benefits, but mostly the challenges stemming from the adoption of Femtocells. The aim is to give a brief overview of the state of the art and the main references used here are [65]-[67]. As clarified in the forthcoming section, one of the distinguishing facts of the interference generated by Femtocells is the large number of interfering devices. As discussed in Section 4, this could be done using homogenous Poisson process for the spatial distribution of Femtocell devices.

In the scenario described above, there will be the need to dramatically increase the indoor capacity in order to enable users with sufficiently high transfer rates and the provision of quality of service (QoS). If, on the one hand, this can be done through conventional Macrocell cellular networks such as the long term evolution (LTE) and its advanced version (LTE-A), in indoor places with limited or non-existing coverage this goal results impossible to achieve. One answer to such a challenging scenario is constituted by Femtocells (see Figure 3-1).

Femtocells aim to improve the indoor coverage, promising to deliver high enough transfer rates. The Femtocell is created around the Femto access point (FAP). The FAP uses one of the typical radio technologies such as UMTS, WiMAx or LTE for the air interface, whilst it uses a broadband optical fibre or digital subscriber line for the backhaul. The advantages arising from using Femtocells are multiples, for both operators and users. The users for example will experience a stronger signal which directly translates into higher reliability and throughput. For the operators, the use of Femtocells opens to the possibility of scaling down the unavoidable congestion of network resources from the Macrocell standpoint. This is simply the consequence of the fact that most of the traffic will be supported over the Internet Protocol backhaul.

Alongside with the benefits arising from the use of Femtocells, the main drawbacks become from the massive deployment of Femtocells equipment. The FAPs are deployed by the end-users without any specific pre-planning and they elude any possibility of control from the network operator. In fact, despite that FAPs are designed to transmit with low power their massive deployment (of the order of millions of customers) inherently carries the problem of limiting the aggregate interference that would be harmful for Macrocell users.

Femtocells could in principle operate in a dedicated portion of the spectrum with respect to the Macrocell. However, studies have shown that the spectral efficiency can be greatly improved if Femtocells and Macrocells operate over the same frequency (Macrocell overlays the Femtocells). As described in [65], co-channel interference will appear with consequent degradation of the Macrocell performance. Thus, the mitigation of aggregate co-channel interference generated by Femtocells would still require the FAPs to incorporate typical solutions that belong to ad-hoc networks such as self-organization and synchronization. The reason why, despite the low power emitted by FAPs, the aggregate interference still represents a problem, is due to the fact that the radio signal does not confine itself only to the area of interest (namely the premises of a customer) [65][66].

From the point of view of sharing the spectrum, the Macrocell users represent the primary service while the Femtocells the secondary one. Solutions to relieve the problem of Macrocell-Femtocell interference can be found in [65]-[67]. Focusing on the problem of co-channel interference generated by Femtocells, the work carried out in [65] reviews several mitigation techniques. For example, under the hypothesis that the Femtocells are synchronized with the Macrocell, two cases of interference are considered: cross-layer (Macrocell and Femtocells belong to different network layers) and co-layer (when they belong to the same network layer). Suggested solutions include power control, radio resource management and self-configuration/organization. An example of self-organization for interference mitigation is shown in [67]. In [66] the authors review several scenarios arising from the unplanned deployments of FAPs. The scenarios call for location uncertainty of the FAPs, parameters reconfiguration at the FAP side and access control mechanisms. One solution claims resource coordination between the Macrocell and the Femtocells for using the spectrum. In addition, the authors of [66] quickly review coordination mechanisms in scenarios in which the interference can be considered both semi-static and dynamic.

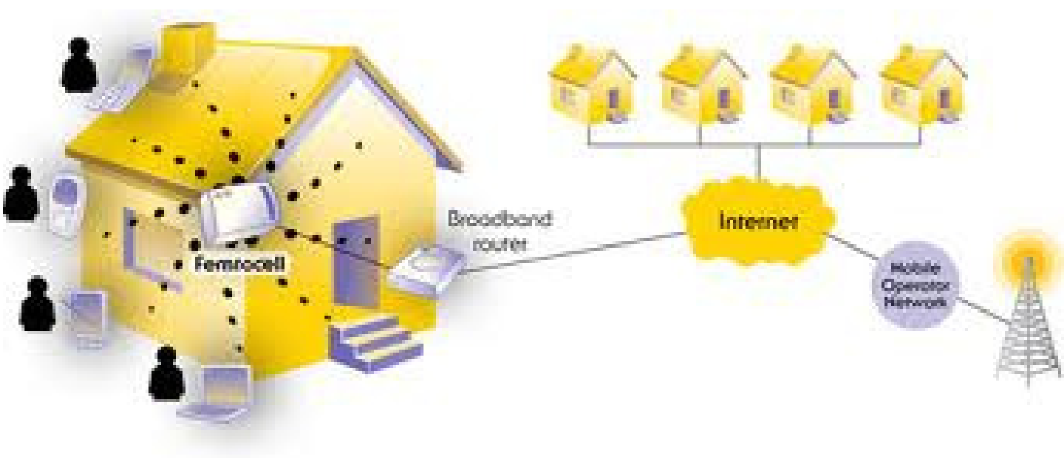

Figure 3-1: Structure of a typical Femtocell scenario from the network perspective.

3.2.2 Scenario2: Opportunistic capacity extension

This scenario depicts a localized region where there is a traffic hot-spot and an opportunistic network is created in order to route the traffic to non-congested access points. It may also include cases such as dynamic spectrum management between Macrocells and underlying micro-, pico- and Femtocells, or 3G traffic offloading towards Wi-Fi.

The generic scenario comprises a congested infrastructure base station (BS), several not-congested APs (part of the operator's infrastructure or not), several devices or nodes to build up the opportunistic network, and one or more terminals that try to connect to the congested BS.

- In a first step, the type of congestion in a heterogeneous context needs to be identified, e.g. in case there is a high level of interference due to simultaneous spectrum access in unlicensed bands, or licensed band systems are overloaded, etc.
- In a second step, the results obtained at the previous step are exploited in order to eventually reconfigure system parameters (if accessible) and/or use re-routing strategies in order to route the traffic via uncongested nodes.

Figure 3-2 shows what described above: the incoming device intends to connect to BS1 but it is instead connected to BS2/Femto-BS/Wi-Fi AP through an opportunistic network.

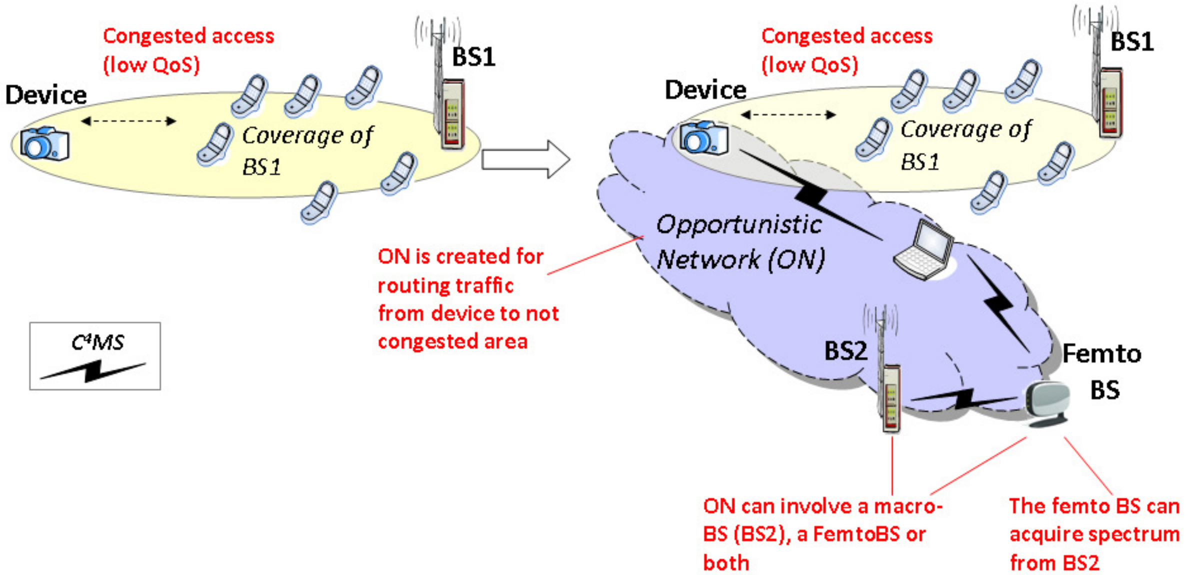

Figure 3-2: Resolving cases of congested access to the infrastructure – Generic case.

This scenario enables devices to maintain the required level of QoS for a wireless communication link even when a congestion situation occurs. In particular, the following two types of congestion situations are considered:

- A system operating in a licensed/unlicensed band is overloaded and cannot guarantee the provision of the required QoS anymore. In this case, the traffic may be re-routed, e.g. based on hot-spots or links via alternative radio access technologies (RATs) in order to avoid any congested link.

- A system operating in an unlicensed band (e.g., Wi-Fi) or licensed band (such as FAPs in a randomly deployed dense environment) is experiencing high levels of interference, since neighbouring APs/BSs are accessing the identical part of the spectrum. Due to this problem, the link throughput is greatly decreased and a congestion situation occurs. In this case, a twofold strategy is typically applied: First, the origin of the interference is identified (which bands are concerned? which Access Points/Base Stations are concerned?) and the concerned APs/BSs are reconfigured in order to avoid the congestion situation if possible (e.g., if the concerned system components belong to a single owner). Typically, it is assumed that the reconfiguration strategy can be applied to resolve at least part of the problem, while further measures are needed in order to fully guarantee the required QoS levels. In particular, re-routing strategies based on opportunistic networks can be adopted to avoid congested links.

3.2.2.1 Use cases

Three generic use cases that might trigger the creation of an Opportunistic Network (ON) are presented in this section while more detailed use cases (which may refer to more than one of these generic scenarios) are analysed in the relative sub-sections.

- *Congestion solving:* The network should be able to detect congestion situations when or even before they occur and then try to create one or more opportunistic networks. These will allow data flows to be re-routed towards not-congested access points and thus free some resources in affected cells. This use case mainly refers to users already connected but their QoS starts to degrade due to congestion and or interference to the Macro-BS and therefore their access needs to be re-routed to a different BS.

- *Congestion access control:* This is a generic use case, where a new incoming user tries to access a congested network access point. An opportunistic network is created in order to re-route its traffic to a decongested area, thus allowing service provisioning to a user that otherwise would have been rejected due to lack of resources.

- *Congestion avoidance (Offloading):* Whenever possible, the operator will try to divert traffic towards infrastructure-less access points (e.g., Wi-Fi APs) so that overlaying cellular (outdoor) network resources are saved. It is a rather proactive behaviour of the operator so as to avoid potential issues and maintain a balanced traffic among the Macro-BSs.

3.2.2.2 Congestion solving: the cell edge users case

Figure 3-3 shows the scenario use case where two users are experiencing a very low level of QoS because

- the neighbouring Macro-BS are heavily loaded,
- the concerned user equipment (UEs) are close to the cell-edge.

Since the demand of radio resources that are required for delivering high data rate services to those cell-edge users could exceed the capability of the network, the concerned devices typically will not be able to achieve their target QoS.

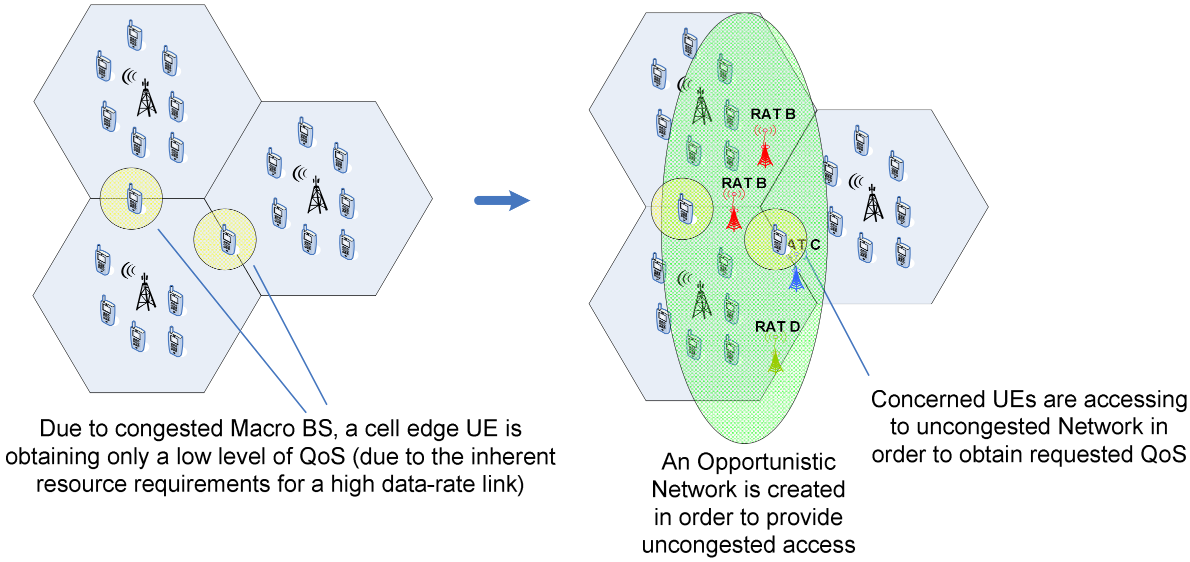

Figure 3-3: Resolving cases of congested access to the infrastructure (congested Macro-BS)

Neighbouring RATs (in this example, “RAT B”, “RAT C” and “RAT D”[3]) are used in order to set-up an opportunistic network and enable high data-rate/high QoS services for the concerned UEs (in particular to those positioned at cell edges). It should be noted that the main focus is on Femtocells able to cover the same service region, and/or on macro BSs (which may be covering neighbouring service area regions; in this case it can be assumed that the traffic is routed to them through Ad-hoc networks).

In the context of Macrocell/Femtocell management (when RAT B/C/D are Femtocells), resolving congested access to a Macrocell can be done by allocating spectrum to Femtocells in the area: the Macrocell can decide the most efficient configuration (in terms of spectrum and power) of the Femtocells with the following objectives:

- offload a number of terminals to the Femtocells so that the load on the Macro-cell does not exceed a threshold;
- minimize Femtocells to Macrocell interferences when both operate over the same band.

It is worth noticing that these two objectives are conflicting: having in fact a high number of terminals capable of connecting to the Femtocell means increasing the power of the FAP, thus causing interference to the Macrocell; minimizing the interferences by reducing the power allocated to the Femtocell means reducing the coverage of the FAP and so the number of terminals that can are served. In this scenario, the Femtocell parameters are adjusted depending on the capability to create opportunistic networks that allow terminals connecting to the Femtocell to relay data from/to neighbouring terminals that are not in coverage of the Femtocell itself.

[3] The new RATs B, C and D either represent Femto-BS for Resource Management between Femto/Macro-BS or RATs which have not been designed in an integrated framework (such as various Wi-Fi flavours, WiMAX, etc.)

3.2.2.3 Congestion solving/avoidance: Macrocell/Femtocell management case

Figure 3-4 shows the allocation of resources to a Femtocell and its integration into an opportunistic network.

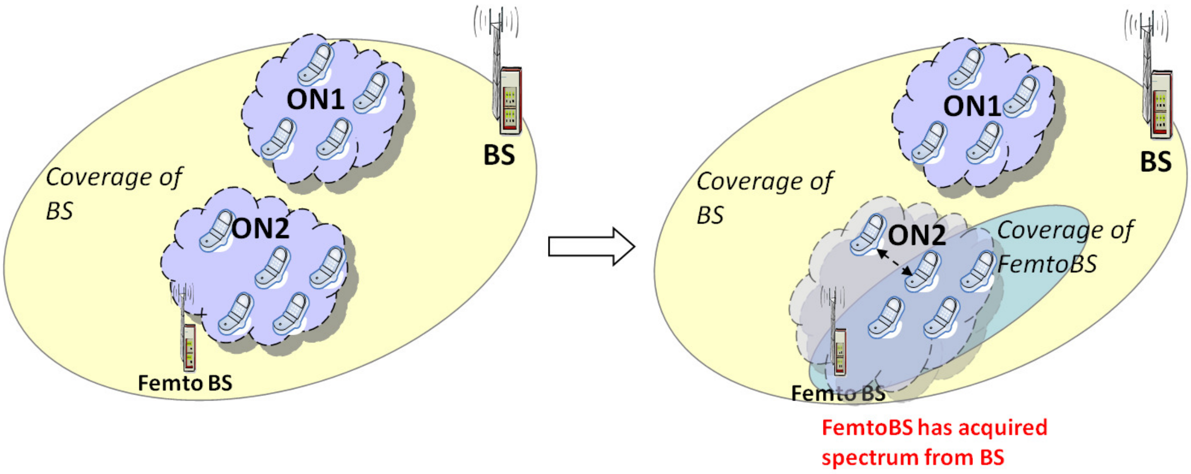

Figure 3-4: Resolving cases of congested access to the infrastructure (Macrocell/Femtocell management).

As shown in Figure 3-4, opportunistic networks (ON1 and ON2) exist between mobile terminals, which have common needs/capabilities. These terminals are connected to the Macro-BS which is supplied with measurements provided by ONs and the Femto-BS is currently off (no resource allocated to it).

As part of the ON suitability determination step, the Macro-BS decides to modify the configuration of ON2 based on the measurements it receives and on the overall level of load it experiences. The objective is to decrease the load on the BS by allocating resources to Femto-BS and having it added to ON2.

As part of the ON reconfiguration step, Femto-BS has allocated resources (spectrum band with associated allowed power levels). Some of the terminals from ON2 stop using the Macro-BS and connect to the Femto-BS. Some other terminals from ON2 (those not under the coverage of the Femto-BS) access Femto-BS through other terminals in ON2 (multi-hop communications) that are in coverage of the Femto-BS. With regard to what specified before, the trade-off is found when the load on the Macro-BS is decreased to reach an acceptable level while the decision on how configuring the Femto-BS ensures acceptable level of interference.

Although this detailed use case mainly addresses issues raised by the generic use cases of congestion solving and congestion avoidance (offloading), it can also be applied to the generic use case of congestion access control.

3.3 Shared Use of Licensed Spectrum in Underlay Mode

"Underlay" spectrum access has, in different sources, been used to mean several things. The common and historical reference is for systems that are causing an interference by their transmissions that is below the noise power spectral density at the primary, typically through transmitting with a very wide bandwidth, for example, such as through impulses transmissions. More recently, underlay spectrum access has often also been used to refer to systems that transmit while causing less than a given threshold of interference power or interference power spectral density at the primary receiver. This section briefly overviews both such cases.

3.3.1 Ultra-Wide Band

UWB technology, which is a radar technology, represents probably the first historical attempt to enable improved forms of spectrum access (i.e., underlay communications). In recent years, UWB has attracted great interest of academia and industry due to the unique characteristics of the signal, which makes it appealing for a large variety of civil applications: short-range communications, Internet, localization at centimeter-level accuracy, high-resolution ground-penetrating radar, through-wall imaging, precision navigation and asset tracking, just to name a few.

A signal is defined to be UWB according to the two following definitions: for a central frequency less than 2.5 GHz its fractional bandwidth (W_f) has to be greater than 20%, whilst above 2.5 GHz its bandwidth (W) has to be at least 500 MHz [17]-[19][68]. The fractional bandwidth of the signal is defined as: $W_f=2(f_h-f_l)/f_h+f_l$, where f_h and f_l stands for the high and low cutoff frequencies measured at either -3 dB or -10 dB, depending on the definition. Already in 2002 the FCC in the USA regulated the use of UWB handheld devices in the huge frequency range 3.1-10.6 GHz. The FCC regulated emission levels of UWB devices to -41.3 dBm/MHz to avoid harmful interference toward systems already existing (e.g., the Global Navigation System - GPS).

The large bandwidth, the simplicity of the transmitted signal that consists of the transmission of a train of baseband nanosecond pulses having a very low level of emitted power (in theory below the noise floor) made UWB attractive for enabling the applications mentioned above. Over time, UWB can be seen as the attempt to bring to the extreme the concepts of a spread spectrum system and the first in its kind to make more efficient use of the wireless spectrum. Mainly two techniques are available to generate an UWB signal. The first approach consists of generating nanosecond pulses and it constitutes the basis for time-hopping UWB systems [69]. The second consist of bonding together frequency bands in order to produce an ultra-wide bandwidth. This last approach was used in [70] and in the literature is referred to as multi-band UWB.

More recently, UWB systems have been classified within the larger group of dynamic spectrum access techniques and in particular the ones that are referred to as underlay communications [60]. In this case, secondary users are forced to transmit with extremely low power levels (below the noise floor) such that the primary user is unaffected by secondary transmissions. With respect to the taxonomy defined in [60], UWB communications break the secondary-usage barrier and the exclusive-usage barrier that are nowadays in force in the allocation of spectrum for wireless services. However, peaks of spectral lines caused by specific modulation schemes reveal that UWB is not totally capable to coexist with other wireless systems without causing harmful interference.

The natural solution that aims to improve the coexistence between secondary UWB devices and primary services goes under the name of detect and avoid (DAA) techniques [71]-[76]. For example, as pointed out in [71], UWB devices might not be able to coexist with other wireless systems despite the restrictive power emission regulations. A study on the coexistence between UWB and other systems like UMTS, GPS and fixed wireless systems is shown in [72]. In this study, UWB devices are limited to indoors (that is the main application of UWB systems) while the victim systems could be either inside or outside the building (that is intended as a commercial/industrial building). Secondary devices make use of the time-hopping UWB signaling scheme.

Literally, DAA means that UWB devices are capable of sensing the power within the band of the victim system and whenever the threshold set for reception is exceeded, UWB devices have to modify their transmission parameters in order to avoid interfering. UWB devices perform these operations on a non-cooperative basis (this is at least the most common way of approaching the problem) with respect to the primary system, which ignores the presence of UWB transmitters. The main limitation of this approach is the need to sense signals as low as the sensitivity of the victim receiver (well below -100 dBm). Therefore, sophisticated measurement instruments are required, which increase the cost of the UWB devices.

In [73] and [74], DAA techniques for UWB devices (also these studies are tailored for time-hopping UWB) potentially interfering with UMTS and WiMAX systems are devised, respectively. The key idea in [72] and [73] is to detect the uplink primary transmission and accordingly adjust transmit power and data rate to reduce/avoid interfering with the victim system. Furthermore, the outcome of the DAA could even consist of suspending completely the transmissions of the secondary devices for the time necessary by the primary UEs to complete network association. A performance metric that could be used in these cases is given by the fraction of time that a period of primary user activity is jammed by UWB devices. In the mentioned papers, the DAA includes two sub-phases: detection and transmission for the purposes mentioned already. For the sake of completeness, as an example, the cooperative approach and the advantages for the UWB system are shown [75].

In [76] DAA technique adapted to the specific scenario of a UWB-WiMAX system is investigated. The study is based on the concept of *low-duty-cycle* and it is applied in the frequency band 3.1-4.8 GHz. The devices this time are using multi-band UWB transmission technology. The study shown in the paper relies also on European regulations for the power emissions of UWB devices in indoors [77]. In essence, the coexistence mechanism consists of defining different thresholds for signal detection and different transmit power levels based on the proximity of a UWB device with respect to the WiMAX receiver. In particular, three zones are identified. In the first zone UWB devices can transmit with a power spectral density of -41.3 dBm and use a threshold for detection of -61 dBm. In the second zone the UWB devices use a threshold of -38 dBm and a power spectral density of -65 dBm/MHz. In the last zone (which implies close proximity to the WiMAX receiver) the emitted power spectral density is set to -80 dBm/MHz for a distance below 36 cm, whereas the threshold for the detection of the signal remains the same.

3.3.2 Interference Threshold

This approach assumes that a known threshold for allowable interference at the primary receiver is enforced or otherwise assumed, whereby the secondary will transmit up to a power level that would cause no more than that interference threshold. A key challenge with such an approach is that, typically, neither the positions, nor propagation/channel characteristics, of/toward the primary receiver from the secondary transmitter are typically known. Correspondingly, it is very difficult if not impossible to ascertain the allowable upper transmit power level of the secondary, especially in dynamic scenarios involving motion of the primary receivers and/or the secondary transmitters. That is not to say, however, that such an approach cannot be useful. If well-known “reference scenarios” for the positions of the primary receivers are defined, such as for TV White Spaces whereby the types of primary receivers, their positions (e.g., locations on/within a building), and motilities (or lack thereof) can be defined with a relatively high certainty, the secondary transmit power limits can be ascertained with a higher confidence level of not causing more than the interference threshold. Such assumptions apply for regulatory modeling of interference, and indeed can be seen in some sense as related to interference threshold models.

Aside from such cases, the most prominent example of such interference limit models is the “Interference Temperature” concept as proposed by the FCC.

3.3.2.1 Interference Temperature Model

The FCC introduced the concept of interference temperature (IT) in 2003, for “quantifying and managing interference” [62]. As described already elsewhere in this document, a CR networks may coexist with the primary user either on a non-interference basis or on interference-tolerant basis. In the first case, as mentioned, the CR devices are allowed to operate only on those bands that are not used by the primary user (i.e., White Spaces). In the second case instead, CR devices can access the same frequency band of the primary user as long as the aggregate interference power falls below a certain threshold. The case in which CR devices can operate simultaneously with the primary transmission is commonly known as the interference temperature case.

When analysing interference-limited CR systems, it is necessary to specify the IT constraint for the primary receiver along with the specification of the transmit power constraint of the CR transmitters. As such, this is the problem of optimizing a system subject to multiple constraints. The limits of interference temperature limited single-antenna CR systems was analysed in [78] in the presence of fading. The capacity and power constrained problem arising in such single-antenna system with fading was investigated in [79]. The work done instead in [80] and [81] investigates interference temperature limited CR systems in multiple input single output (MISO) and multiple input multiple output (MIMO) cases, respectively.

It is important mentioning that the FCC recently dropped the concept of interference temperature declaring it as *not a workable concept* [82]. This was due to the observation made by several industries that the concept of interference temperature, if adopted, would have resulted in an increased interference in the frequency bands where it would have been used.

3.4 Spectrum Commons and Related Models: Interference among Secondary Systems

3.4.1 In Opportunistic Secondary Spectrum Access Scenarios: TV White Spaces

Interference may occur among secondary systems in cases of secondary spectrum usage, for instance among the secondary systems using UHF TV White Space frequency bands. In the particular case of TV White Space, numerous secondary systems are either defined or being defined for operation in TV White Space, including ECMA-392 [83], IEEE 802.22 [84], IEEE 802.11af [85], IEEE 802.15.4m [86], IEEE 1900.7 [87], among others. Considering that in many locations the number of channels available for TV White Space access will be very limited, the interference that these systems cause on each other could quickly lead to a situation where the available White Spaces become unusable for secondary access.

In the case of TV White Space, a number of opportunities exist to do things better than in the case of ISM and other unlicensed bands. In such a case, there is already a database entity that, especially for Ofcom and CEPT other proposed rules [88] [89][90], would be able to not only manage secondary access to protect the primary, but also potentially could operate outside of its proposed purpose in managing the interference powers among secondary systems. Such as case, from the regulator's point of view, is nevertheless out of scope of consideration, and could also be seen as medalling in fair competition between users. There are scenarios, however, such as in ASA and related concepts, where such management could be applicable. If a spectrum owner were to provide its own database to allow opportunistic access of its spectrum, e.g., for a fee, then that spectrum owner could validly manage the powers among the secondary systems to avoid interference, as well as potentially implementing far more complex management concepts than just transmission power adaptation.

Aside from such possibilities, interference among secondary systems is subject to many of the same considerations and challenges as interference in unlicensed bands. It is noted that, however, there are different sets of equipment operating in White Space compared with unlicensed bands, due to various factors such as maturity of technology, contributions and spectrum opportunities and the desire to develop systems that can take advantage of opportunities better, as might become available in White Space, and tougher regulatory rules and challenges such as transmission masks, among others.

3.4.2 In Conventional Unlicensed Spectrum: ISM bands

The case of spectrum sharing and interference in conventional unlicensed spectrum like for example ISM (2.4 GHz) and U-NII (5 GHz) bands is referred as uncontrolled commons or open spectrum access [60]. In this scenario any one can operate as many devices as he want and no specific rules have been defined to avoid or reduce interference. Regulation bodies like FCC or ECC only require that a certain maximum peak power is not exceeded. Therefore several devices belonging to independent systems can be active at the same time in the same portion of spectrum. As previously indicated, if each single system is only trying to maximizing its own performance without considering external factors the so called “tragedy of commons” is expected to happen [91]. For this reason, although standards are rapidly getting more and more performing (e.g: IEEE 802.11n) creation of reliable, revenue generating services in unlicensed spectrum continues to be less than viable due to this weakness. An additional limitation is represented by the multitude of different systems and standards operating in the same spectrum band. This make difficult to define techniques to mitigate possible interference scenarios. For this reason many efforts to avoid "the tragedy of commons" didn't encounter much resonance in the industry. In [59] one of these efforts referred as "Managed Commons" has been presented together with the main desirable characteristics for a good commons management protocol.

3.4.3 In Unlicensed bands: Use of Opportunistic Wi-Fi Networks for Resolving Interference among different RATs

3.4.3.1 When all nodes can be reconfigured

Moving beyond the cellular framework, Figure 3-5 shows the use case where interference occurs in RATs B, C and D which are accessing unlicensed spectrum, e.g. Wi-Fi spectrum at 2.4 GHz, opportunistically. Also, it is assumed that RATs B, C as well as the cellular network are not designed in an integrated framework (as it would be the case for GSM and various 3rd Generation Partnership Project (3GPP) flavours such as UMTS, HSPA, LTE, etc.). In fact, various independently designed RATs are used and exploited in an optimum way in order to fill in available bands and to provide access to the users affected by network congestion. This approach is a clear distinction compared to the Self-Organizing Networks (SONs) solution envisioned in 3GPP. In the given scenario, the different RATs transmit over the same portion of the band thus creating interference and greatly reducing the overall QoS. In this case, the UEs are typically used to identify the interference creating entities. Afterwards, the transmission parameters of the identified nodes are reset assuming that the required changes can actually be implemented (i.e., nodes belonging to a single owner).

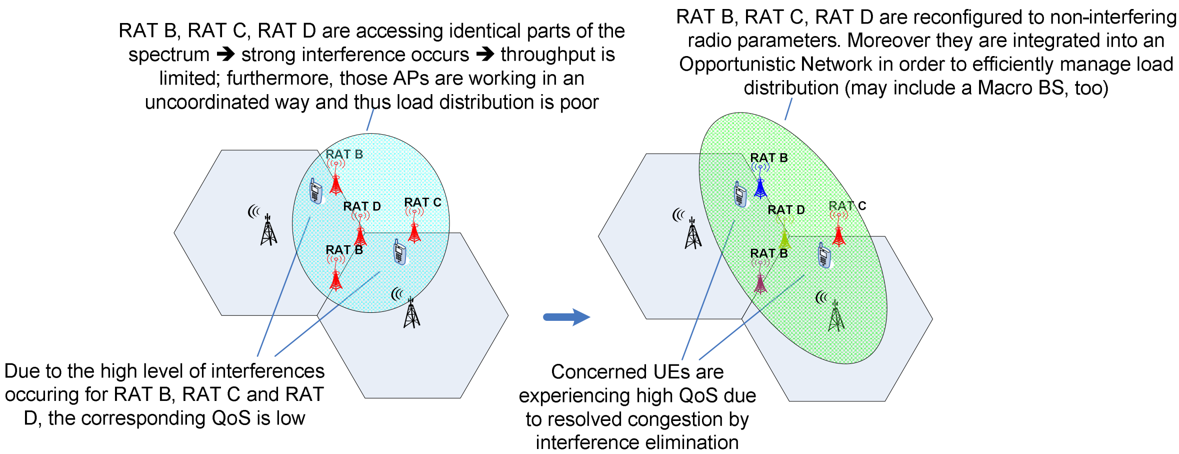

Figure 3-5: Resolving interference issues when nodes can be reconfigured.

3.4.3.2 When some nodes cannot be reconfigured

Figure 3-6 shows a use case similar to the one described in Section 3.4.3.1 and depicted in Figure 6, i.e., where interference occurs in RATs B, C and D which are accessing unlicensed portions of the spectrum such as the Wi-Fi spectrum at 2.4 GHz, opportunistically. The difference consists in the fact that some RATs are out of control of any management entity for ONs and their parameters cannot be set/reset. Consequently, an ON has to be organized in a way that only those RATs that can coexist on a non-interfering basis are included. Those are reconfigured such that no interference occurs inside the ON and maximum QoS can be therefore achieved.

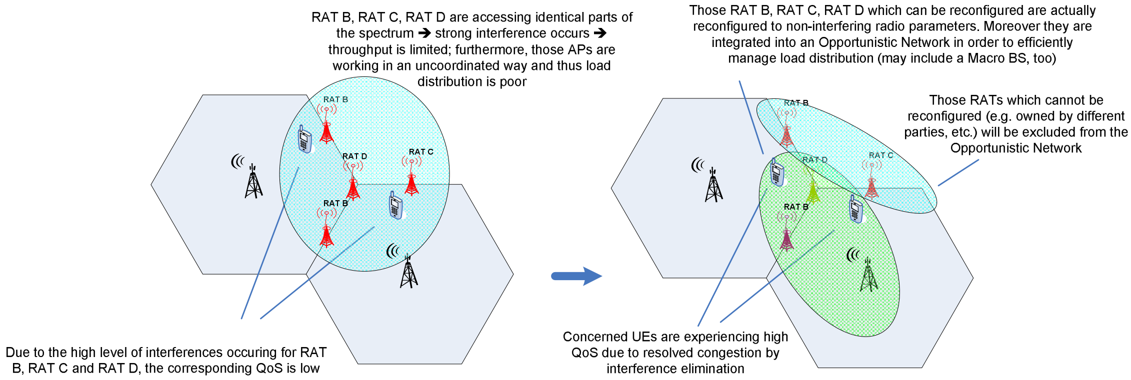

Figure 3-6: Resolving interference issues when some nodes cannot be reconfigured.

4. Models of Wireless Interference

The aim of this section is to present a thorough though succinct overview of some fundamental aspects connected with the modelling of the aggregate interference in wireless systems. This quite basic approach will be at the end extended to the specific case of cognitive radios. Referring to the generic $\mathbb{R}^d$ space and a point *y* in it, the aggregate interference measured at the location *y* can be written as follows

$$I(y) = \sum_{x \in \mathrm{T}} P_x h_x l \| y - x \|, \tag{1}$$

where T denotes the set of active transmitters, P_x is the transmitted power of node *x*, h_x is the (power) channel fading coefficient for the link between *x* and *y* and $l\|y-x\|$ denotes the path-loss due to the distance affecting the link between the two nodes. In the remainder of this document the analysis of the interference is clearly important for interference-limited networks such as cognitive radio systems.

Aggregate interference plays a major role in many aspects of management and optimization of wireless networks. In essence, aggregate interference in the shared wireless channel has a number of implications on network performance. One of the main working assumptions in wireless communications, made from the system standpoint, is to determine an exclusion region around the transmitter-receiver pair in order to obtain a communication free from interference [92][93]. This is the typical way of proceeding in many papers dealing with MAC protocols, for example. These papers try, to some extent, to enable access to the wireless channel in such a way to reduce (or minimize) the probability that two or more packets collide at the same receiver, thus causing multi user interference (MUI).

Despite all the attempts to minimize the aggregate interference between communication systems sharing the same frequency band at the same time and location, the problem still exists. Depending on the radio technology used, narrowband or ultra wideband, the type environment where the network has to operate (urban or countryside), performance may vary quite dramatically. In a realistic environment, the location of the wireless devices with respect to the receiver, the time of arrival of the received packets and the different levels of received power affect the performance of a wireless link. All these effects fall in the set of near-far effects. Therefore, in realistic scenarios where packets suffer from collisions, if a packet is received correctly, although in principle it collided with other concurrent transmissions, is said to capture the intended receiver. This effect is known in the literature of MAC protocols as the capture effect. Often the capture is defined as follows

$$g_{i,0} P_i > P_\vartheta \left(\sum_{j \neq i} g_{j,0} P_j + N_W \right), \tag{2}$$

where P_i is the transmit power of the *i*th terminal[4], while the sum represents the aggregate interference power, N_W is the additive white Gaussian noise with two-sided power spectral

[4] When power control is applied it holds that $P_i \neq P_j$.

density $N_0/2$ and P_ϑ is the threshold (referred to as capture power ratio) for accepting the packet of node i and it typically depends on the application. The terms $g_{i,0}$ and $g_{j,0}$ denote the power gains introduced by the channel in the test link and in the jth interfering link, respectively. Typically, they incorporate random propagation effects such as power-law decay, fading and shadowing. The power-law decay can be expressed as r^{-2b}, where parameter b is the typical path-loss exponent that equals 1 in free space. The term r^{-2b} is itself a random variable (r.v.) that follows some statistical distribution. The work done in [94] shows that, under the assumptions that fading, shadowing and locations of individual transmitters are independent, for a large number of stations (theoretically going to infinity) and under very broad conditions, the capture ratio in (2) depends only on the capture power ratio γ and on the path-loss exponent b.

4.1 Validity of Gaussian modelling for the interference

The capture model has been successfully applied to model realistic performance of packet switched radio networks under various transmission schemes and propagation effects. For example, capture was used to model the performance of mobile spread spectrum systems and more in general the basic but important case of a slotted Aloha (S-Aloha) network. Models have been developed to account for different modulation schemes, fading effects and shadowing. In all cases, modelling of the interference assume a central role. In brief, the capture model has bridged the algorithmic approach usually taken at levels of the OSI model higher than the physical layer and typical propagation effects affecting radio signals. In most or even all the studies, modelling the interference as the result of the superposition of individual and independent radio transmitters displaced in space has represented one of the primarily tasks, though very challenging. Modelling the aggregate interference as a Gaussian process is appealing due to its simplicity and direct use of the central Limit Theorem (CLT) in the presence of a large number of interferers. Despite this model has been used, soon it received criticisms as it does not account for the spatial distribution of the nodes.

In [95] and [96] the spatial capacity of a multihop S-Aloha network and the benefit owed to spatial reuse have been investigated, respectively. Both papers model the distribution of nodes in space as a two dimensional Poisson Point Process (PPP) as show in (3), with λ the intensity function of the point process and $||A||$ denotes the Lebesgue measure of set A. In particular, [95] models the throughput of the multihop network as the result of a spatial process in which packets from the devices are received correctly when no other nodes transmit within the same region of space. In [96] it is shown how spatial reuse can be introduced in the study of the performance of a multihop network when nodes are at least three hops apart. Moreover, network topologies that allow spatial reuse are discussed. In particular, [96] shows a previous result in which nodes are arranged on the vertices of equilateral triangles repeated over the network topology. Assuming that each node has a range of r=1 meters, the average distance between nodes is surprisingly equal to 2.

$$P\{k\ nodes\ in\ \mathrm{A}\} = \frac{(\lambda\|A\|)^k}{k!} e^{-\lambda\|A\|} . \tag{3}$$

When tackling the problem of studying the performance multihop network from a geometrical perspective, one interesting result can be obtained by computing the average distance among nodes. Referring to Figure 4-1, nodes are uniformly deployed inside the circle. The length of the arc XY is given by $2x\cos^{-1}(\vartheta)$, with $\cos\vartheta = x/2R$. Assuming now that a point is uniformly distributed over the elemental area [x,x+dx], the corresponding probability density function (pdf) can be written as follows

$$f_R(x) = \frac{2x\cos^{-1}\left(x/2R\right)}{\pi R^2}dx\,. \tag{4}$$

Therefore, the average distance of a point over the elemental area from *A* can be expressed as

$$d(R) = \frac{1}{\pi R^2}\int_0^{2R} 2x^2\cos^{-1}(x/2R)dx = \frac{16R}{\pi}\int_0^{\pi/2}\vartheta\cos^2\vartheta\sin\vartheta d\vartheta = \frac{32}{9\pi}R\,, \tag{5}$$

where the above integral was obtained changing first variable as $y=x/2R$ and then setting $\theta=\cos^{-1}y$. The result given in (5) can be used to find the general case of the average distance ($l(R)$) between any two points of the circle. This can be obtained using a result from stochastic geometry known as the Crofton's theorem on the mean values, which states that

$$\frac{\partial}{\partial r}l(r) = 2\left(d(r) - l(r)\right)\frac{2}{r}\,, \tag{6}$$

where in the above expression $d(r)$ is expressed in terms of (5). Multiplying (6) by r^4 and integrating by parts in [0,R] the following results is obtained

$$l(r) = \frac{128}{45\pi}R\,. \tag{7}$$

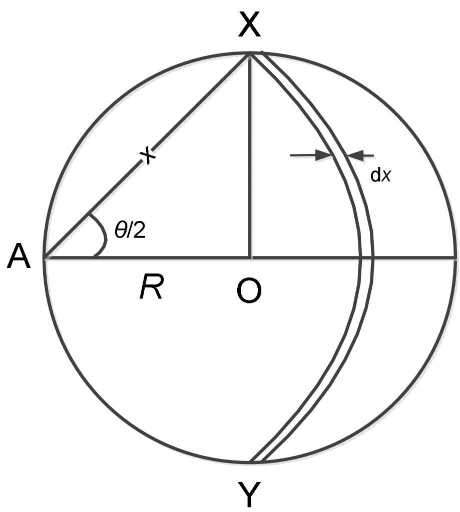

Figure 4-1: Geometrical model for deriving the average distance between two points uniformly distributed inside the circle.

Clearly the simple geometric approach shown above does not incorporate any realistic propagation effect which in reality impacts on the reception of the radio signal. For example, this limitation is removed in [97] where optimal transmission ranges are derived for a spread spectrum multihop packet radio network for an environment affected by Rayleigh fading and log-normal shadowing. The main result shown in [97] is the derivation of the transmission range of a device so that, on average, it has the optimum number of neighbours. Furthermore, this work enhances the one made in [98] where optimum transmission ranges were found for a packet switched radio network but with simpler channel propagation effects.

As mentioned already above, the assumption of the Poisson distribution of the devices over space and the Gaussian modelling of the distribution of the aggregate interference power provided already a good insight of the network behaviour. This has represented a fundamental step that bridged together the systemic approach with the physics of the radio signal propagation. Examples aligned with this view can be found in [99]-[101]. However, these papers started debating the validity of the Gaussian assumption for modelling the interference power distribution. For instance, one hit that unhinged this conjecture came out when studying the performance of impulse radio UWB systems. In fact, the work done in [102] and [103] showed that the Gaussian approximation is too poor to predict accurately the performance.

The tool of stochastic geometry provides an excellent mean to devise the performance of packet switched radio networks in which devices generate harmful interference affecting each other's behaviour. The core contribution of this approach consists of modelling the nodes of a wireless network as a point process (PP). This approach was already pursued in the seminal papers [37][38] and [98] just to name a few. More recently this modelling approach have been rediscovered and adapted to more recent scenarios, radio technologies and networks. This is evident from [16][23]-[27][54][104]-[106]. In particular, [105] and [106] challenge the validity of the spatial Poisson model for the sake of obtaining an accurate prediction of the network behaviour.

Accordingly to such recent trend in communications, the next sections are devoted to review how stochastic geometry is helpful for modelling the behaviour of a wireless network where the aggregate interference assumes the key role.

4.2 Stable distributions

Historically, modelling the distribution of the aggregate interference power has witnessed important progresses especially with the two seminal papers [37] and [38]. In particular, both papers subsume that the distribution of the aggregate interference power generated by a Poisson field of interferers belongs to the family of stable distributions. Stable distributions belong to the family of heavy tail distributions. A typical example of one-side heavy tail distribution is the Pareto distribution. Two-side heavy tail distributions are the Cauchy and Lévy distributions. A probability distribution is considered heavy-tailed when the tails of such distribution are not exponentially bounded or, in other words, the tails are heavier than the exponential distribution.

This section is concentrated on the family of stable distributions, which belong to the two-tail distributions. Stable distributions can be considered as a result of the generalization of the CLT dealing with the sum of independent and identically distributed (iid) r.vs. whose variance is not finite. Thus, the Normal Gaussian distribution can be seen as particular case of stable distributions. In general, there is no closed form expression for the cumulative distribution function (CDF) and the pdf of stable distributions except for the Cauchy and Lévy distributions which represent special cases.

A univariate Cauchy distributed r.v. *x* is characterized by the following pdf and CF[5]:

$$f(x) = \frac{1}{\pi\gamma\left[1+\left(\frac{x-\delta}{\gamma}\right)^2\right]}, \qquad -\infty < x < \infty \tag{8}$$

$$\phi(\omega) = \exp\left(\delta i\omega - \gamma|\omega|\right),$$

where $i=\sqrt{-1}$ is the imaginary unit. On the other hand, a Lévy distributed r.v. *X* is characterized by the following pdf and CF:

$$f(x) = \sqrt{\frac{\gamma}{2\pi}}\frac{1}{(x-\delta)^{3/2}}\exp\left(-\frac{\gamma}{2(x-\delta)}\right), \qquad \delta \le x < \infty \tag{9}$$

$$\phi(\omega) = \exp\left(\delta i\omega - \sqrt{-2i\gamma\omega}\right),$$

At this point it can be given the first formal definition of a univariate stable distributed r.v. *X*. The following discussion on stable distributions will rely on [107] for notation and the definition of related concepts.

Definition 1: A r.v. *X* is stable or stable in the broad sense if for X_1 and X_2 independent copies of *X* and any positive constants k_1 and k_2 and positive numbers *c*, *d* $\in \mathbb{R}$ the following equality holds

$$k_1X_1 + k_2X_2 \overset{d}{=} cX + d, \tag{10}$$

where the equality above holds in distribution. The r.v. is strictly stable or stable in the narrow sense if (10) holds with *d*=0 for ant value assigned to k_1 and k_2. A r.v. *X* is symmetric stable if it is stable and symmetrically distributed around zero, that is *X*=-*X* in distribution. In other words, (10) states that the shape of *X* is unchanged under addition operation.

Definition 2: A r.v. *x* is stable distributed $S(\alpha,\beta,\gamma,\delta,1)$[6] if and only if it exists a r.v. *Z* having the following CF

$$E\exp(i\omega z) = \begin{cases} \exp\left(-|\omega|^{\alpha}\left[1 - i\beta sign(\omega)\tan\frac{\pi\alpha}{2}\right] + i\delta\omega\right) & \alpha \ne 1 \\ \exp\left(-|\omega|\left[1 + i\beta\frac{2}{\pi}sign(\omega)\log(w)\right] + i\delta\omega\right) & \alpha = 1 \end{cases}, \tag{11}$$

where the log() stands for the natural logarithm and in distribution it holds that

[5] The CF of a r.v. *x* is defined as E{exp(i*ωx*)}.

[6] The notation $S(\alpha,\beta,\gamma,\delta,1)$ will be abbreviated in $S(\alpha,\beta,\gamma,\delta)$ in the remainder of this text.

$$x \stackrel{d}{=} \begin{cases} \gamma z + \delta & \alpha \neq 1 \\ \gamma z + \left(\delta + \beta \frac{2}{\pi} \gamma \log \gamma \right) & \alpha = 1 \end{cases}$$

Therefore, in this case *X* has the following CF:

$$E \exp(i\omega x) = \begin{cases} \exp\left(-\gamma^{\alpha} |w|^{\alpha} \left[1 - i\beta sign(w) \tan \frac{\pi\alpha}{2} \right] + i\delta w \right) & \alpha \neq 1 \\ \exp\left(-\gamma |w| \left[1 + i\beta \frac{2}{\pi} sign(w) \log(w) \right] + i\delta w \right) & \alpha = 1 \end{cases}, \quad (12)$$

The four parameters which are entries of the stable distribution are defined as follows

- α: index of stability or characteristic exponent defined in (0,2]
- β: skewness defined in [-1,1]
- γ: scale parameter or dispersion defined in $[0, \infty)$
- δ: location parameter define for all $\mathbb{R}$.

It is important to remark few facts related to the stable distribution: parameter γ must not be confused with the standard deviation and parameter δ must be confused with the mean. In addition, since α and β determine the shape of the distribution they can be interpreted as shape parameters.

At this point it is clear that the Gaussian, Cauchy and Lévy distributions can be seen as special cases of the family of stable laws. Thus, the Gaussian distribution can be seen as $\mathcal{S}(2,0,\gamma,\delta)$ with γ properly set with respect to the standard deviation. The Cauchy distribution is $\mathcal{S}(1,0,\gamma,\delta)$ and the Lévy distribution is $\mathcal{S}(1/2,1,\gamma, \delta)$. When γ =1 and δ =0 the stable distribution is said *standardized*. On the other hand, β =0 define the important case of the family of symmetric stable distributions ($\mathcal{S}\alpha\mathcal{S}$). For symmetric stable distribution the CF reduces to

$$\phi(\omega) = \exp\left(-\gamma \|\omega\|^{\alpha}\right) \quad (13)$$

Some general properties of the stable distributions are:

1. All (non-degenerate[7]) stable distributions are continuous distributions with an infinitely differentiable density.
2. **Reflection property**: for any α and β, let the r.v. $Z \sim \mathcal{S}(\alpha,\beta)$ and $Z(\alpha,-\beta) \stackrel{d}{=} -Z(\alpha,\beta)$. Therefore, the density and distribution function of *Z* satisfy $f(x|\alpha,\beta)=f(-x|\alpha,-\beta)$ and $F(x|\alpha,\beta)=1-F(-x|\alpha,-\beta)$.
3. **Scaling property**: Let the r.v. $X \sim \mathcal{S}(\alpha,\beta)$ with $\alpha \neq 1$ and let k_1 be a positive real constant. Then, $k_1X \sim \mathcal{S}(\alpha,\text{sign}(k_1)\beta, |k_1|^{\alpha}\gamma)$

[7] A degenerate distribution is the probability of a r.v. which takes only a single value.

4. **Decomposition property**: if the r.v. $X \sim \mathcal{S}(\alpha,0,\gamma)$ then it can be decomposed as $X = \sqrt{V}Z$, where in this case the r.v. Z is Gaussian $Z \sim \mathcal{N}(0,2\gamma^{2/\alpha})$ and $V \sim \mathcal{S}(\alpha/2,1,\cos(\pi\alpha/2))$.

Stable distributions will assume an important role when modelling the distribution of the aggregate interference power generated by an infinite number of nodes distributed over space according to a PPP. Below are shown some plots for stable distributions and different values of the four defining parameters discussed above.

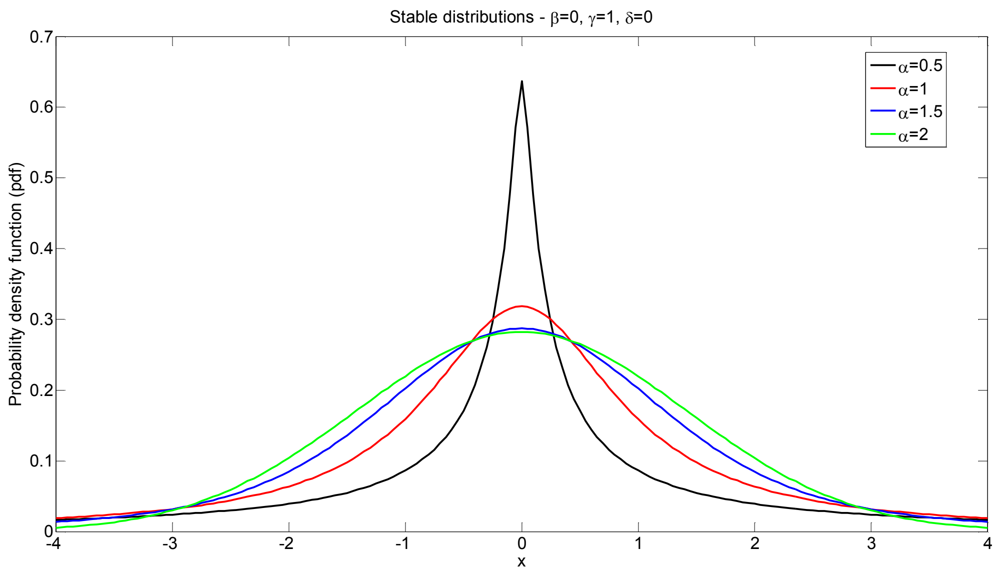

Figure 4-2: Probability density function of a symmetric stable distributed r.v.

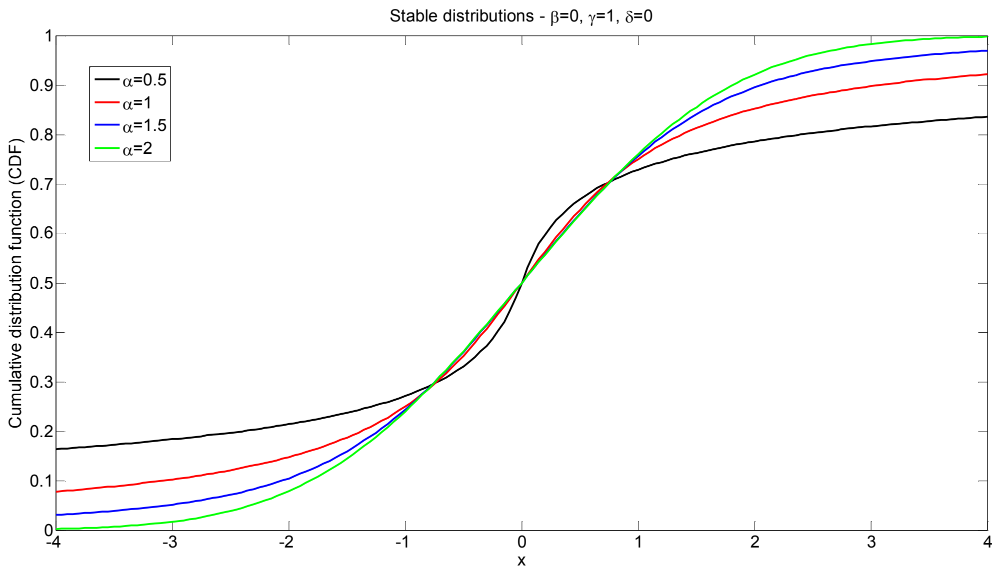

Figure 4-3: Cumulative distribution function of a symmetric stable distributed r.v.

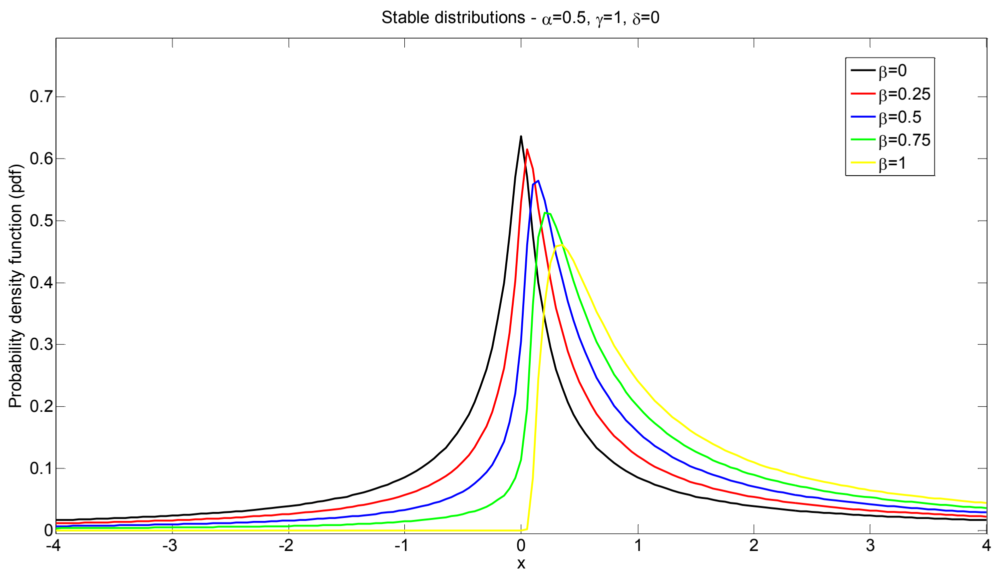

Figure 4-4: Probability density function of a skewed stable distributed r.v.

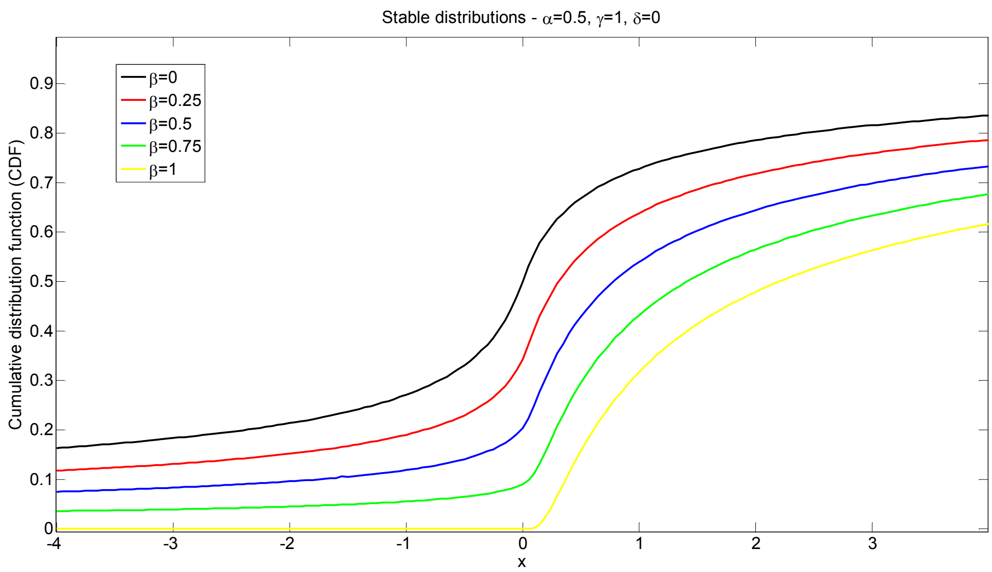

Figure 4-5: Cumulative distribution function of skewed stable distributed r.v.

4.2.1 Useful facts

An important function that will be often used to compute the distribution of the aggregate interference is the Gamma function, which is defined as

$$\Gamma_a(z) = \int_0^\infty t^{z-1} e^{-t} dt, \tag{14}$$

considering that $\Gamma(z) = (z-1)!$ if *z* assumes only integer values. Another function that will be used is the standard Q-function, whose expression is the following

$$Q(x) = \frac{1}{\sqrt{2\pi}} \int_x^\infty e^{-x^2/2} dx. \tag{15}$$

Furthermore, the following two integrals will be used during the following calculations

$$\int_0^\infty \frac{1-\cos(zt)}{t^{\alpha+1}}dt = \frac{\Gamma(1-\alpha)\cos(\pi\alpha/2)}{\alpha}|z|^\alpha, \tag{16}$$

$$\int_0^\infty \frac{1-\phi_0(t)}{t^{\alpha+1}}dt = \frac{\Gamma(1-\alpha)\cos(\pi\alpha/2)}{\alpha}E|Z|^\alpha \tag{17}$$

Where ϕ(*t*) is the CF of the aggregate interference. To solve the last integral it was used the following property of the Gamma function $\Gamma(1-\alpha)=\Gamma(2-\alpha)/(1-\alpha)$.

Channel propagation effects such as fading and shadowing greatly affect the reception of a radio signal and so reduce the throughput of a communication link. For the specific case of Rayleigh fading, the general result prescribes computing the parameters of the stable distribution that models the aggregate interfering process

$$EZ^\alpha = 2^{\alpha/2}\Gamma(1+\alpha/2) \tag{18}$$

For Nakagami-*m* fading instead

$$EZ^\alpha = \frac{\Gamma(m+\alpha/2)}{\Gamma(m)}\left(\frac{\mathrm{K}_m}{m}\right)^{\alpha/2}, \tag{19}$$

Where $\mathrm{K}_m = EZ^2$. Finally for log-normal shadowing with variance σ^2 instead

$$EZ^\alpha = \exp\left\{\frac{1}{2}\alpha^2\sigma^2\right\} \tag{20}$$

As it shall be seen later, the multivariate LePage series representation will provide us with an important tool to characterize the aggregate interference under the assumption of PPP. The definition of a spherically symmetric (SS) r.v. (respectively random vector) is provided in Definition A5 in Section 0.

Definition 1 (LePage series):
Let us consider a real random vector $\boldsymbol{Y}=[Y_1,Y_2, ...,Y_d]$ with Y_i SS α-stable r.vs. Thus, the vector $\boldsymbol{Y}$ is SS α-stable if the joint CF is of the following form

$$\phi(t) = \phi(t_1,...,t_d) = \exp\left(-\gamma\left|\sum_{i=1}^{d} t_i^{\,2}\right|^{\alpha/2}\right). \tag{21}$$

Theorem 1: Let $\{\tau_i\}$ denote the arrivals of a Poisson process and let $\boldsymbol{X}_i$ be SS iid vectors in $\mathbb{R}^d$, independent on τ_i, with $E|\boldsymbol{X}_i|^\alpha<\infty$, then $\boldsymbol{Y}$ can be written as follows

$$\boldsymbol{Y} = \sum_{i=1}^{\infty} \tau_i^{-1/\alpha} \boldsymbol{X}_\mathrm{i}, \tag{22}$$

and it almost surely converge to SS stable random vector with CF as in equation (13).

In order to show the way the interference is modelled, it will also be useful the distribution of the distance of the nodes with respect to their intended receiver. Assuming the nodes uniformly distributed over space and denoting with $r \leq R$ the r.v. of the distance between source and destination, the probability to find a node inside the ring of thickness dr is

$$f_R(r) = \frac{2r}{R^2} dr \ . \tag{23}$$

4.2.2 Probability of detecting the primary transmission without interference

In the remainder, the computation of the distribution of the aggregate interference power is particularly important when typical propagation effects such as fading and shadowing are superimposed on top of the link distance loss. Essentially, three cases will be considered hereafter: Rayleigh fading, Nakagami-*m* fading and shadowing.

It is important to remark that the Rayleigh fading is a special case of Nakagami fading with m=1. Shadowing is instead modelled as lognormal r.v. The analysis starts with the derivation of the probability of detection. This probability is particularly important in CRNs as it quantifies how much secondary transmissions could affect the reception of a primary transmission. It can be said that an event of miss-detection causes harmful interference to the primary service. Referring mainly to the work done in [16], the probability of detecting the primary transmission is defined as

$$P_d = 1 - P_{out} = P\left\{ P_t r^{-2b} \prod_j Z_j \geq P_\vartheta \right\}, \tag{24}$$

where P_out defines the outage probability of the primary link, P_θ is the threshold power, Z_j accounts for the number the propagation effects (i.e., fading and shadowing) and b is amplitude loss coefficient that will be useful later when introducing the interference in the calculation.

It is known that when a transmission is affected by Rayleigh fading only (shadowing is neglected in the first place), the distribution of the received signal power is exponentially distributed. Thus, for a given distance r between a primary receiver and the primary transmitter which transmits with fixed power P_t, the pdf of the received power is $f_X(x) = \frac{r^{2b}}{P_t} \exp\left(-x \frac{r^{2b}}{P_t} \right)$ that yields a mean value P_t / r^{2b}. Therefore, (24) can be explicitly computed for j=1, with Z_1 exponentially distributed, as follows

$$P_{d,Ray}^{(No-Int)} = \exp\left\{ -P_\vartheta \frac{r^{2b}}{P_t} \right\}. \tag{25}$$

When considering Nakagami-*m* with *m*>1 distributed fading, the power of the received signal is a r.v. whose distribution can be modelled as Gamma distributed. Avoiding technicalities, the detection probability is

$$P_{d,Nak}^{(No-Int)} = 1 - \frac{1}{\Gamma(m)} \gamma_{inc}\left(m, \frac{P_\vartheta r^{2b}}{P_t} m \right), \tag{26}$$

where $\gamma_{inc}(z,x) = \int_z^x t^{z-1} e^{-t} dt$ is the lower incomplete gamma function. For integer values of *m* (26) simplifies into

$$P_{d,Nak}^{(No-Int)} = 1 - \frac{(m-1)!}{\Gamma(m)} \left(1 - \sum_{k=0}^{m-1} \frac{\nu_1^{\,k} e^{-\nu_1}}{k!} \right) \tag{27}$$

$$\nu_1 = \frac{P_\vartheta r^{2b}}{P_t}$$

Introducing also the shadowing, the probability of detection is essentially the probability that

$$P_{d,shadowing}^{(No-Int)} = P_G\left\{ e^{2\sigma G_s} \geq \frac{P_\vartheta r^{2b}}{P_t} \right\},$$

where G_s is a Normal random variable. Thus, by means of the standard Q-function shown in (15) , the probability of detection is obtained as

$$P_{d,Shadowing}^{(No-Int)} = Q\left(\frac{1}{2\sigma} \ln\left(\frac{P_\vartheta r^{2b}}{P_t} \right) \right). \tag{28}$$

The last case includes both shadowing and fading. Considering the general case of Nakagami-*m* fading and log-normal shadowing, the probability of detection is obtained by averaging the following probability w.r.t the shadowing

$$P_{d,All}^{(No-Int)} = 1 - \frac{1}{\Gamma(m)} E_{G_s}\left\{ \gamma_{inc}\left(m, \frac{P_\vartheta r^{2b}}{P_t e^{2\sigma G_s}} m \right) \right\}. \tag{29}$$

In [16] it is proposed the approach of developing the exponential term that accounts for the shadowing with the Gauss-Hermite series, which allows computing the expectation above.

4.3 Spatial interference model

The reference scenario explaining how the distribution of the aggregate interference power is calculated in shown in Figure 4-6. The figure shows that nodes are distributed over space according to a point process with respect to the common receiver which is placed at the origin of the reference system. Clearly, despite the number of nodes can be high, what really matters is the number of active transmitters. The transmission of each device can arrive from different distances and encounter different levels of fading and shadowing. Furthermore, nodes could also adopt different transmit powers and/or data rates. These two possibilities, although pertaining to a cognitive radio network, shall not be considered in the remainder of this document.

As it will be shown in the following sections, existing literature showing the way the aggregate interfering process is modelled consists of different approaches. Regardless of that, when the interferers are distributed according to a PPP, the distribution of the aggregate interference power belongs to the family of stable distributions with location parameter δ=0 and with the other parameters that depend on the characteristics of the radio signal, the fading and the shadowing. Namely, these are approaches are based on *i*) the theory of shot noise and elements of stochastic geometry; *ii*) modelling based on the LePage series representation of the aggregate interference and *iii*) an approach relying more on standard probability theory.

As presented in [106], despite the Poisson distribution of nodes allows determining the distribution of the aggregate interference power with tractable maths, how realistic this assumption could be is arguable. In fact, the assumption of an infinite number of interferers might be quite unrealistic with quite a few devices. This document considers then the Binomial point process (BPP), which is however closely related to the PPP. At last, it will be given a glimpse of the generalization of PPP when the density of the nodes is not homogeneous. The removal of this assumption claims for the possibility to model networks wherein nodes are clustered over space. Namely, these processes are referred to in a very general sense as Cox point processes. For the sake of having a self-contained document, a short tutorial introducing the basics of stochastic geometry is provided in Section 0.

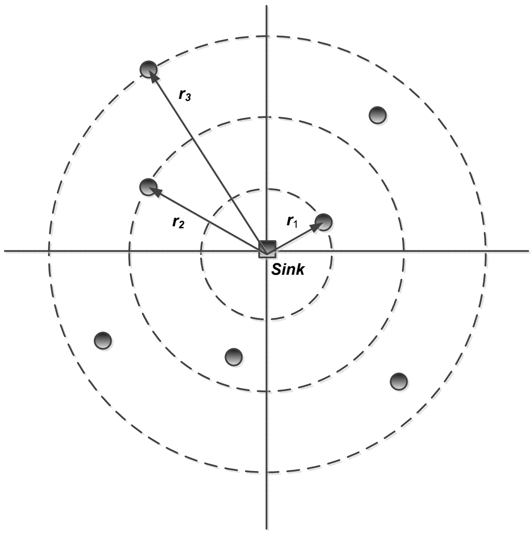

Figure 4-6: Scattering of points (or interferers) on the two-dimensional plane.

4.3.1 Aggregate interference based on Poisson distribution

Before showing the main result used here in case of PPP, it is necessary to give few more notions of point processes in general. Referring to Definition A6 in Section 0, for a PP *X*, let *N*(*B*) denote the number of point in the set *B*, $N(B)=n(x_B)$. Upon these hypothesis, *X* is a point process *iff* *N*(*B*) is a r.v.

Definition 2: The intensity measure of a PP is a function $\Lambda(B)=EN(B)$. If it there exists a Lebesgue-measurable function λ so that $\Lambda(B)=\int_B \lambda(\xi)d\xi$. Such a function is called the intensity function.

An immediate consequence of the above result is that a PP *X* is homogeneous *iff* the intensity function *λ* is a constant.

Definition 3: A PPP *X* with locally finite measure Λ the following properties:

1. For a compact set *W* and $B \subseteq W$, *N*(*B*) is Poisson distributed with parameter $\Lambda(B) < \infty$
2. For $\forall n \in \mathbb{N}$ and pairwise disjoint sets $B_1,\ldots,B_n$ it holds that $N(B_1),\ldots,N(B_n)$ are independent with $\Lambda(B_i) < \infty$.

Definition 4 (Laplace functional): Let *f* be a non-negative measurable function of bounded support and Λ the measure of the point process. The Laplace functional of Λ is

$$L_\Lambda(f) = E\exp\left\{-\int_{R^d} f(x)\Lambda(dx)\right\}. \quad (30)$$

Definition 5 (moment measures): For a point process *X* defined over the Borel set $B \subseteq \mathcal{B}^d$, the *j*th order moment measure is

$$M^{(j)}(B) = E\sum_{\xi_1,\ldots\xi_1 \in X} \mathbf{1}_{[(\xi 1,\ldots\, \xi n)\ \text{in}\ B]}, \quad (31)$$

whereas the *j*th order factorial moment measure is calculated as

$$V^{(j)}(B) = E\sum_{\xi_1,\ldots\xi_1 \in X}^{\neq} \mathbf{1}_{[(\xi 1,\ldots\, \xi n)\ \text{in}\ B]}, \quad (32)$$

where the last sum denotes that it is made over the *j*-tuple of mutually distinct points ξ_i. It can be noticed that the first order moment measure and the first moment factorial measure coincides with the intensity function of the point process.

Theorem 2: For any compact set *W* and Borel set $B \subset W$, a point process *X* on *W* is completely defined by the set of void probabilities[8], which are the probabilities that

$$P\{N(B)=0\} = \frac{(\nu_d(W) - \nu_d(B))^n}{\nu_d(W)^n}$$

Proof:

In order to prove the theorem it is necessary to show that

$$\begin{aligned} &P\{X(B)=0 \mid X(W)=n\} = P\{X(B)=0, X(W)=n\} / P\{X(W)=n\} = \\ &= P\{X(B)=0\}P\{X(W \setminus B)=n\} / P\{X(W)=n\} \end{aligned}. \quad (33)$$

The last equality equals the thesis stated in the proposition, and thus completing the proof.

Theorem 3 For any compact set *W* and Borel set $B \subset W$, the void probabilities of a PPP are defined *iff* it exists an intensity measure $\Lambda(B)$.

[8] This result that can be demonstrated easily for PPP and BPP is however generally valid.

Proof:
Assuming that $\exists\Lambda(B)<\infty$, it suffices to apply the result of Theorem 2 with the void probabilities of the PPP as $\exp\{-\Lambda(B)\}$. Referring also to Definition A4 in Section 0, assuming the point process is Poisson, let now $\{B_i\}$ be a set of bounded pairwise disjoint sets representing the interior of $\mathbb{R}^d$. Consider the r.v. N_i of set B_i, so that N_i is Poisson distributed with intensity measure $\Lambda(B)$. Upon condition on $N_i = n$, the point process is Binomial. If the BPP that can be constructed on the sets B_i that are independent in *i,* the void probability can be written as

$$P\{n(X)=0\}=\prod_i P\left(n\left(X_{B_i}\right)=0\right)=\prod_i\sum_{n=0}^{\infty}P\left(n\left(X_{B_i}\right)=0\mid N_i=n\right)P\left(N_i=n\right)$$

Using the Poisson assumption on N_i, it can be written that

$$\prod_i\sum_{n=0}^{\infty}\left(1-\frac{\Lambda\left(B\cap B_i\right)}{\Lambda\left(B_i\right)}\right)^n e^{-\Lambda(B_i)}\frac{\Lambda\left(B_i\right)^n}{n!}=$$

$$=\prod_i e^{-\Lambda(B_i)}e^{\Lambda(B_i)-\Lambda(B\cap B_i)}=\prod_i e^{-\Lambda(B\cap B_i)}=e^{-\sum_i\Lambda(B\cap B_i)}=e^{-\Lambda(B)},$$

and this concludes the proof.

Corollary 1: let *X* be a PPP with intensity measure Λ defined on the compact set *W*. For any Borel set $B\subset W$ with $\Lambda(B)<\infty$, conditionally on *N*(*B*)=*n*, X_B is BPP with *n* points on *B* and measure Λ restricted to B.
Proof:
Using the last equality in (33) and being the void probability of a PPP is $\exp\{-\Lambda(B)\}$, equation (33) can be explicitly written as

$$\frac{e^{-\Lambda(W)}\dfrac{\Lambda(W\setminus B)^n}{n!}e^{-\Lambda(W\setminus B)}}{\dfrac{\Lambda(B)^n}{n!}e^{-\Lambda(B)}}=\left(\frac{\Lambda\left(W\setminus B\right)}{\Lambda\left(B\right)}\right)^n$$

Corollary 1 proves Theorem 2 for the specific case of a PPP and BPPP.

Proposition 1: A Homogeneous PPP is stationary and isotropic.
Proof:
Referring also to Section 0 let us consider two homogeneous PPPs *X* and *X*+*s* with the same constant intensity function *λ* for any $s\in\mathbb{R}^d$. Similarly to what done above, upon conditioning on the number of points of the point processes, the void probabilities of the two PPPs can be written as $\exp\{-\lambda(B)\}$ and $\exp\{-\lambda(B-s)\}$. It can be now noticed that the Lebesgue measures of the two PPPs coincide, thus proving the proposition.

Theorem 4: Referring to Definition 4, the Laplace functional for a PPP with measure Λ

$$L_\Lambda(f)=\exp\left\{-\int_{R^d}\left(1-e^{-f(x)}\right)\Lambda\left(dx\right)\right\}. \tag{34}$$

Theorem 5 (Campbell's theorem): Let us now consider a point process *X* with measure *Λ* a non-negative measurable function *f* and a distribution *F* it holds that

$$E\left(\sum_{x\in X} f(x)\right) = \int \sum_{x\in X} f(x)F(d\varphi) = \int_X \int_{R^d} f(x)\Lambda(dx)F(d\varphi) = \int f(x)\Lambda(dx)\,. \quad (35)$$

In case of a stationary process the above equations simplifies to

$$E\left(\sum_{x\in\Psi} f(x)\right) = \lambda \int f(x)dx\,. \quad (36)$$

4.3.1.1 Modelling the distribution of the aggregate interference amplitude

The derivation of the distribution of the aggregate interference power when the nodes are distributed over space according to a PPP starts with the work developed in [37] and [98]. It is important to remark that it will be first developed the distribution of the amplitude of the aggregate interference. In this case, parameter *b* shall denote the amplitude loss coefficient, whereas the power loss coefficient is 2*b*.

The reference scenario is shown in Figure 4-6 and the starting point for modelling the interference is (1). However, (1) can be rewritten in a more suitable way as follows

$$I = \sum_{i=1}^{\infty} a(r_i) \prod_j Z_{i,j} = \sum_{i=1}^{\infty} a(r_i) Z_i\,, \quad (37)$$

where, given *i*, Z_j=1 for *j*=0 whereas it accounts for fading and shadowing when *j*>0, as anticipated in Section 4.2.2. The term *a*(*r*) models instead the distance of the link of the *i*th interferer

$$a(r_i) = \frac{K_i}{r_i^b}\,, \quad (38)$$

where K_i depends on the transmitted power and other characteristics of the radio technology used. It is now necessary to observe that (38) goes to zero for $r->\infty$ but to infinity as soon as *r*->0: $a(r)->\infty$. In this last case (38) does not hold unless the link loss is defined as $a(r) = \min(r^{-b}, s)\forall s > 0$. For *j*=0, conditioning on *n* interfering devices deployed over a surface of area *A* and radius *R*, the aggregate interference becomes $I = \sum_i a(r_i)$, where the number of nodes *n* is a Poisson distributed r.v. of intensity *λ*.

$$P\{k\ nodes\ in\ \mathrm{A}\} = \frac{(\lambda\|A\|)^k}{k!} e^{-\lambda\|A\|}\,. \quad (39)$$

Theorem 6 (Probability theory approach) [37] [98]: The distribution of the aggregate interference amplitude generated by a Poisson field of interferers distributed over a surface of area $\|A\| = \pi R^2$ in the Euclidean space *d*=2, with the aggregate interference modelled as in (37) and measured at the unique receiver located at the origin of a reference system, it exhibits a CF equal to

$$\phi_I(\omega) = \exp\left\{-\gamma\|\omega\|^{\alpha}\right\}, \quad (40)$$

with $\gamma = -\lambda C_d K^{\alpha} \int_0^{\infty} x^{-\alpha} \phi_0(x) dx$, C_d defined in equation (75) and Φ_0 the CF of a SS r.v. corresponding to a single interferer. As already mentioned in (13) this is the CF of $S\alpha S$ random variable.

Proof:

In order to prove the theorem, the first stage is to consider a finite number *k* of interferers with the *i*th placed at distance r_i from the receiver. Therefore, the CF of the aggregate interference with *k* interfering active links having distance r_i is

$$\phi_{I_k}(\omega \mid r) = E e^{j\omega I_k} = \prod_{i=1}^{k} e^{j\omega I_i} \ . \tag{41}$$

The unconditional CF is obtained taking a double expectation over both distance and number of active links.

$$\phi_I(\omega) = E_r \left\{ E_k \phi_{I_k}(\omega \mid k, r) \right\}.$$

Using Fubini's theorem these two expectations can be exchanged. Assuming that $r_i=r$, $K_i=K$ $\forall$ *i* the CF of the interferences becomes

$$\phi_I(\omega) = \sum_{k=0}^{\infty} \frac{\left(\lambda \|A\|\right)^k}{k!} e^{-\lambda \|A\|} \left(E_r \phi_{I_k}(\omega \mid k, n) \right), \tag{42}$$

where using (23) it is obtained that

$$E_r \phi_{I_k}(\omega \mid r, k) = \left(\int_0^R \frac{2r}{R^2} e^{j\omega Z a(r)} dr \right)^k = \left(\int_0^R \frac{2r}{R^2} \phi_0(a(r)\omega) dr \right)^k .$$

Computing now the sum in (42) the following expression is obtained

$$\phi_I(\omega) = \exp\left[\lambda C_d R^2 \left(\int_0^R \frac{2r}{R^2} \phi_0(a(r)\omega) dr - 1 \right) \right], \tag{43}$$

where Φ_0 is the CF accounting for the terms K_i and Z_i in (37) that are the projection (at the receiver) of a random vectors ***K*** and ***Z*** into multidimensional vectors (i.e., basis of the vector space). Integrating by parts (43) and noticing that $a(r) -> 0$ as $r -> \infty$ (or equivalently $\phi_0(a(r)\omega) -> 1$) (42) becomes

$$\phi_I(\omega) = \exp\left[\lambda C_d \left(\int_0^{\infty} r^2 \frac{d\phi_0(a(r)\omega)}{dr} dr \right) \right]. \tag{44}$$

Making now the change of variable *t*=*a*(*r*), (47) can be rewritten as follows

$$\phi_I(\omega) = \exp\left[\lambda C_d K^{\alpha} \left(\int_0^{\infty} t^{-\alpha} \frac{d\phi_0(t\omega)}{dt} dt \right) \right], \tag{45}$$

where *α*=-2/*b*.

The analysis continues relying on Definition A5 in Section 0, which allows restricting to the case in which ***Z***[9] is an SS vector. After making the last change of variable as $x=\omega t$ it is obtained that

$$\phi_I(\omega) = \exp\left[-\lambda\|\omega\|^{\alpha} C_d K^{\alpha}\left(\int_0^{\infty} x^{-\alpha}\phi_0'(x)dx\right)\right]. \quad (46)$$

After reorganizing the terms in the equation above, it can be seen that this corresponds to (40) with the aggregate interference $I \sim S\left(\alpha, \gamma = -\lambda C_d K^{\alpha}\int_0^{\infty} x^{-\alpha}\phi_0(x)dx,\ \beta = 0, \delta = 0\right)$.

Corollary 2: Complying with the result in Theorem 6 the following facts hold

- for b=2 => α=1, (40) reduces to Cauchy distribution (that is (8) for d=1)
- for b=4 => α=1/2 , (40) reduces to the Leví distribution (that is (9) for d=1).

Theorem 7 (LePage series approach) [38][108]: Using the definition of the aggregate interference given in (37) and writing the amplitude of the interference as in (38), relying also on Definition 1 and Theorem 1 (LePage series representation), the CF of the interference amplitude has the form shown in equation (40).

Theorem 8 (Stochastic geometry approach) [16][104]: Using the definition of the aggregate interference given in (37) and relying also on Theorem 6 and Theorem 7, the distribution of the aggregate interference amplitude is $S\alpha S$ with parameters

$$\begin{aligned}
&\alpha = 2/b \\
&\beta = 0 \\
&\gamma = -\lambda\pi C^{-1}{}_{2/b} E|Z_i|^{2/b}, \\
&\delta = 0 \\
&C_\alpha = \begin{cases} \dfrac{1-\alpha}{\Gamma(2-\alpha)\cos(\pi\alpha/2)} & \alpha \neq 1 \\ \dfrac{2}{\pi} & \alpha = 1 \end{cases}
\end{aligned} \quad (47)$$

Proof:

The proof relies on the definition of Laplace functional (see Definition 4) for the specific case of a PPP given in Theorem 4, it relies also on the result provided by the Campbell's theorem (see Theorem 5), equation (37) for the definition of the overall interference (in case of j>0) and the amplitude of the ith interferers as in (38). Furthermore, unit transmit power is assumed and the set of distances of the active interferers $r_i \in \mathrm{I}_a$ are inside a ball of unit

[9] It is supposed here that the terms K_i incorporate all the characteristics of the radio signal, which are fixed for all the interfering devices. Therefore, the analysis focuses mainly on the terms Z_i.

radius (see Section 0 for the formal definition). Therefore, the CF of the aggregate interference can be written as

$$\phi_I(\omega) = \exp\left[-\lambda 2\pi \int_{I_a} \left[1-\phi_0\left(a(r)\omega\right)\right] r dr\right] = \exp\left[-\lambda 2\pi \int\int_{Z} \left[1-e^{r^{-b} i\omega Z}\right] r dr f_Z(z) dz\right], \quad (48)$$

Where $Z = \left\{Z : \left|Z^2\right| < P_g r_g^{-b}\right\}$. It is worth noting that expression in (48) is equivalent to (46) as it is evident after some manipulations. In order to prove the theorem it is used the hypothesis that *Z* is spherically symmetric so as to obtain that

$$\phi_0(\omega) = Ee^{i\omega Z} = E\cos(\omega Z) + iE\sin(\omega Z) = E\cos(\omega Z),$$

where the expectation of the sin(ωZ) is zero as a consequence of the hypothesis that vector *Z* is SS. Integrating by parts it is obtained the following intermediate result

$$\int_0^\infty \frac{1-\cos(tZ)}{t^{1+\alpha}} d\omega = \frac{1}{\alpha}\int_0^\infty \frac{\phi_0{}'(t)}{t^\alpha} dt.$$

The way of solving the above integral was shown in (16) which provide the way of computing explicitly the integral in (48) (or equivalently in (46)).

$$\int_0^\infty \frac{\phi_0{}'(t)}{t^\alpha} dt = \Gamma(1-\alpha)\cos(\pi\alpha/2) E|Z|^\alpha = E|Z|^\alpha \frac{\Gamma(2-\alpha)}{1-\alpha}\cos\pi\frac{\alpha}{2}, \quad (49)$$

where the integral was computed taking into account the definition of the Gamma function given in (14) and that $\Gamma(1-\alpha) = \int_0^\infty t^{-\alpha} e^{-t} dt$. The result shown in equation (49) completes the proof of the theorem.

Corollary 3 (Parameters of the Stable distribution) [108]:
Under the hypotheses of previous theorems, parameter γ of the symmetric stable distribution can be expresses as

$$\gamma = -\lambda K^\alpha C_d C_\alpha^{-1} E|Z|^\alpha .$$

Using (18), (19) and (20) respectively in case of Rayleigh fading, Nakagami-*m* fading and lognormal shadowing the expectation in the expression above can be rewritten as

$$E|Z|^{\alpha} = \begin{cases} \left(\frac{4}{\pi}\right)^{\alpha/2} \Gamma\left(1+\frac{\alpha}{2}\right) & Rayleigh \\ \frac{\Gamma(m+\alpha/2)}{\Gamma(m)}\left(\frac{K_m}{m}\frac{2}{\pi}\right)^{\alpha/2} & Nakagami-m \\ \exp\left(\frac{1}{2}\alpha^2\sigma^2\right) & Lognormal \\ \exp\left(\frac{1}{2}\alpha^2\sigma^2\right)\left(\frac{4}{\pi}\right)^{\alpha/2}\Gamma\left(1+\frac{\alpha}{2}\right) & Lognormal\ and\ \text{Rayleigh fading} \end{cases}, \quad (50)$$

4.3.1.2 Modelling the distribution of the aggregate interference power

Based on the theory reviewed in previous sections, it is now possible characterize the distribution of the aggregate interference power.

Theorem 9 (Probability theory approach) [98]: Complying with the hypothesis and the result of Theorem 6, it can be shown that the CF of the aggregate interference power is

$$\phi_I(\omega) = \exp\left[-\lambda\pi\Gamma(1-\alpha)e^{-\pi\alpha/2}\|\omega\|^{\alpha}\right], \quad (51)$$

Proof:

Referring to (37) the aggregate interference power is derived for *j*=0. After simple mathematical manipulations similar to those done in Theorem 6, equation (46) reduces to

$$\phi_I(\omega) = \exp\left[-\lambda\|\omega\|^{\alpha} C_d\left(\int_0^{\infty} x^{-\alpha}e^{i\omega x}dx\right)\right].$$

The proof is completed replacing the value of C_d for *d*=2 and using the Gamma function in (14).

Theorem 10 (Stochastic geometry approach) [16]: Following the hypotheses and results shown in Theorem 8, the aggregate interference power is stable distributed with the stable distribution having the following parameters

$$\begin{aligned} \alpha &= 1/b \\ \beta &= 1 \\ \gamma &= -\lambda\pi C^{-1}{}_{1/b}K^{1/b}E|Z|^{1/b}, \\ \delta &= 0 \end{aligned} \quad (52)$$

where C_{α} was defined in (47).

Proof:
This theorem can be proved in a similar fashion to Theorem 8 but removing the hypothesis that vector *Z* is spherically symmetric. Therefore the CF of the aggregate interference power is rewritten first as follows

$$\phi_I(\omega) = \exp\left[-\lambda C_d \int_0^{\infty} [1 - \phi_0(a(r)\omega)] r dr \right].$$

Similarly to Theorem 6, after changing variable it is obtained that

$$\phi_I(\omega) = \exp\left[-\lambda C_d K^{\alpha} |\omega|^{\alpha} \frac{1}{\alpha} \int_0^{\infty} \frac{1 - e^{isign(\omega)Zt}}{t^{1+\alpha}} dt \right].$$

The proof continuous using the following result that was already shown in (17)

$$\int_0^{\infty} \frac{1 - \phi_0(Zt)}{t^{\alpha+1}} dt = \frac{\Gamma(1-\alpha)}{\alpha} |Z_i|^{\alpha} [\cos(\pi\alpha/2) - isign(z)\sin(\pi\alpha/2)]. \quad (53)$$

Taking now the expectation w.r.t. Z_i (where the subscript can be dropped since it is assumed that each interferer is subject to independent and identically distributed propagation effects) on both sides of (53), the equation reduces to

$$\int_0^{\infty} \frac{1 - E\{e^{isign(\omega)Zt}\}}{t^{\alpha+1}} dt = \frac{\Gamma(1-\alpha)}{\alpha} E|Z|^{\alpha} [\cos(\pi\alpha/2) - isign(\omega)\sin(\pi\alpha/2)]. \quad (54)$$

After few more manipulations, the theorem is proved.

Theorem 11 (Shot noise approach) [104]: Modelling the aggregate interfering process as in (1), using the definition of Laplace functional (see Definition 4) in Theorem 4 for the specific case of a PPP, the probability of a success for a reference transmission, with the interference occurring within a *d*-dimensional ball *b*(0,*R*) centred in correspondence of the unique sink is

$$p_s = \exp\left(-\lambda q C_d R^d E\left(|h|^2\right)^{\alpha} \Gamma(1-\upsilon) P_{\vartheta}^{\ \alpha} \right), \quad (55)$$

where *q* is the probability a node is active, P_{ϑ} is the threshold for detection and $\alpha = d/\upsilon$, $\upsilon = 2b$ is the power loss coefficient and $|h|^2$ is the channel fading coefficient in terms of power.

Proof:
The proof of the theorem is carried out for the specific but very important case of Rayleigh fading. In general, the success probability can be written as follows

$$p_s = P\left\{|h|^2 S > P_{\vartheta}(I + N_W)\right\},$$

where $S = R^{-\nu} P_t$. In the specific case of Rayleigh fading it becomes that

$$p_s = \exp\left(-P_9 \frac{R^{\upsilon}}{P_t} N_W\right) \underbrace{E \exp\left(-P_9 R^{\alpha} I\right)}_{\text{Laplace functional}}. \quad (56)$$

It is worth noting that the hypothesis of Rayleigh fading allows decomposing the problem in two terms: the noise component and the interference component. The interference term in (56) is in practise the Laplace functional computed in $s = P_9 R^{\alpha}$.

The proof of this theorem relies on the Laplace functional of a PPP, which can be computed directly using the Campbell's theorem (see Theorem 5) as follows

$$L_I(s) = \exp\left\{-\lambda C_d \int_0^{\infty} dr^{d-1} E_h\left[1 - e^{-s|h|^2 r^{-\upsilon}}\right] dr\right\}. \quad (57)$$

It is in fact well-known that if the fading of the signal's amplitude is Rayleigh, the power of the signal follows an exponential distribution. Integrating by parts (57), it can be obtained that

$$L_I(s) = \exp\left\{\lambda C_d E_h\left[\int_0^{\infty} r^d s|h|^2 \upsilon r^{-\upsilon-1} e^{-s|h|^2 r^{-\upsilon}} dr\right]\right\}.$$

Furthermore, making the change of variable $s|h|^2 r^{-\upsilon} = t$, $dt = -\upsilon r^{-\upsilon-1} s|h|^2 dr$, the Laplace functional can be rewritten as

$$L_I(s) = \exp\left\{-\lambda C_d s^{d/\upsilon} E_h\left[\int_0^{\infty} \left(|h|^2\right)^{d/\upsilon} t^{-d/\upsilon} e^{-t} dt\right]\right\}.$$

It can be now recalled the definition of the Gamma function shown in (14), and writing $\alpha = d/\upsilon$ and that $\Gamma(1-\alpha) = \int_0^{\infty} t^{-\alpha} e^{-t} dt$, the Laplace functional can be written as

$$L_I(s) = \exp\left\{-\lambda C_d s^{\alpha} E\left(|h|^2\right)^{\alpha} \Gamma(1-\alpha)\right\}.$$

Using a slightly modified version of equation (18) for the moments of the Rayleigh distributed fading, the Laplace functional is finally written as follows

$$L_I(s) = \exp\left\{-\lambda C_d s^{\alpha} \Gamma(1+\alpha)\Gamma(1-\alpha)\right\} = \exp\left(-\lambda C_d s^{\alpha} \frac{\pi\alpha}{\sin(\pi\alpha)}\right),$$

where the last expression is obtained using the Euler's reflection formula. This expression allows making the following observation:

1) for $\alpha \geq 1$ ($v \leq d$): the overall interference if asymptotically infinite as an infinite number of interferers (infinite network) give a non-zero power contribution. For a finite network the interference would be instead finite.

2) for α<1 (ν>d): the interference is finite but the moments of the interference (e.g., the first moment representing the average interference power) are not finite due to the discontinuity of the path-loss at the sink (origin of the reference system).

It is finally worth noting that the proof is concluded assuming $s = P_g R^{\alpha}$ and N_W=0 in (56).

Proposition 3 (*n*th nearest neighbour) [109] [110]:
In a random network where nodes are distributed over a *d*-dimensional Euclidean space according to an homogeneous PPP of constant intensity λ, the pdf of the distance between the unique traffic sink (located at the centre of the reference system) and its *n*th neighbour (or transmitter) follows an Erlang distribution

$$f_{R_n}(r) = r^{2n-1}(\lambda C_d)^n \frac{d}{(n-1)!} \exp\left(-\lambda C_d r^d\right). \quad (58)$$

Remarks
Before concluding this part, it can be noted that the theorems shown above allow modelling the distribution of the aggregate interference amplitude by means of different approaches developed throughout time. The most important fact is that all these approaches lead to the same conclusion that the interference distribution belongs to the family of the stable distributions when the nodes are displaced according to a homogeneous Poisson point process.

4.3.2 Aggregate interference based on Binomial point processes

The use of stochastic geometric tools for the study of random network graphs has gained increasing popularity and current research trend is also to consider point processes other than Poisson. One attempt in this direction is found in [105], where BPPs are considered. The reason for using BPPs rather than PPPs is that it is sometimes important to model the performance of a (wireless) network as a function of the number of users. Regard to this aspect, the theory of PPPs assumes an infinite number of nodes and they work mainly on spatial densities. It can noticed anyway that using a BPP yields more accurate results when deriving the effect of the aggregate interference generated by a small number of interferers (e.g., below 10 interfering devices) but the two models almost overlap when the number of interferers is greater than or equal to 15 [105]. The remainder of this section is devoted to show some results related to BPPs. Proofs are in this case only sketched or omitted as the procedure is very similar to what shown already for Poisson point processes. However, the interested reader is reminded to the specific articles available from the list of references provided for a more in-depth discussion.

The foundation of the theory of BPP can be found in Proposition A1 placed in Section 0 and in Section 4.3.1. Considering the case of exactly *N* transmitting nodes displaced independently and uniformly inside a *d*-dimensional ball $b_d(0,R)$, the density of the nodes can be written as $\lambda = N / C_d R^d$.

Theorem 12 (Interference distribution for a BPP network) [105]: Consider a random network with exactly *N* transmitting nodes and $\lambda = N / C_d R^d$. In general, the moment generating function (or the Laplace functional) of the BPP can be stated as follows

$$M_I(s) = \left(1 - \frac{\lambda}{N}\int_{R_1}^{R_2} E_h\left[\left(1 - \exp\left(-sgr^{-\upsilon}\right)\right)dC_d r^{d-1}\right]dr\right)^N, \tag{59}$$

where $R_1<R_2<R$, $g=|h|^2$ is the channel power gain coefficient and v is the power loss exponent .

Proof:
The complete proof can be found in [105] but the starting point consists of writing the probability distribution of k nodes within the annulus of inner radius R_1 and outer radius R_2

$$P_N(k) = \binom{N}{k}\left(\frac{R_1{}^d - R_2{}^d}{R^d}\right)^k\left(1 - \frac{R_1{}^d - R_2{}^d}{R^d}\right)^{N-k}. \tag{60}$$

As mentioned, the full proof of the theorem is omitted but it is worth noting that it continues similarly to what shown already for PPPs.

The theory of BPP developed herein gives the opportunity to introduce the concept of cumulants that was anticipated in Section 2 (for an in-depth discussion on this aspect the reader can refer to [47][54] although the analysis is developed there for Poisson point processes). The nth cumulant is defined as the derivative of the logarithm of the moment generating function as follows

$$\kappa_n = (-1)^n \frac{\partial^n}{\partial s^n}\ln\left(M_I(s=0)\right). \tag{61}$$

As it is shown in [105], this way of approaching the problem allows finding closed and simple form expressions for the moments of a r.v.

Remark
It can also be noted that equation (59) yields the expressions derived in previous sections for PPPs when R_1=0, R_2->∞ and N->∞.

Proposition 4 (*n*th nearest neighbour) [105] [111]: Consider a random network with exactly N nodes independently and uniformly distributed in a d-dimensional ball $b_d(0,R)$. Let $\lambda = N / C_d R^d$ and $r \in [0, R]$, the pdf of the nth nearest neighbour w.r.t. the sink location ca be written as follows

$$f_{R_n}(r) = \frac{d}{R}\frac{B(n-1/d+1, N-n+1)}{B(N-n+1, n)}\beta\left(\left(\frac{r}{R}\right)^d; n-1/d+1, N-n+1\right), \tag{62}$$

where $\beta(x; R_1, R_2)$ is the beta density function defined as

$$\beta(x;y_1,y_2) = \left(1/B(y_1,y_2)\right)x^{y_1-1}(1-x)^{y_2-1}.$$

The CCDF of the *n*th nearest neighbour has instead the following expression

$$\overline{F_{R_n}}(r) = \sum_{j=0}^{n-1} p^j (1-p)^{N-j} = I_{1-p}(N-n+1,n), \tag{63}$$

Where *p* is the probability of a random point defined in Proposition A1 in Section 0.

$$I_x(y_1,y_2) = \frac{\int_0^x t^{y_1-1}(1-t)^{y_2-1}dt}{B(y_1,y_2)}.$$

Finally, the *i*th moment of the *n*th distant neighbour is expressed as

$$ER_n{}^i = \begin{cases} \dfrac{R^i\Gamma(1+N)\Gamma(i/d+n)}{\Gamma(n)\Gamma(i/d+N+1)} & n+i/d>0 \\ \infty & otherwise \end{cases}, \tag{64}$$

where $\Gamma(y+n)/\Gamma(y)$ denotes the rising Pochhammer symbol. In particular, closed form expressions of the *n*th distant neighbour are particularly appealing when computing for example the average signal-to-interference-plus-noise-ratio (SINR) in a wireless network.

4.3.3 Probability of detecting the primary transmission with interference

Similarly to what showed in Section 4.2.2, the derivation of the distribution of the aggregate interference is helpful for determining the probability of detecting the transmission of a PU from the point of view of a CR network. All the derivations shown hereafter are based on the assumption that nodes are distributed over space according to a homogeneous PPP with intensity λ. Therefore, the distribution of the aggregate interference power follows a stable distribution with parameters given in equation (52). The results shown in this section are mainly based on the work done in [16]. Differently from Section 4.2.2 the probability of detecting the primary user's transmission relies on the SINR=$P_{ru}/(I+N_W)$. The model developed in [16] considers the power received from the transmission of the PU (e.g., the PU transmits a beacon to signal its presence) at the location of a reference secondary device. The interference is modelled as in equation (37), with the received power of the PU transmission computed as follows

$$P_{ru} = \frac{P_t}{r^{2b}} \prod_j Z_j . \tag{65}$$

The condition upon which secondary devices are able to detect the PU transmission is

$$P_d = 1 - P_{out} = P\{SINR \geq P_\vartheta\}. \tag{66}$$

Based on equation (66), the detection probability can be computed by means of two alternative ways

$$P\{SINR \geq P_\vartheta\} = \begin{cases} E_I\left\{P_{\{Z_j\}}\left\{\prod_j Z_j \geq \frac{r^{2b}}{P_t} P_\vartheta(I+N_W) \mid I\right\}\right\} \\ E_{\{Z_j\}}\left\{F_I\left(\frac{P_t \prod_j Z_j}{r^{2b} P_\vartheta} - N_W\right)\right\} \end{cases}. \tag{67}$$

The two ways of computing the probability of detection can be used interchangeably based on computational convenience. The remainder of this section is dedicated to write the expressions for the probability of detection in the some specific cases of Section 4.2.2.

When only the effect of the path-loss is considered, the probability of detecting the PU's transmission is expressed as follows

$$P_{d,path-loss} = F_I\left(\frac{P_t}{r_0^{2b} P_\vartheta} - N_W\right), \tag{68}$$

where r_0 stands for the distance between the primary transmitter and the reference secondary receiver.

In case the effects of path-loss and Nakagami-*m* fading are considered, the probability of detection becomes

$$P_{d,Nak} = 1 - \frac{1}{\Gamma(m)} E_I\left\{\gamma_{inc}\left(m, \frac{r_0^{2b} P_\vartheta(I+N_W)m}{P_t}\right)\right\}, \tag{69}$$

where γ_{inc} is the lower incomplete Gamma function already introduced already in Section 4.2.2. In case of Rayleigh fading (*m*=1) equation (69) reduces to

$$P_{d,Ray} = \exp\left(-\frac{r_0^{2b} N_W}{P_t} P_\vartheta\right) \exp\left[\left(-\frac{\pi\lambda C_{1/b}^{-1}\Gamma(1+1/b)}{\cos(\pi/2b)}\right)\left(\frac{K r_0^{2b}}{P_t} P_\vartheta\right)^{1/b}\right]. \tag{70}$$

As mentioned already, the model is sophisticated enough to account also for shadowing. As such, the probability of detecting the PU's transmission with path-loss and lognormal distributed shadowing is the following

$$P_{d,Shadowing} = E_I\left\{Q\left(\frac{1}{2\sigma}\ln\left(\frac{r_0^{2b}(I+N_W)}{P_t} P_\vartheta\right)\right)\right\}, \tag{71}$$

Where Q() denotes the Gaussian Q function recalled in equation (15).

The last case reviewed here takes into account path-loss, Nakagami-*m* fading and lognormal shadowing. Thus, the probability of detection can be written as follows

$$P_{d,All} = 1 - \frac{1}{\Gamma(m)} E_{Z_0,I}\left\{\gamma_{inc}\left(m, \frac{r_0^{2b}(I + N_W)m}{P_t e^{2\sigma Z_0}} P_\vartheta\right)\right\}. \quad (72)$$

In the particular case of Rayleigh fading (*m*=1), equation (72) can be rewritten as follows

$$P_{d,All} = E_{Z_0}\left\{\exp\left(-\frac{r_0^{2b} N_w}{P_t e^{2\sigma Z_0}} P_\vartheta\right)\left(-\frac{\pi\lambda C_{1/b}^{-1} e^{2\sigma^2/b^2}\Gamma(1+1/b)}{\cos(\pi/2b)}\right)\left(\frac{K r_0^{2b}}{P_t e^{2\sigma Z_0}} P_\vartheta\right)^{1/b}\right\}. \quad (73)$$

Before concluding this section, it is important to observe that the results shown here differ from the work done in [16] as they do not include the duty-cycle of the interfering nodes. The main motivation to do this is that such a simple term is unsuitable to catch the real complexity of the protocols sitting on top of the physical layer. In fact, this additional degree of freedom would require a deeper modelling of the network protocols, which is out of scope of the current deliverable.

4.4 Cluster-based models

In previous sections it was given a concise but exhaustive description of the most advanced analytical tools that are used nowadays for modelling the distribution of the aggregate interference power in wireless networks. The two main setups considered above are PPP and BPP. It was pointed out that for a sufficiently large number of nodes, the interference distribution obtained with the BPP overlaps with that of the PPP. Despite the wide use of the Poisson assumption for the nodes distribution, it is now useful raise the question of whether this assumption is realistic in a real network. Many authors have in fact argued that often natural and man-made processes do not have the features characterizing a Poisson process, which therefore is a useful but not totally realistic working assumption. In this respect, the work done in [106] shows that the adoption of the Logistic distribution would be more appropriate to model a realistic deployment of wireless devices over space.

Most of the literature and the analysis developed so far in this deliverable have reviewed the simplest form of point processes, which is the homogeneous PPP. As mentioned, this assumption makes workable many steps of the mathematical analysis shown above, which remains anyway not trivial. For the sake of completeness, below is given the flavour of other available point processes with the content mainly extracted from [104] [112].

- Germ-grain model: This is one of the most celebrated models in stochastic geometry which, in its simplest form, is the Boolean model that is the basic for BPPs and PPPs. In this respect, typical terminology includes the germs (points of the PPP) and primary grains, the ball of radius *r* around points.
- Cox point process: It is also referred to as doubly stochastic process and it is obtained by relaxing the hypothesis of constant intensity measure typical of a PPP. A realization of a Cox process is Poisson conditioned upon the intensity measure. Therefore, the probability distribution of a Cox process is obtained by defining a probability distribution of the random measure and deconditioning with respect to the random measure. Typical examples of a Cox process includes: mixed Poisson process (PPP with randomized intensity measure); π(x) thinning process (where the

thinning – probability to retain/delete a point of the PP - is not only a probability but a random process).

- Neyman-Scott point process: It represents the typical example of a Poisson cluster process and it is the result of homogeneous independent clustering of stationary PPPs. The random number of points inside a reference cluster is referred to as the number of daughter points while parent points form a stationary PPP with intensity λ. The Matérn cluster model is a particular class of these types of point processes when the number of points inside a cluster is Poisson distributed.
- Matérn hard-core point process: It is essentially a dependent thinning applied to a stationary PPP. The typical Matérn hard-core process is a dependent thinning where constituent points are not allowed to lie close together than a certain minimum distance. The thinning can be done using the Palm retaining probability of a typical point.
- Gibbs point process: Originally used to describe the energy equilibrium states of subsystems taking part to a large close physical system it has been also adopted for modelling the behaviour of large wireless networks. It associated to the concept of Gibbs measure and in brief it is based on the concept that a point process can be formed starting from an initial PP (e.g., Poisson) and then altered by means of a probability distribution.

5. Simulation tools to model interference in cognitive radio networks.

This section is dedicated to review some of the simulation tools that can be used to quantify the aggregate interference power generated by cognitive radio networks over a primary link. A number of simulators are nowadays available including licensed and unlicensed tools. Licensed tools include Matlab and Opnet for example. Unlicensed tools include ns-2, ns-3, OMNET++ and SEAMCAT. All of them have pros and cons however it is worth mentioning that, SEAMCAT is the official tool used by ECC/CEPT to carry out compatibility studies. The other mentioned simulators find applications in modelling many different aspects of the behaviour of wireless and wired networks. Therefore, the remainder of this section will focus on describing the essentials of SEAMCAT simulator, which is used with the specific purpose of modelling interference and which is officially adopted by European regulatory bodies.

SEAMCAT is a software tool based on Monte-Carlo simulation method which is developed within CEPT since the year 2000 and that allows simulating different interference scenarios with the purpose of addressing compatibility studies between different radio technologies operating in the same or adjacent frequency bands. It was developed by CEPT/ECC Working Group Spectrum Engineering (WGSE) within its sub-entity SEAMCAT Technical Group (STG) [113] and it is freely downloadable from European Radio Office (ERO) website.[10]

More in specific, SEAMCAT is a tool conceived for the evaluation of co-existence studies in terms of the evaluation of transmitter/receiver mask, unwanted emissions (spurious out-of-band), blocking/selectivity, etc. It cannot be considered however as a tool for system planning purposes [114]. Despite that, SEAMCAT offers a degree of flexibility to simulate point-to-point and point-to-multipoint connections, broadcasting systems (e.g., terrestrial systems such as DTVB), short range devices and land mobile systems. SEAMCAT can flexibly use any user-defined propagation model. The built-in propagation model allows modelling the victim link, the interfering link, the interference path and CDMA/OFDMA modules. For example, in [115] it is shown a research work on the interference analysis for the coexistence between WLAN and Bluetooth. Monte-Carlo simulations provide a tool for statistical analysis throughout several realizations (e.g., thousands) of the wanted random process. In case of using SEAMCAT for modelling the probability that a system interferes with another one, Figure 5-1 illustrates the essentials of the procedure built-in the simulator. The right hand side of the figure shows the behaviour of the victim system when the event of interference occurs. In other words, the event “interference occurs” when the minimum permissible carrier-to-interference ratio (C/I) is exceeded. Therefore, the probability to interfere with another system is the statistics that is collected by counting the number of times in which the event of interference effectively occurred and averaging with respect to the total number of simulations.

ECC is actively involved in the adoption of new technologies such as cognitive radio within the leading group SE43 that deals with CR systems in the frequency range 470 – 790 MHz

[10] Available at www.ero.dk/seamcat.

(i.e., TV White Spaces). As shown in [116] [117], SEAMCAT allows Monte-Carlo simulations of the interference produced by CR devices operating the in TV White Spaces when the interference is measured at the location of the White Space receiver (victim receiver). In particular, the work done in [117] considered two simulation scenarios: 1) the case of one CR device operating in the TV White Spaces transmitting in an adjacent channel and located outside the coverage area of the DTVB station and 2) up to three CR devices transmit inside the coverage area and in one of the adjacent frequency channels of the DTVB station. The main result of this work was determining, by means of SEAMCAT simulations, the in-block power limit of a channel (i.e., the amount of power that the CR device can use for transmission in that channel) for given separation distances between the interferer and the victim receiver.

Another similar work similar to the one made in [117] is shown in [118]. There, SEAMCAT is used to simulate several interference snapshots and so compute the probability that the CR devices can interfere with one victim, like made of wanted transmitter - victim receiver. In this work the concept of spectrum emission mask (SEM) and blocking emission mask (BEM) is considered. One surprising result of this work is that, for a BEM over 6 MH bandwidth of a DTVB channel and for a distance between primary transmitter and primary receiver below 2 Km, the number of CR devices that are allowed to transmit simultaneously is approximately “600”.

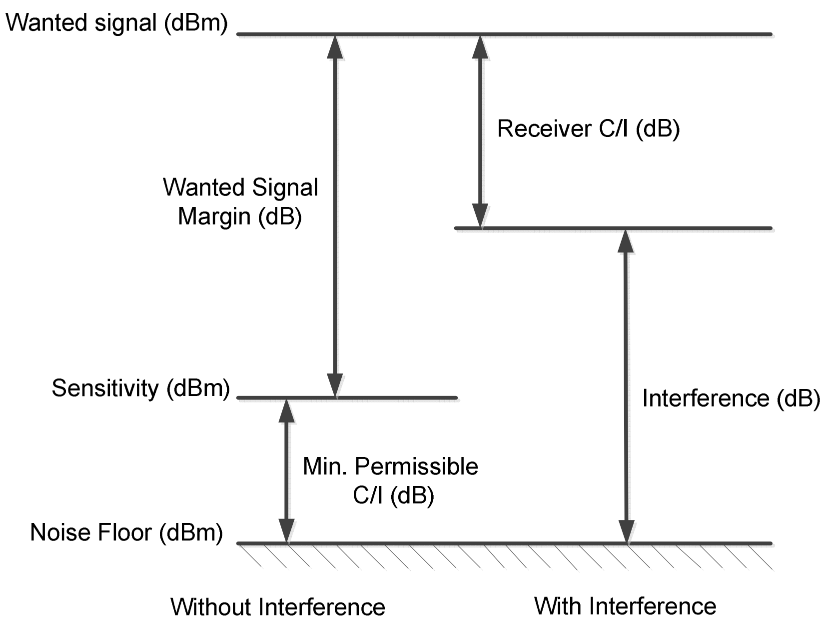

Figure 5-1: Power levels used to determine presence/absence for the event of interference.

6. Advantages/Disadvantages of the reviewed models

This section provides a summary of the main results previously shown on the aggregate interference power generated by CR devices. The above discussion has led us to explore the use of stochastic geometry tools for modelling the distribution of the aggregate interference occurring in a random network graph, when the interference is modelled at the unique receiver that is placed at the origin of the reference system (the work done in [53] showed that this is worst interference scenario). The study done in previous sections has also reviewed available simulation tools capable of estimating the impact of the aggregate interference generated by CR devices to a primary transmission. Despite the many available tools the discussion focused on the CEPT/ ECC official tool SEAMCAT.

Analytical tools such as those based on stochastic geometry provide already an advanced way of modelling the aggregate interference with respect to invoking the Gaussian CLT. Despite that, these models still suffer from many unrealistic assumptions although at this point they offer the advantage of incorporating important propagation effects such as fading, shadowing, sensing schemes and primary receiver's location.

Simulation tools have the advantage of letting users testing many specific scenarios, even to a level of detail quite refined. This would be quite difficult with analytical tools which rather deem to show reference performance. Despite that simulators can be extremely useful in testing network behaviour with a level of complexity almost as close as to the real system, they suffer from the problem of an awkward and slow development that sometimes it does not allow timely predictions. This aspect is particularly relevant during the process of creating new international standards for wireless communications. Furthermore, the results obtained with a simulator are difficult to evaluate as they could be greatly affected by internal assumptions of the simulator and limitations of the random seed generators in providing sufficient event diversity.

The discussion above highlights that all the tools have pros and cons but the findings obtained with one individual tool should be compared with the results that can be obtained with others, or to field measurements, in order to show the reliability of the results. In order to compare the different tools, a list of the critical aspects that can be used for comparison between them is provided below:

- *Complexity*: this aspect is concerned with the complexity of a tool (analytical or simulation) other than computational power.
- *Computational power*: it accounts for the computational power that is required to run a software tool in order to obtain meaningful results.
- *Reliability*: it refers to the reliability of the obtained results for predicting the behaviour of a wireless network.
- *User's experience*: an experienced user might privilege the adoption of analytical tools rather than simulations or vice versa, based on the acquired experience, thus affecting also the goodness of the results that are going to be obtained.

7. Standardization Perspective

Standardization is an important step in the bringing of concepts to markets. Standardisation is necessary in cases where multiple entities are producing products for a similar purpose, especially if those different products have to interact or be compatible in some way, with each other or with a another common third party entity or element. Of course, in the case of communications, equipment/products of different manufacturers, operators, and other entities are naturally interacting, so must follow a standard. The alternative is that eventually one product from one manufacturer will win the fight and dominate the market for compatibility reasons, but this is not preferable due to competition concerns. The development of and adherence to standards is therefore the only way forward.

As regards interference management and higher-level requirements, it is noted that standards must follow the regulations, including emission requirements, interaction with a geolocation database in the case of TV White Space, and other aspects. Hence, all standards follow regulatory rules and in some cases even try to predict them, as well as the associated requirements. A good example of this is the IEEE 802.22 standard and working group [84], which since the inception of its work has gone from being spectrum sensing-based to having to incorporate aspects of geolocation database interaction in line with changes in regulations. This has been an aspect of the delay in producing the baseline IEEE 802.22 standard.

Concerning the key issue of interference management and standards thereof, standardisation is generally a voluntary option, such that in many bands it is not possible to enforce a standard—with notable exceptions such as bands allocated for a particular owner and purpose that follows a standard, an example being as LTE. It is therefore not possible to rely on such a standard for interference management, unless it is the case that regulators impose a standard for such a purpose or assisting such a purpose. Although regulators have been interested in feeding from standardisation and incorporating associated ideas, including some aspects of standards to help specify the regulatory requirements, the use of a given standard for all aspects of interference management by a regulator, developed for that particular purpose, would be a big change.

If the standards that will be interfering in a given spectrum band are all under the same entity, it is easier to impose coexistence rules upon them that will implicitly assist the management of interference. A good example of this is provided by the IEEE 802.19 working group [119], which considers coexistence (implicitly of IEEE standards) in unlicensed frequency bands. This working group requires that all new IEEE 802 standards operating in the given unlicensed spectrum submit a “Coexistence Assurance” document, which specifies the standards that the new standard could mutually interfere with in the given unlicensed spectrum, measures for mitigation of that interference, and the associated coexistence performance. IEEE 802.19, however, recognises the particular issues of TVWS, given the wide range of systems that will operate in TVWS currently under development. It has therefore initiated a task group, IEEE 802.19.1, that is considering the issue of such coexistence in TV White Space specifically [120]. Various proposals for management of interference based on 802.19.1 have been proposed, and for simplifying managing coexistence.

7.1 Limits on the aggregate interference

Following the actions undertaken by the US FCC that opened up significant parts of the TV spectrum for unlicensed use, other countries in the world have considered to apply similar measures [121] [122] [123]. The FCC selected a value of the maximum transmit power for devices operating in the White Spaces in unlicensed fashion. The FCC also defined the so called *erosion margin*, which quantifies how much the TV service can degrade and thus the tolerable amount of interference that CR devices can inject in TV bands. A zero erosion margin would imply zero white spaces. This margin is particularly important as it allows determining how far the CR devices (referred to as White Spaces Devices) have to be from television receivers, taking into account in-band interference and the interference caused by transmissions on adjacent channels.

As seen from the literature related to this topic, interferences (intentional or unintentional) represent one of the major challenges from the perspective of designers. The interference is not only intended as the degradation of a primary service (e.g., televisions service) and thus the need to protect it but also to the fact that the TV broadcasting service will affect CR devices. This latter aspect is known as *pollution* [124]. The aspect of interference is strictly connected to the concept of how much a radio system can be interfered before experiencing performance degradation. The higher is the resilience the more a system could operate in hostile (i.e., interfered in this case) environments. Initial estimations of the White Spaces and of interference margins have started in the USA but similar ones can be found in Europe as well. For example, [63] shows calculation of the maximum interfering power and field strength that a primary service can tolerate in case of the TV broadcasting service, PMSE systems, radio astronomy services and aeronautical navigation systems.

7.2 TV White Spaces estimation in the USA

The work done in the seminal papers [124] and [125] represented a fundamental step to understand the amount of White Spaces that could be available for communications before and after the digital switch-over (DSO) of analog TV. A similar work for Europe is available from [126], whereas a test bed used to measure the amount of White Spaces in the UK is available from [129].

The work done in [124] deems to evaluate the amount of White Spaces that are available in the USA for cognitive radios, with a 6 MHz TV channel width and a 4 W of equivalent radiated power (ERP). Here it is taken an approach that includes the *protection* viewpoint (for protecting the receivers of the primary service from the aggregate interference) and pollution viewpoint (the primary service affecting the availability and quality of spectrum for cognitive devices). Results are in terms of the average number of white space channels per location (this accounts for the area as normalization factor) or per person (this accounts for the population density as normalization factor). The study, regardless of the viewpoint, assumes the FCC's transmitters database and the ITU propagation model (ITU-R P-1536-3). The results are shown for UHF and VHF frequency bands considering different acceptable pollution levels with and without adjacent channels interference (i.e., in this case TV transmitters operating on channels other than the selected one). White space channels for the pollution viewpoint are more available in the low VHF band. For the protection viewpoint, with a zero watt transmitter, there are almost 19 white space channels per person in the low UHF. However, as soon as the transmit power of the secondary users is increased this number reduces dramatically. When also fading is taken into account, the erosion margin introduced in the previous section is found to be around 1dB, as ruled out by the FCC. Beyond an erosion margin of 0.1 dB, there is a gain of almost 20 available white space channels per person.

The work done in [125] deems to evaluate the available capacity (intended as the Shannon information-theoretic capacity) within the White Spaces throughout the US, fulfilling also the FCC constraints for the protection of the TV service. The computation is carried out applying propagation models approved by the FCC for this matter. For a TV channel of 6 MHz width, a TV signal with 4 W ERP in each channel and a single link of 1 Km and 10 Km, the result shows a huge amount of White Spaces. As pointed out by the authors this result is misleading as a single link is not a meaningful target. As soon as the effect of interference piles up, the amount of White Spaces changes dramatically. Two important aspects are highlighted by this work: the importance of the propagation models that are selected and the regulatory aspects incorporated which greatly affect the final result and the definition of an exclusion-radius, which is the real footprint of a White Space transmitter for the purpose of sharing. A very interesting insight is provided by dividing the capacity of White Spaces in a given area by the population density. This shows that, on a long term, a user receives up to 10 Kbits/sec which goes up to 720 Kbits/sec over a shorter term. The paper concludes with an insight of economic effects that arise from using White Spaces taking again into consideration the density of people.

7.3 TV White Spaces in the European Context

The work done in [126] is one of the first attempts to quantify the amount of White Spaces available in Europe and it is somewhat similar to [124] and [125]. The study investigates the situation of White Spaces in Europe taking into account the area of interest and density of the population. The erosion margin is set to 1 dB and the frequency range is 470-790 MHz, which is what remains of the European digital dividend. In terms of propagation models, it is used the ITU model and the Longley-Rice irregular terrain model. The study, with and without adjacent channels interference, is conducted for European countries like Austria Belgium, Czech republic, Denmark, Germany, The Netherlands, Luxemburg, Slovakia, Sweden, Switzerland and the United Kingdom. The approach, if compared to the previous papers already cited, is based on the protection viewpoint. Using TV network data, for the United Kingdom, this study managed to derive the protection region before and after the switch-over of analogue TV in terms of the minimum field strength. Thus, the required field strength in dB is computed as follows

$$E^{(Ana\log)} = \gamma + 20\log_{10} f - 111.5 \tag{74}$$
$$E^{(Digital)} = \gamma + 20\log_{10} f - 150.1 + SNR_{req},$$

Where γ is the erosion margin and SNR_{req} is the value required to protect the TV service. The study confirms that the amount of White Spaces available in Europe is less than in the USA, as also stated in [127]. For the entire evaluated European region the average availability of white space channels is around 25% by area compared to the USA (or 18% by population).

Based on various academic, industrial and regulatory input the ECC produced its landmark report ECC159 in January 2011 on the technical and operational requirements for the use of cognitive radio in TV white space in 470-790 MHz band. The report considers the use of sensing and geolocation-based approaches to minimise risk of harmful interference to the incumbents. The following incumbent protection cases are considered:

- Protection of the broadcasting service in the UHF band
- Protection of wireless microphones in Programme Making and Special Events (PMSE)
- Protection of Radio Astronomy (RAS) in the 608-614 MHz
- Protection of aeronautical radio navigation (ARNS) in the 645-790 MHz band
- Protection of Mobile/Fixed services in bands adjacent to the band 470-790 MHz

The ECC Report 159 defines the requirements for the operation of white space devices (WSDs) (i.e. cognitive radios) under the geo-location based approach [128]. Specific requirements are provided for WSD deployment using a master/slave architecture. It identifies the information which needs to be communicated by the WSD to the geo-location database and vice versa.

A key element in the geo-location database approach is that the WSD will be providing its location information to the database which will then be used by the database to calculate and output information containing a list of **allowed frequencies and their associated maximum transmit powers** to the WSD. The Report also provides guidance to administrations on a general methodology for this input/output translation process that needs to be carried out between the WSD and the database as well as some examples of the algorithms that can be used in the calculations to be performed by the database. The approach of providing example algorithms is motivated by the need to enable flexibility for administrations to adapt the framework to their national circumstances (e.g. national DTV planning model, specific national quality requirements, etc.). The algorithms and underlying modelling assumptions made on a national level can nevertheless have a significant influence on the effectiveness of the protection of incumbent users and therefore have to be chosen very carefully.

A reference implementation by ACROPOLIS project of the ECC approach to TV white space is described in ACROPOLIS deliverable D14.4.

7.4 OFCOM Cambridge Trials on TV White Spaces

The UK's OFCOM started considering the exploitation of TV white space in 2006 with various studies, reports and public consultations. This led to the OFCOM decision in 2011 to undertake the Cambridge Trials by a consortium of stakeholders (broadcaster, PMSE users, white space equipment makers, geolocation database providers) to carry out field tests and measurements of several aspects, including

- Considerations for the protection of wireless microphones by the PMSE community
- Performance of TV white space base station for mobile and fixed broadband applications
- Measurements on DVB-T protection ratios in the presence of interference from white space devices.

An OFCOM report gives the overview of the Cambridge Trial and experimental work to measure the effective amount of White Spaces in the Cambridge White Space Trial test bed [129]. This test bed was designed to help Ofcom in achieving its proposal of license-exempt access to White Spaces. The objective of the test bed is twofold: i) make a number of in-depth tests and measurements focusing on the requirements for the protection of existing services and ii) help industry to understand the benefits arising from White Space spectrum. The test bed consists of 8 base stations deployed in urban and rural environments with 5 assigned in urban locations. The technology used includes 6Harmonics, Adaptrum, KTS and Neul. In urban locations, the maximum allowed transmitted power was set in the order of 125 dBm of EIRP for base stations and mobile terminals. For rural areas the tested link included a directional antenna transmitting over a distance of approximately 6 Km. Tests ran from August to November 2011 in UHF bands. Plots of experimental data, after processing, show that the use of spectrum is reasonably stable over a time scale of months and mostly clear of harmful interference. One interesting finding of this experimental study was the provision of a broadband Internet service in rural areas through white space technology. The broadband access achieved nearly 8 Mbits/sec in downlink and 1.5 Mbits/sec in uplink. This trial also allowed concluding that a path loss of 140 dB constitutes the minimum requirement for the provision of the broadband service.

7.5 Protection of PMSE Applications

The PMSE (Programme making and special events) use case represents a socially and economically important professional user community that already shares the TV white spaces with broadcasters in the UK and elsewhere. It includes large outdoor concerts, outdoor collection of footage for news gathering and TV programmes, and widespread use of wireless microphones in theatres and conference halls.

In order to protect PMSE, relevant EIRP restrictions need to be applied on WSDs operating in the geographic cells around the PMSE events. A cell is typically defined as a 100m x 100m pixel. The protection approach is to limit the interference at the PMSE receiver such that the sensitivity of the equipment is not degraded beyond an acceptable margin [130, 131].

To achieve this, the interference from WSD, weighted by the receiver ACS value should be in the range below the receiver's noise floor. Figure 7-1 shows the degradation in receiver sensitivity as function of I/N [130].

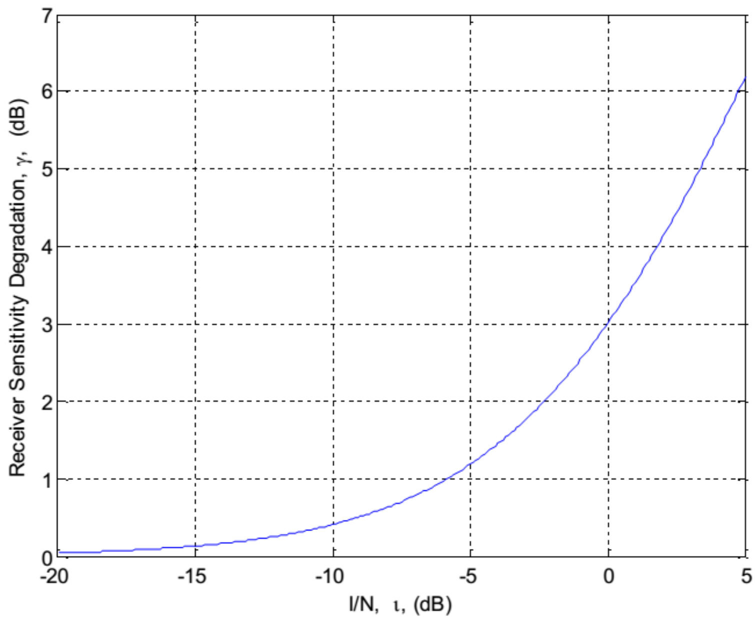

Figure 7-1: Degradation in receiver sensitivity as function of I/N [130]

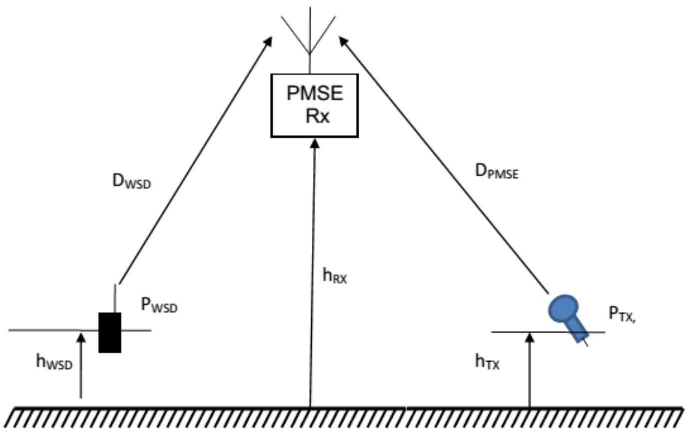

(a) Reference geometry between a PMSE receiver and the WSD transmitter

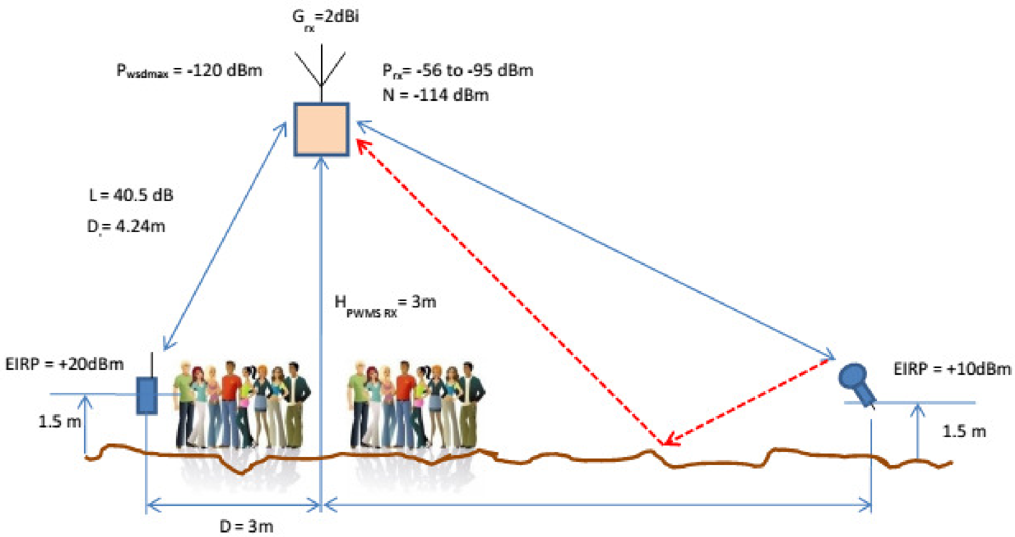

(b) Scenario: Outdoor events e.g. Street fair, foot race, etc

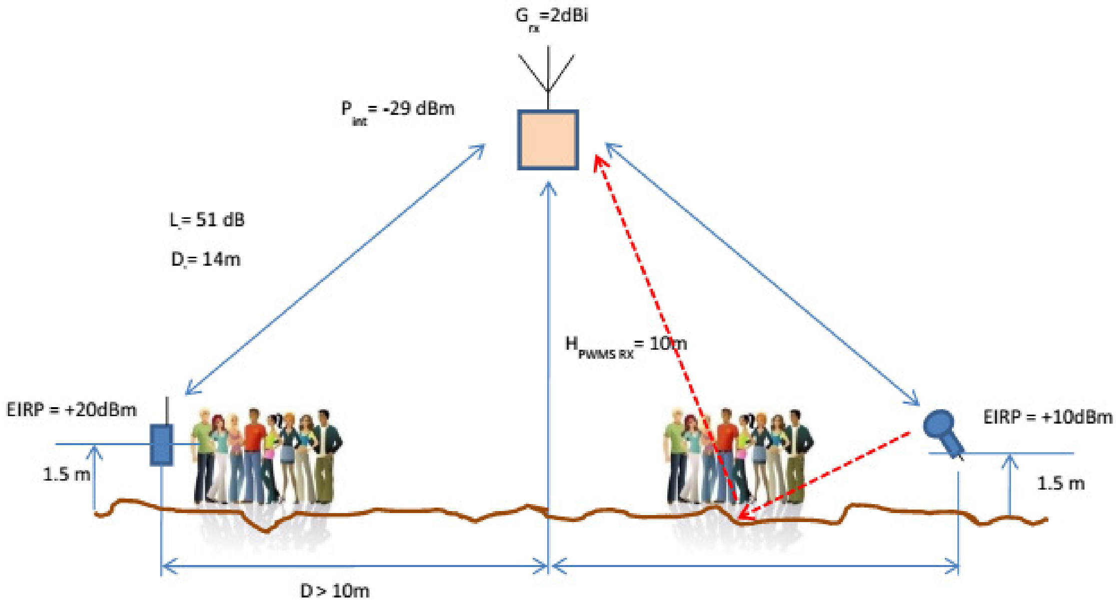

(c) Indoor scenario: Concert hall, theatre, etc

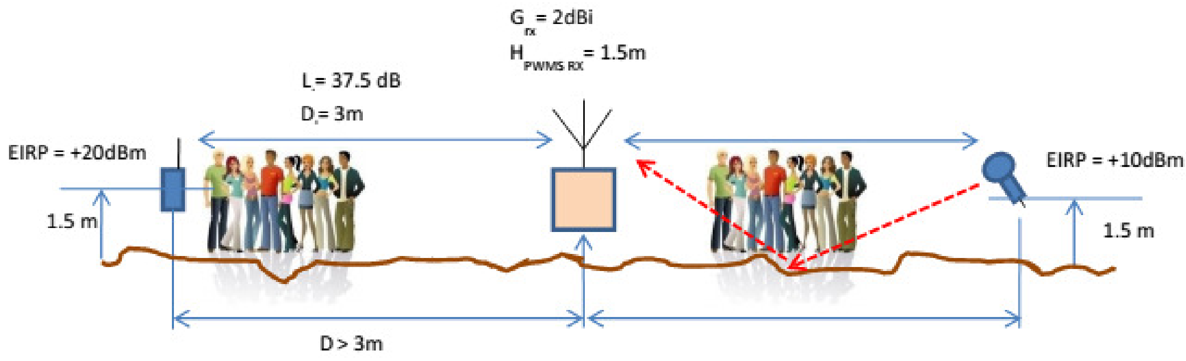

(d) Indoor scenario: Meeting room, conference centre

Figure 7-2: Reference geometry in typical PMSE scenarios [130]

7.5.1 PMSE Receiver Performance and Protection Ratios

For the Cambridge Trials, in order to identify the amount of protection required for PMSE operations, trial participants carried out *protection ratio measurements* involved the set up shown in Figure 7-3 [130], [131]. The tests involved a sample of commercially available PMSE receivers, along with digital and analogue radio microphones.

The protection ratio, specified for a particular frequency offset, defines the maximum level of interference that can be tolerated without noticeable impairment to the demodulated audio signal. The protection ratio is measured as being the *ratio of the wanted to interfering signal strengths* at the maximum interfering signal that results in an unimpaired audio signal.

An arbitrary signal was generated with waveforms captured from an LTE base station (BS) and user terminal. Typical results of protection ratios, with LTE base station as a WSD, are shown in Figure 7-4.

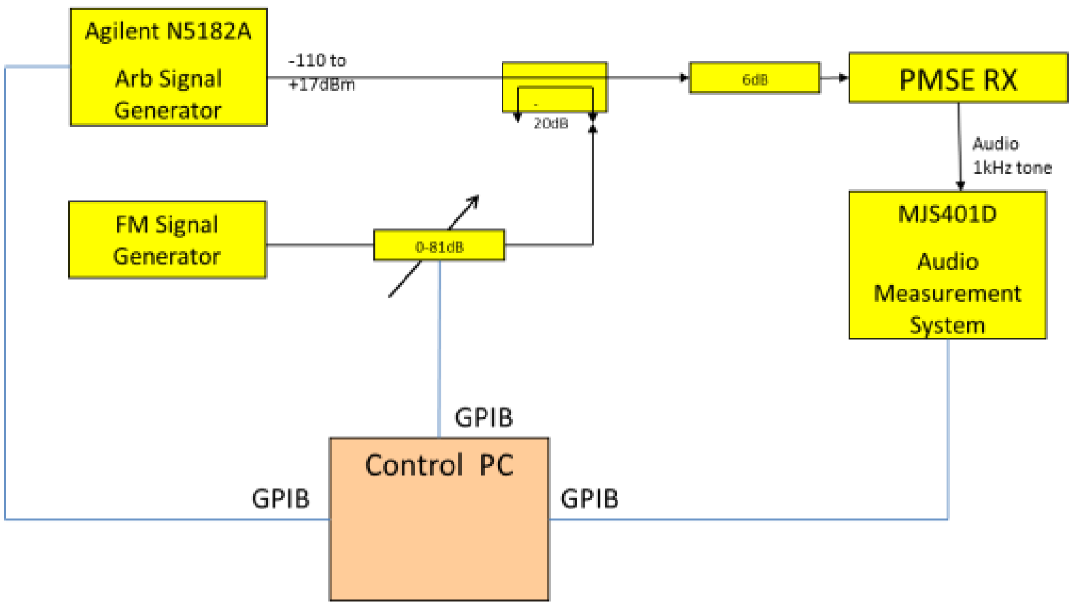

Figure 7-3: Test arrangement for PMSE Protection Ratios [130]

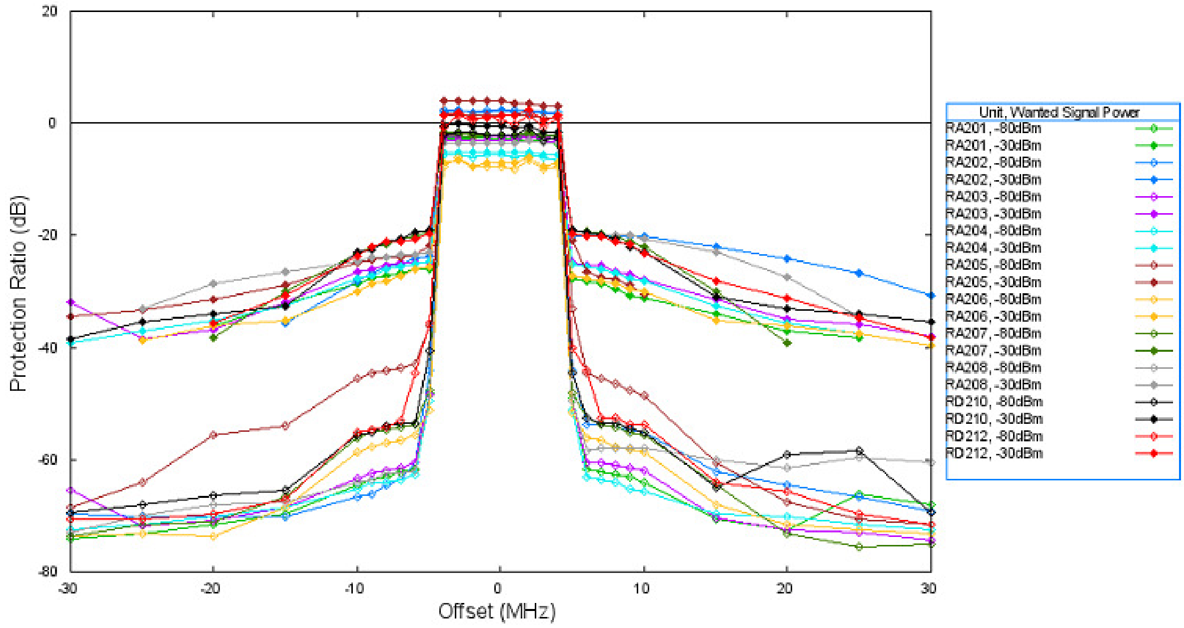

(a) LTE base station interference at 100% traffic

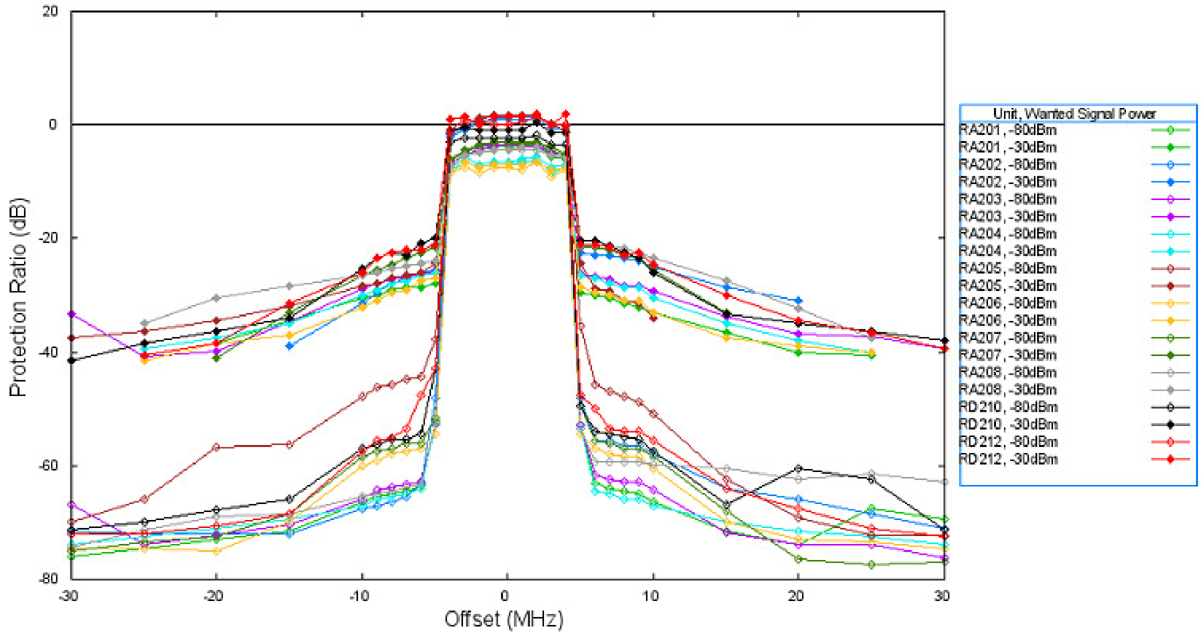

(b) LTE base station interference at 50% traffic

Figure 7-4: Protection ratios for PMSE from LTE base station as a WSD [130]

The test indicated that protection ratio values for both the high and low power wanted signals are different; the worse adjacent channel protection ratio for the -30dBm wanted signal is as a result of the receiver being overloaded (both wanted and interfering signal powers are large in this case).

The tests reported in [130], [131] found that the adjacent channel (+-10MHz) minimum protection ratio is better than 55dBm for the non-overloaded case, irrespective of the waveform used. The worst co-channel protection ratio is around 6dB.

7.6 Protection of DVB-T Receivers

In the presence of cognitive radio, specifically of the white space devices in the UHF band, protection of Digital Terrestrial Television (DTT) receivers is required to ensure the quality of DVB-T reception is free from unwanted interference from WSD signals in the adjacent UHF bands.

BBC carried out tests in 2011-12 on a range of candidate technologies and assessed DVB-T receiver performance in the UK context [132]. Fourteen popular models of commercially available receivers were tested representing integrated digital television (IDTV), set top boxes (STBs) and programmable video recorders (PVRs). The interference from WSDs was generated through a vector signal generator to replay a waveform recorded from candidate WSD radio technology.

Figure 7-5 to 7-8 show the test set up for DVB-T testing, different WSD waveforms and typical test results for protection ratios.

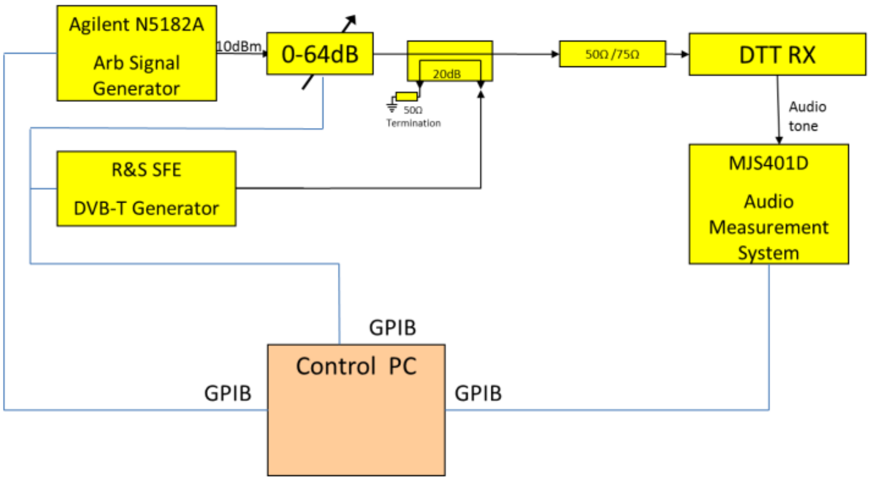

Figure 7-5: DVB-T Test Setup [132]

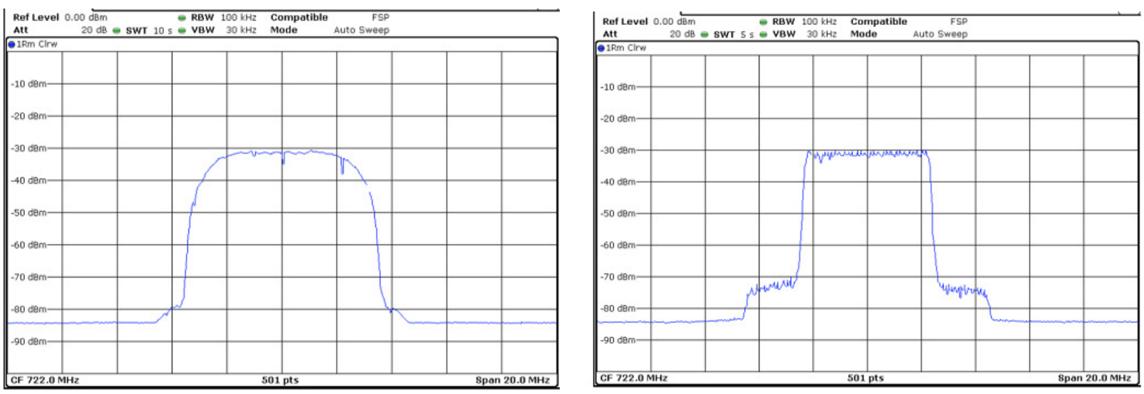

Figure 7-6: Waveforms of different WSDs [132]

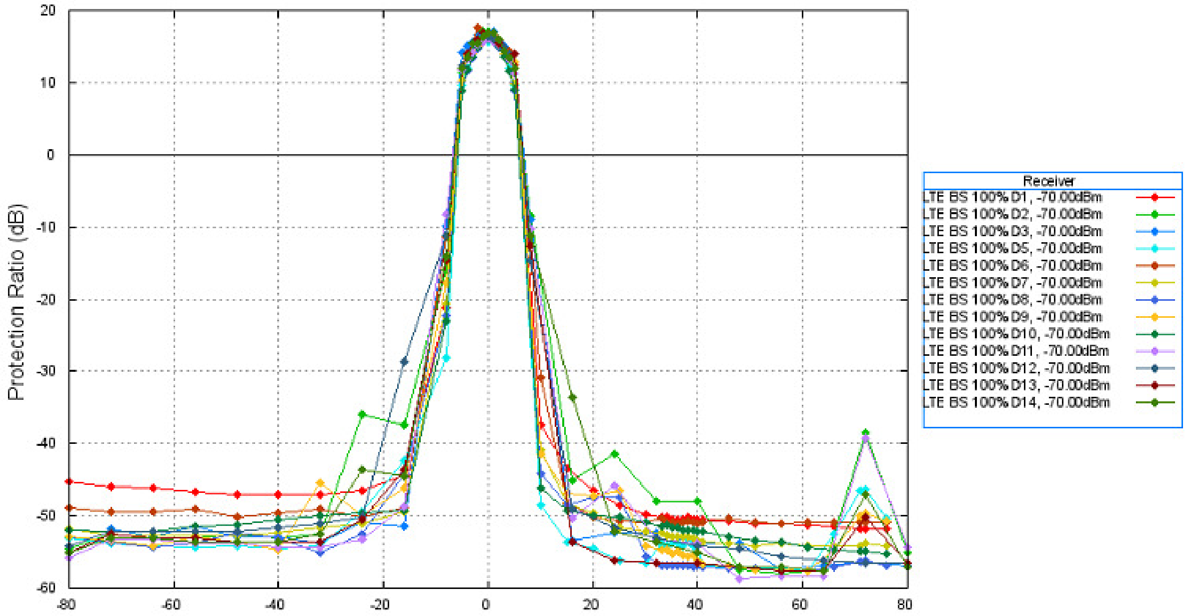

Figure 7-7: Protection ratio for different receivers at LTE base station 100% and DTT Signal level of -70dBm [132]

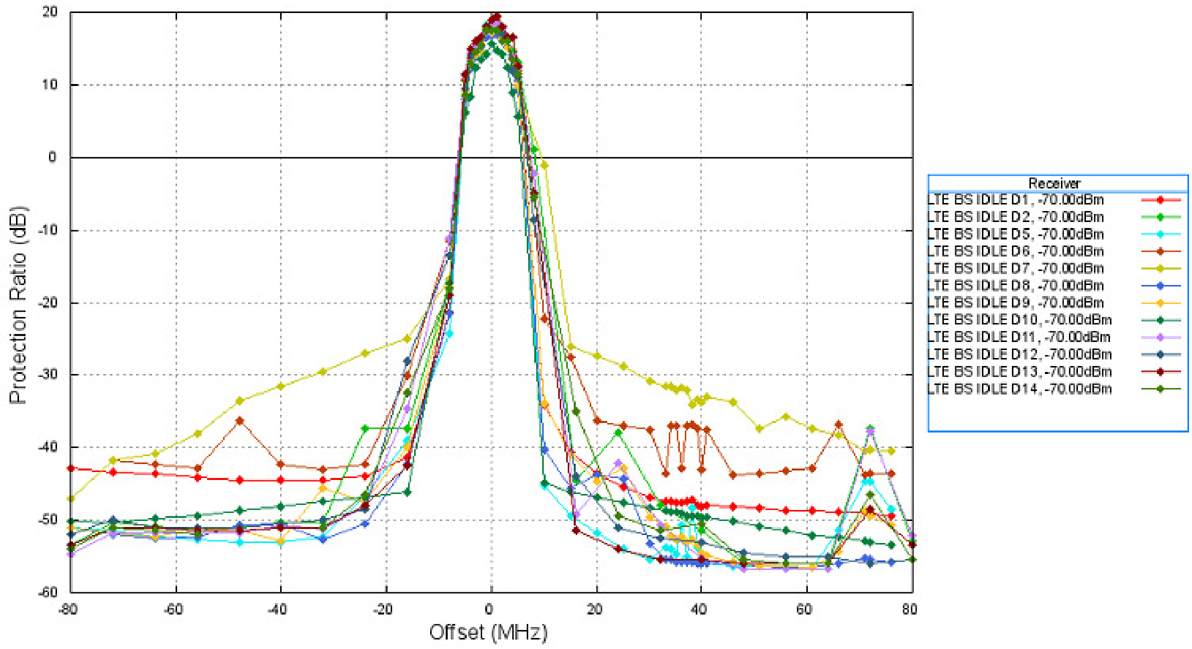

Figure 7-8: Protection ratio for different receivers at LTE base station idle and DTT Signal level of -70dBm [132]

The results of these tests show a considerable variation in performance of DTT receives. Whereas high-end receivers appeared to be fairly resilient to interference from WSD signals, other receivers were found to be vulnerable to the WSD waveforms used in the tests. Broadcast-like signals (e.g. LTE base station at 100% traffic) were dealt with by the receivers without interference. However, burst-like signals (e.g. low traffic CPE signals) result in up to a 30dB degradation in protection ratios.

As a consequence, the authors in [132] recommend the use of a highly conservative protection ratio values in the UK in order to protect the majority of existing consumer grade DVB-T receivers (largely in the form of low cost set-top boxes used to adapt old analogue TV receivers to DTT reception). The authors concluded that the geolocation database approach to TVWS was feasible provided that the database could take into consideration the various WS technologies and the predicted field strength at the DTT receiver location.

7.7 Spectrum and Environment Measurements Supporting Interference Prediction and Assessment

Spectrum and environment measurements for general characterisation purposes are key ways of assessing both the availability of spectrum for opportunistic use and other forms of sharing, and the potential interference that could result. Moreover, in-the-field measurements, aligned with estimation approaches in some scenarios represent means of monitoring, locating and mapping potential interference effects.

One area in which some extensive related work has been done given its interest in the community and given a number of positive initiatives in regulatory circles is TV white spaces. The prior sections have concentrated heavily on aspects of TV white spaces. Here we concentrate more generally on other bands.

Within ICT-ACROPOLIS, extensive measurements have been done within in London in July 2011 (see, e.g., [133], [134]). These measurements and the ensuing analysis concentrate heavily on correlation aspects of the traffic, and particularly temporal and spatial correlation, both of which have profound implications for the characteristics of the availability of spectrum for sharing, and associated design implications for the systems that must implement sharing. The measurements assessing temporal correlation were taken at a fixed location for a long duration, whereas the measurements assessing spatial correlation were done through maintaining one measurement system at a fixed location, and moving other measurements systems with respect to that, ensuring that the times of the measurements are accurately logged so that the measurements from exact the same time can be compared thereby ruling out temporal variation effects in assessing the spatial comparison. Such a concept could be implemented through drive testing, as covered in Deliverable 9.3 [135], were such drive-testing supported by the time-stamps of a GPS system, for example. Moreover, the understanding of correlation aspects through such measurements can assist in the calculations done by radio environment mapping, also covered in Deliverable 9.3, noting that there is a direct link between correlation and variance, which of course exists by definition if the covariance measure is used.

In [133], spatial correlation aspects have been assessed at a number of different locations in London as part of the July 2011 campaign. On the one hand this work applies the semi-variogram measure to assess spatial correlation, letting the parameter of the semivariogram be the distance between measurement locations considered, instead of a time or frequency separation. In this case the natural estimator for the spatial semivariogram becomes the empirical variogram of Matheron. The main challenge in applying this semivariogram definition to the data set is that the number of individual measurement locations within a measurement area is not very large, resulting in a high estimation variance at an individual bin of this histogram style estimator. This phenomenon is illustrated in Figure 7-9, showing the spatial empirical semivariograms for the GSM1800 downlink band for the Oxford Street and Wimbledon measurement areas. Clearly while in some cases the shape of the semivariogram is as expected, using this approach for characterizing spatial correlations in our data sets is not very effective.

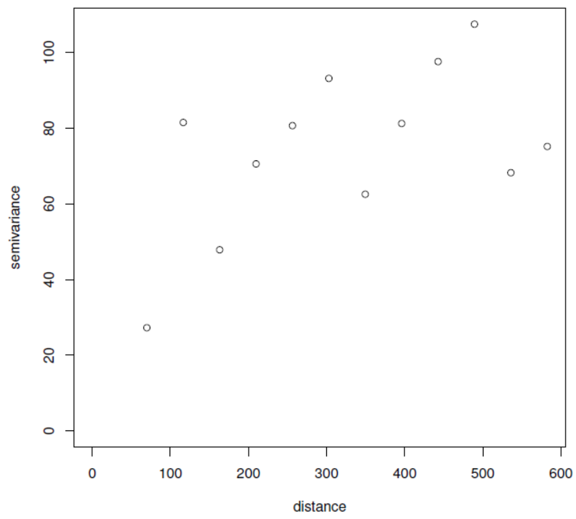

(a)

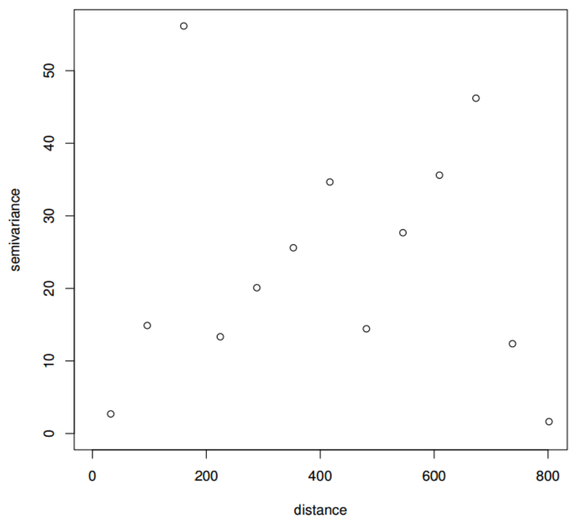

(b)

Figure 7-9: Spatial variograms for GSM1800 downlink band for measurement locations in (a) Trafalgar Square and (b) Wimbledon Stadium [133]

Because of these estimation difficulties with the spatial empirical semivariogram, this work also foregoes the attempt to characterize spatial correlations as function of distance, and instead compute “global” measures of spatial autocorrelation, resulting in a single number for the whole measurement site. This increases the available data the correlation measure is computed for, and will significantly increase the reliability of our estimates. As the measure of spatial autocorrelation we adopt Moran’s *I*.

Table 7.1 gives the values of Moran’s *I* for different statistics based on the measurements on the GSM900 downlink band, assessed in this measurement campaign. Clearly, the spatial structure of the data sets varies significantly across the measurement areas. In the residential and suburban locations high spatial autocorrelations can be observed, whereas in Heathrow area and more central downtown locations correlations become much lower or even insignificant. This is in part due to the intrinsic effects of network structure and deployment, and also in the case of Heathrow due to measurement locations being rather far apart from each other. It is also interesting to note that the choice of statistic used has a strong impact on the correlation coefficient. Typically the analysis in the literature has focused on the random field corresponding to the (linear) mean power spectral density, given in the second column of the table. However, the results show that also the tail behavior of the mean PSD distribution can feature high spatial correlations.

				Tail behavior / percentiles			
Location	Mean	Mean (dB)	Median	0.05	0.25	0.75	0.95
Oxford Street	0.33	-0.04	0.30	0.62	0.42	0.27	0.21
Trafalgar Square	0.05	0.14	0.03	0.35	0.08	-0.16	0.24
Wimbledon Tennis Court	0.31	0.33	0.12	0.57	0.37	0.04	0.59
Residential Area	0.53	0.49	0.59	0.25	0.42	0.65	0.27
Business Area	0.20	0.13	0.12	-0.04	0.10	0.21	0.18
Suburban Area	0.60	0.18	0.42	0.81	0.73	0.52	0.56
Heathrow Airport	-0.17	-0.01	0.02	-0.04	-0.01	-0.25	-0.24

Table 7-1: Values of Moran's *I* for different measurements statistics for the GSM900 downlink [133]

8. Conclusions

This report has focused on the issue of interference generated by cognitive radio networks to primary user communications, as well as other spectrum sharing cases, particularly concentrating on the issue of aggregate interference. The proliferation of innovative wireless technologies and corresponding services lead to the serious problem of spectrum shortage. The paradigm of cognitive radio, as well as other spectrum sharing regimes, may therefore represent a possible solution that opens the way to unconventional forms of use that deviate from the typical command and control or exclusive use ideology.

Such agile spectrum access where cognitive radios might access different frequency bands, anytime and anywhere, requires particular attention to the problem of aggregate interference. Most of the work behind cognitive radio is founded on the assumptions that cognitive radio devices can detect the presence of the primary user's transmissions and they do not cause significant degradation of the licensee's performance. Even if only one of these assumptions doesn't carry, the concept of cognitive radio is of greatly reduced importance and viability. Accordingly, sophisticated analytical and simulation tools are needed to predict the impact of aggregate interference on the performance of the primary user.

The relevant scenarios for addressing the important problem of interference in this document have been selected among the existing taxonomy of spectrum sharing principles. Therefore, the selected scenarios were: TV White Spaces, Femtocells, UWB and spectrum sharing among equal unlicensed users. This deliverable has reviewed existing approaches that have been adopted for modelling of the aggregate interference throughout time. The starting point is the observation that the typical Gaussian approximation of the aggregate interfering process that pours out from the application of the central limit theorem is appealing but at the same time wrong. Beside analytical tools, this deliverable has spent some time reviewing existing simulation tools for estimating the impact of wireless interference. Among the variety of existing tools, this deliverable paid particular attention on the SEAMCAT simulator developed within CEPT.

The most advanced analytical tools used for modelling aggregate interference borrow concepts from stochastic geometry. The most widely used assumption is that nodes are scattered over space according to a homogeneous Poisson point process. This assumption allows for analytical tractability although not completely realistic. Results originated from the application of stochastic geometry as well as from standard probability theory lead to the conclusion that the distribution of the aggregate interference power belongs to the family of heavy tail distributions known as stable distributions. It was also shown that realistic propagation effects (e.g., fading) are reflected in the computation of the parameters of the stable distribution. Recent papers have the merit of empowering the analysis also with the capability of accounting for specific sensing schemes, cooperation among the secondary users and different positions of the primary receivers.

This report has shown that the design of a wireless cognitive system cannot be made without accounting for the effect of the aggregate interference they could generate. This aspect should gain increasing relevance and never be neglected in any future design. As the Poisson displacement of the nodes is not completely realistic, more studies on aggregate interference modelling, simulations as well as measurements are needed.

Finally, in recent years, practical work in the UK under "The OFCOM Cambridge Trials on TV white spaces") has focussed on determining the safe conditions for the deployment of cognitive radio in the UHF band. Based on the measurements carried out in the trials, participants have established the protection ratios for the incumbents (DTT and PMSE users) to determine the maximum WSD power levels and channel separation from the incumbents. These protection ratios will form the basis of regulatory limits in future while considering the allowable use of different white space technologies by secondary users while minimising the risk of harmful interference to primary users.

Appendix. A short tutorial on stochastic geometry

This section is devoted to summarize some general concepts of stochastic geometry that are useful to understand how models of the aggregate interference can be developed.

Definition A1: A set *A* has the following properties

1. It is said to be open if for each *x* in *A* it exists a positive real number *ε*>0 such $b(x,\varepsilon) \subset A$, where *b*(*x*,*ε*) denotes the ball centred at *x* and with radius *ε*.
2. it is closed if its complement A^c is open.
3. It is bounded if $A \subset b(a,r)$ for *r*>0 and a location point *a*.
4. the interior of the set is the union of all open sets contained in *A*.
5. the closure of A is the intersection of all closed sets containing *A*.
6. A set $A \subset \mathbb{R}^d$ is said to be compact if it is closed and bounded.

Definition A2: In measure theory, the concept of *σ*-algebra is a system $\boldsymbol{\chi}$ of subsets of a set A_x satisfying the following properties

1. $A_x \in \boldsymbol{\chi}$
2. If $A_x \in \boldsymbol{\chi}$ then $A^c_x \in \boldsymbol{\chi}$
3. If $A_1, A_2, \ldots \in \boldsymbol{\chi}$ then $\bigcup_{x=1}^{\infty} A_x \in \boldsymbol{\chi}$
4. $0 \in \boldsymbol{\chi}$
5. If $A_1, A_2, \ldots \in \boldsymbol{\chi}$ then $A_1 \setminus A_2 \in \boldsymbol{\chi}$
6. If $A_1, A_2, \ldots \in \boldsymbol{\chi}$ then $\bigcap_{x=1}^{\infty} A_x \in \boldsymbol{\chi}$
7. If $A_1, A_2, \ldots, A_n \in \boldsymbol{\chi}$ then $\bigcup_{x=1}^{n} A_x \in \boldsymbol{\chi}$ and $\bigcap_{x=1}^{n} A_x \in \boldsymbol{\chi}$

Remark A1: The family of Borel sets $\mathcal{B}^d$ on $\mathbb{R}^d$ represents the smallest possible *σ*-algebra.

Remark A2: In order to develop the concepts related to measure theory, the following facts are going to be used:

1. A set A_x and its *σ*-algebra constitute a measurable space,
2. A function *f*: $A_x \rightarrow \mathbb{R}$ is said to be $\boldsymbol{\chi}$-measurable if for all Borel sets $B \in \mathcal{B}^1$ the inverse image $f^{1}(B)=\{x \in A_x : f(x) \in B\}$ belongs to the *σ*-algebra $\boldsymbol{\chi}$ associated with A_x.

Definition A3: A particular example of measurable function is the indicator function of a measurable set A

$$\mathbf{1}_A = \begin{cases} 1 & for\ x \in A_x \\ 0 & otherwise \end{cases}$$

Definition A4: The measure on $[\boldsymbol{\chi}, A_x]$ is a function $\mu : \boldsymbol{\chi} -> [0,\infty]$ satisfying the following properties

- $\mu(0)=0$,

- $\mu\left(\bigcup_{x=1}^{\infty} A_x\right) = \sum_{x=1}^{\infty} \mu(A_x)$, for all disjoint sets in $\boldsymbol{\chi}$
- $\mu(A \setminus B) = \mu(A) - \mu(B)$

A first important example of measure is the Dirac delta function defined on a set A_x, which equals one for all x in A_x and zero otherwise. The second example is given by the *Lebesgue measure* v_d. The Lebesgue measure for d=1 represents the length, for d=2 the area and for d=3 the volume of a measurable set. The Dirac and Lebesgue measures are quite different in that the first operates on single points, whereas the second assigns measure zero to a point.

Although the concepts presented here can be extended to any measurable space, for practical reasons, the results are tailored to the Euclidean space. Hereafter, it will be referred to as the volume of the d-dimensional ball generalized to a d-dimensional space, with unit radius centred at the origin of the reference system (b(0,1)) with respect to the receiver as follows

$$C_d = \frac{\pi^{d/2}}{\Gamma(1+d/2)}, \tag{75}$$

which clearly corresponds to C_1=1 for d=1, C_2=π for d=2 and C_3=4/3 π. The denominator is the Gamma function for integer values (i.e., Γ(n)=(n-1)!).

For a function f: A_x->$\mathbb{R}$ the integral with respect to the measure has the following properties:

- $\int \mathbf{1}_{Ax}\, d\mu = \mu(A_x)$
- $\int f d\mu = \int f \mu(dx)$
- $\int \mathbf{1}_{[a,b]} f\, dv = \int_{[a,b]} f\, dv$, (for the Lebesgue measure)
- $\int \mathbf{1}_{Ax} f\, dv = \int_{A_x} f\, dv$, (for the Lebesgue measure)

If a generic measurable space that is defined by the triplet $[\Omega, \mathrm{A}_x, P]$ is such that P(Ω)=1, it is called a probability space and P is the probability measure. If X is a r.v. such that $\int |X(w)| P(dw) < \infty$ then the expectation of X can be computed as $E\{X\} = \int |X(w)| P(dw) = \int_{-\infty}^{\infty} x dF(x)$, with F the CDF of X.

Definition A5: A r.v. X is said to be spherically symmetric if its pdf depends only on |X|. Furthermore, the product between a univariate r.v. and SS r.v. that are independent from each other is itself a SS r.v.

Definition A6 (Point process): Let $\mathcal{B}^d$ be the Borel σ-algebra in $\mathbb{R}^d$ and $B_0^d \subseteq \mathcal{B}^d$ be the system of all bounded Borel sets. A point process X is a measurable mapping from the abstract probability space $[\Omega, \mathrm{A}_x, P]$ to $N_{lf} = \{x \subseteq \mathbb{R}^d : n(x_B) < \infty \forall B \in B_0{}^d\}$, where $x_B = x \cap B$ and $n(x_B)$ denotes the cardinality of the set. Furthermore, when N_{lf} is equipped with a σ-algebra it implies that $n(x_B)=N$, $\forall N \in \mathbb{N}$.

Proposition A1 (Random point): Let us consider a point ξ uniformly distributed in a compact set $W \subset \mathbb{R}^d$. This point is a random point if for all Borel sets $B \subset W$ it holds that

$$P\{\xi\} = \frac{\nu_d(B)}{\nu_d(W)}. \tag{76}$$

As a consequence, a random-point pattern of *n* points ($\xi_1 \ldots, \xi_n$) uniformly distributed over space forms a BPP.

For the sake of completeness, the useful summary on the properties of a spatial point process on the Euclidean space $\mathbb{R}^d$ given in [104] allows a few dichotomies:

- A PP is said to be simple if the multiplicity of a point over space is one; otherwise it is not
- A PP is said to be stationary if the resulting spatial process results invariant by translation.
- A PP is said to be isotropic if the resulting spatial process is invariant to rotation.
- A PP is said to be marked if it assigns labels to the points of the process, which are typically independent of the PP.
- A PP can be Poisson or not. If it is Poisson, it can be homogeneous or non-homogeneous, as it was discussed in Section 4.4.

It is important to remark that a homogeneous PPP is both stationary and simple.

9. References

[1] J. Mitola, “Cognitive radio: An Integrated Agent Architecture for Software Defined Radio,” Ph.D. dissertation, KTH Royal Inst. of Technol., Stockholm, Sweden, 2000.

[2] D13.2, “Context and Interference Aware Coding and Decoding”. ACRPOPOLIS deliverable, Nov. 2012.

[3] FCC, “Policy Task Force Report (et docket-135)”, 2002.

[4] M. A. McHenry, “NSF Spectrum Occupancy Measurements Project Summary,” *Shared Spectrum Company*, 2005.

[5] FCC, “Notice of proposed rulemaking, in the matter of facilitating opportunities for flexible, efficient and reliable spectrum use employing cognitive radio technologies (et docket no. 03-108) and authorization and use of software defined radios (et docket no. 00-47), FCC 03-322,” Dec. 2003.

[6] S. Haykin, “Cognitive radio: Brain-empowered wireless communications,” *IEEE J. Sel. Areas Commun.*, vol. 23, no. 2, pp. 201–220, Feb. 2005.

[7] I. F. Akyildiz, W. Lee, M. C. Vuran, and S. Mohanty, “Next Generation/Dynamic Spectrum Access/Cognitive Radio Wireless Networks: A Survey,” *Computer Networks*, vol. 50, no. 13, pp. 2127–2159, Sep. 2006.

[8] Q. Zhao and B. M. Sadler, “A Survey of Dynamic Spectrum Access,” *IEEE Signal Process. Mag.*, vol. 24, no. 3, pp. 79–89, May 2007.

[9] A. Goldsmith, S. A. Jafar, I. Maric, and S. Srinivasa, “Breaking Spectrum Gridlock with Cognitive Radios: An Information Theoretic Perspective,”*Proc. IEEE*, vol. 97, no. 5, pp. 894–914, May 2009.

[10] A. Ghasemi, and E. S. Sousa, “Spectrum Sensing in Cognitive Radio Networks: Requirements, Challenges and Design Trade-Offs,” *IEEE Commun. Mag.*, vol. 46, no. 4, pp. 32–39, Apr. 2008.

[11] Cabric, S. M. Mishra, and R. W. Brodersen, “Implementation Issues in Spectrum Sensing for Cognitive Radios,” in *Proc. Asilomar Conf. on Signals, Systems, and Computers*, Pacific, Grove, Nov. 2004, pp. 772– 776.

[12] A. Sonnenschein and P. M. Fishman, “Radiometric Detection of Spread- Spectrum Signals in Noise,” *IEEE Trans. Aerosp. Electron. Syst.*, vol. 28, no. 3, pp. 654–660, Jul. 1992.

[13] R. Tandra and A. Sahai, “SNR Walls for Signal Detection,” *IEEE J. Sel. Topics Signal Process.*, vol. 2, no. 1, pp. 4–17, Feb. 2008.

[14] R. Tandra, S. M. Mishra, and A. Sahai, “What is a Spectrum Hole and What Does It Take to Recognize One Extended Version,” *Proc. IEEE*, vol. 97, no. 5, pp. 824–848, May 2009.

[15] M. Z. Win, “A Mathematical Model for Network Interference,” IEEE Communication Theory Workshop, Sedona, AZ, May 2007.

[16] M. Z. Win, P. C. Pinto, and L. A. Shepp, “A Mathematical Theory of Network Interference and its Applications,” *Proc. IEEE*, vol. 97, no. 2, pp. 205–230, Feb. 2009, special issue on *Ultra-Wide Bandwidth (UWB) Technology & Emerging Applications*.

[17] M. Z. Win and R. A. Scholtz, “Impulse radio: How it works,” *IEEE Commun. Lett.*, vol. 2, no. 2, pp. 36–38, Feb. 1998.

[18] ——, “Ultra-Wide Bandwidth Time-Hopping Spread-Spectrum Impulse Radio for Wireless Multiple-Access Communications,” *IEEE Trans. Com- mun.*, vol. 48, no. 4, 8p. 679–691, Apr. 2000.

[19] M. Z. Win, “A Unified Spectral Analysis of Generalized Time-Hopping Spread-Spectrum Signals in the Presence of Timing Jitter,” *IEEE J. Sel. Areas Commun.*, vol. 20, no. 9, pp. 1664–1676, Dec. 2002.

[20] R. A. Scholtz, “Private Conversation,” University of Southern California, Sep. 1997, Los Angeles, CA.

[21] J. H. Winters, “Private conversation,” AT&T Labs-Research, Mar. 2001, Middletown, NJ.

[22] L. A. Shepp, “Private conversation,” AT&T Labs-Research, Mar. 2001, Middletown, NJ.

[23] P. C. Pinto and M. Z. Win, “Communication in a Poisson Field of Interferers – Part I: Interference Distribution and Error Probability,” *IEEE Trans. Wireless Commun.*, vol. 9, no. 7, pp. 2176–2186, Jul. 2010.

[24] ——, “Communication in a Poisson Field of Interferers – Part II: Channel Capacity and Interference Spectrum,” *IEEE Trans. Wireless Commun.*, vol. 9, no. 7, pp. 2187–2195, Jul. 2010.

[25] A. Rabbachin, T. Q. Quek, P. C. Pinto, I. Oppermann, and M. Z. Win, “Non-coherent UWB Communication in the Presence of Multiple Narrowband Interferers,” *IEEE Trans. Wireless Commun.*, vol. 9, 2010, to appear.

[26] P. C. Pinto, A. Giorgetti, M. Z. Win, and M. Chiani, “A Stochastic Geometry Approach to Coexistence in Heterogeneous Wireless Networks,” *IEEE J. Sel. Areas Commun.*, vol. 27, no. 7, pp. 1268–1282, Sep. 2009, special issue on *Stochastic Geometry and Random Graphs for Wireless Networks*.

[27] P. C. Pinto and M. Z. Win, “Spectral Characterization of Wireless Networks,” *IEEE Wireless Commun. Mag.*, vol. 14, no. 6, pp. 27–31, Dec. 2007, special Issue on *Wireless Sensor Networking*.

[28] J. F. Kingman, *Poisson Processes*. Oxford University Press, 1993.

[29] S. Chandrasekhar, “Stochastic Problems in Physics and Astronomy,” *Rev. Modern Phys.*, vol. 15, no. 1, pp. 1–89, Jan. 1943.

[30] S. E. Heath, “Applications of the Poisson Model to Wireless Telephony and to Cosmology,” Ph.D. dissertation, Department of Statistics, Rutgers University, Piscataway, NJ, Mar. 2004, thesis advisor: Professor Lawrence A. Shepp.

[31] M. Y. Vardi, L. Shepp, and L. Kaufman, “A statistical Model for Positron Emission Tomography,” *J. of the American Statistical Association*, vol. 80, no. 389, pp. 8–20, Mar. 1985.

[32] M. Beil, F. Fleischer, S. Paschke, and V. Schmidt, “Statistical Analysis of 3D Centromeric Heterochromatin Structure in Interphase Nuclei,” *Journal of Microscopy*, vol. 217, pp. 60–68, 2005.

[33] D. L. Snyder, “Filtering and Detection for Doubly Stochastic Poisson Processes,” *IEEE Trans. Inf. Theory*, vol. 18, no. 1, pp. 91–102, Jan. 1972.

[34] J. R. Pierce, “Optical Channels: Practical Limits with Photon-Counting,” *IEEE Trans. Inf. Theory*, vol. 26, no. 12, pp. 1819–1821, Dec. 1978.

[35] J. R. Pierce, E. C. Posner, and E. R. Rodemich, “The Capacity of the Photon Counting Channel,” *IEEE Trans. Inf. Theory*, vol. 27, no. 1, pp. 61–77, Jan. 1981.

[36] J. L. Massey, “Capacity Cut-off Rate, and Coding for Direct Detection Optical Channel,” *IEEE Trans. Commun.*, vol. 29, no. 11, pp. 1615–1621, Nov. 1981.

[37] E. S. Sousa, “Performance of a Spread Spectrum Packet Radio Network Link in a Poisson Field of Interferers,” *IEEE Trans. Inf. Theory*, vol. 38, no. 6, pp. 1743–1754, Dec. 1992.

[38] J. Ilow, D. Hatzinakos, and A. N. Venetsanopoulos, “Performance of FH SS Radio Networks with Interference Modelled as a Mixture of Gaussian and Alpha-Stable Noise,” *IEEE Trans. Commun.*, vol. 46, no. 4, pp. 509– 520, Apr. 1998.

[39] C. C. Chan and S. V. Hanly, “Calculating the Outage Probability in a CDMA Network with Spatial Poisson Traffic,” *IEEE Trans. Veh. Technol.*, vol. 50, no. 1, pp. 183–204, Jan. 2001.

[40] F. Baccelli, B. Błaszczyszyn, and F. Tournois, “Spatial Averages of Coverage Characteristics in Large CDMA Networks,” *Wireless Networks*, vol. 8, no. 6, pp. 569–586, Nov. 2002.

[41] X. Yang and A. P. Petropulu, “Co-channel Interference Modelling and Analysis in a Poisson Field of Interferers in Wireless Communications,” *IEEE Trans. Signal Process.*, vol. 51, no. 1, pp. 64–76, 2003.

[42] J. Orriss and S. K. Barton, “Probability Distributions for the Number of Radio Transceivers which Can Communicate with One Another,” *IEEE Trans. Commun.*, vol. 51, no. 4, pp. 676–681, Apr. 2003.

[43] S. P. Weber, X. Yang, J. G. Andrews, and G. de Veciana, “Transmission Capacity of Wireless Ad-hoc Networks with Outage Constraints,” *IEEE Trans. Inf. Theory*, vol. 51, no. 12, pp. 4091–4102, Dec. 2005.

[44] O. Dousse, F. Baccelli, and P. Thiran, “Impact of Interferences on Connectivity in Ad-hoc Networks,” *IEEE/ACM Trans. Netw.*, vol. 13, no. 2, pp. 425–436, Apr. 2005.

[45] O. Dousse, M. Franceschetti, and P. Thiran, “On the Throughput Scaling of Wireless Relay Networks,” *IEEE Trans. Inf. Theory*, vol. 52, no. 6, pp. 2756–2761, Jun. 2006.

[46] L. Song and D. Hatzinakos, “Cooperative Transmission in Poisson Distributed Wireless Sensor Networks: Protocol and Outage Probability,” *IEEE Trans. Wireless Commun.*, vol. 5, no. 10, pp. 2834–2843, Oct. 2006.

[47] A. Ghasemi and E. S. Sousa, “Interference Aggregation in Spectrum-Sensing Cognitive Wireless Networks,” *IEEE J. Sel. Topics Signal Process.*, vol. 2, no. 1, pp. 41–56, Feb. 2008.

[48] R. Menon, R. M. Buehrer, and J. H. Reed, “On the Impact of Dynamic Spectrum Sharing Techniques on Legacy Radio Systems,” *IEEE Trans. Wireless Commun.*, vol. 7, no. 11, pp. 4198–4207, Nov. 2008.

[49] W. Ren, Q. Zhao, and A. Swami, “Power Control in Spectrum Overlay Networks: How to Cross a Multi-Lane Highway,” *IEEE J. Sel. Areas Commun.*, vol. 27, no. 7, pp. 1283–1296, Sep. 2009.

[50] E. Salbaroli and A. Zanella, “Interference Analysis in a Poisson Field of Nodes of Finite Area,” *IEEE Trans. Veh. Technol.*, vol. 58, no. 4, pp. 1776–1783, May 2009.

[51] H. Inaltekin, M. Chiang, H. V. Poor, and S. B. Wicker, “The Behaviour of Unbounded Path-Loss Models and the Effect of Singularity on Computed Network Characteristics,” *IEEE J. Sel. Areas Commun.*, vol. 27, no. 7, pp. 1078–1092, Sep. 2009.

[52] F. Baccelli, B. Błaszczyszyn, and P. Mu¨hlethaler, “Stochastic Analysis of Spatial and Opportunistic Aloha,” *IEEE J. Sel. Areas Commun.*, vol. 27, no. 7, pp. 1105–1119, Sep. 2009.

[53] V. Chandrasekhar and J. G. Andrews, “Uplink Capacity and Interference Avoidance for Two-Tier Femtocell Networks,” *IEEE Trans. Wireless Commun.*, vol. 8, no. 7, pp. 3498–3509, Jul. 2009.

[54] A. Rabbachin, T. Q. S. Quek, Shin Hyundong, M. Z. Win, “Cognitive Network Interference”, *IEEE J. Sel. Areas Commun.*, vol. 29, no. 2, pp. 480–493, Feb. 2011.

[55] A. Rabbachin, T. Q. S. Quek, M. Z. Win, “Statistical Modelling of Cognitive Network Interference”, *IEEE GLOBECOM - Wireless Commun. Symp.*, 2010.

[56] A. Rabbachin, G. Baldini, T. Q. S. Quek., “Aggregate Interference in White Spaces”, *Int. Symp. on Wireless Commun*. Systems, 2010.

[57] R. K. Ganti and M. Haenggi, “Interference and Outage in Clustered Wireless Ad-hoc Networks,” *IEEE Trans. Inf. Theory*, vol. 55, no. 9, pp. 4067–4086, Sep. 2009.

[58] K. Gulati, B. L. Evans, J. G. Andrews and K. R. Tinsley, ``Statistics of Co-Channel Interference in a Field of Poisson and Poisson-Poisson Clustered Interferers'', *IEEE Trans. on Signal Proces.*, vol. 58, no. 12, Dec. 2010, pp. 6207-6222.

[59] J. Peha, “Spectrum Sharing Through Spectrum Policy Reform and Cognitive Radio”. *Proc. of the IEEE* , vol. 97, no. 4, April 1997.

[60] M. M. Buddhikot, “Understanding Dynamic Spectrum Access: Models, Taxonomy and Challenges”. *Proc. of IEEE Dyspan* 2007, 17-21 April 2007.

[61] S. Forge, R. Horvitz and C. Blackman, "Perspectives on the Values of Shared Spectrum Access".Final Report for the European Commission, Feb. 2012.

[62] P. Kolodzy, “Spectrum Policy Task Force Report”, ET Docket No. 02-135, Nov. 2002.

[63] ECC Report 159 “Technical and operational requirements for the operation of cognitive radio systems in the ‘white spaces’ of the frequency band 470-790 MHz”.

[64] G. Mansfield, “Femtocells in the US Market-Business Drivers and Consumer Propositions”. Femtocells EUROPE, ATT, London UK, June 2008.

[65] [61] D. L. Perez, A. Valcarce, G. de la Roche and J. Zhang, “OFDMA Femtocells: A Roadmap on Interference Avoidance”. *IEEE Commun. Mag.*, Sept. 2009.

[66] K. Zheng, Y. Wang, W. Wang, M. Dohler and J. Wang, “Energy-Efficient Wireless In-Home: The Need for Interference-Controlled Femtocells”. *IEEE Wireless Commun.*, Dec. 2011.

[67] F. Pantisano, K. Ghaboosi, M. Bennis and R. Verdone, “A self-Organizing Solution for Interference Avoidance in TDD Underlay Femtocells”. *Proc. of the Forty Fourth Asilomar Conference on Sig. Sys. and Commun.*, 2010.

[68] L. yang and G. B. Giannakis, “Ultra-Wideband Communications: an Idea Whose Time Has Come*”. IEEE Signal Proc. Mag*., vol. 21, no. 6, pp. 26-54, Nov. 2004.

[69] “IEEE std 802.15.4 (2011): Wireless Medium Access Control (MAC) and Physical Layer (PHY) Specifications for Low Rate Wireless Personal Area Networks (LR-WPANs),” The Institute of Electrical and Electronics Engineers, Inc., Standard, Roll-up of all IEEE Std 802.15.4 and its amendments before end of 2011, Sept. 2011.

[70] ECMA-368: High Rate Ultra Wideband PHY and MAC Standard, December 2007.

[71] R. Macchi, "Rev. of UWB and FS Coexistence Report (Annex 5-1)", M1720R0 SE24, CEPT SE24 Meeting 17, Mainz (Germany), Sept. 2002.

[72] R. Giuliano and F. Mazzenga, “On the Coexistence of Power-Controlled Ultrawide-Band Systems With UMTS, GPS, DCS1800, and Fixed Wireless Systems”. *IEEE Trans. on Vehicular Technology*, vol. 54, no. 1, Jan. 2005.

[73] A. Durantini, R. Giuliano, F. Mazzenga, J. Hernandez and M. B. Villarroya, “Detect and Avoid Procedure for UWB Interference Mitigation on Narrowband Systems”. *Proc. of 3rd Int. Symp. on Wireless Commun. Sys., (ISWCS’06)*, pp. 428-432, Sept. 2006.

[74] A. Durantini, R. Giuliano, F. Mazzenga and F. Vatalaro, “Performance Evaluation of Detect and Avoid Procedures for Improving UWB Coexistence with UMTS and WiMAX Systems”. *Proc. of IEEE Int. Conf. on Ultra-Wideband*, pp. 501-506, Sept. 2006.

[75] R. Giuliano, F. Mazzenga, J. H. Pablo and I. A. Benedé, “Performance of Cooperative and Non-Cooperative Detect and Avoid Procedures for UWB”. *Proc. of 16th Mobile and Wir. Commun. Sum. (IST)*, July 007.

[76] E. Cano, A. Rabbachin and J. Fortuny, “Performance Analysis of WiMax Systems in the Presence of MB-OFDM UWB Interference”. *Proc. of the 6th Int. Symp. on Wir. Commun. Sys. (ISWCS)*, Sept. 2009.

[77] European Commission Decision 2007/131/EC, “Allowing the Use of the Radio Spectrum for Equipment Using Ultra-Wideband Technology in a Harmonized Manner in the Community”, Feb. 2007.

[78] A. Ghasemi and E. S. Sousa, “Fundamental Limits of Spectrum-Sharing in Fading Environments”. *IEEE Trans. on Wirel. Commun.*, vol. 6, no. 2, pp. 649-658, 2007.

[79] X. Kang, Y.-C.Liang, A. Nallanathan, H. K. Garg and R. Zhang, “Optimal Power Allocation in Cognitive Radio Networks: Ergodic capacity and Outage capacity*”. IEEE Trans. Wirel. Commun.*, vol. 8, no. 2, pp. 940-950, 2009.

[80] H. Y. Kong and Asaduzzaman, “On the Outage of Interference Temperature Limited CR-MISO Channel”. *IEEE Journal of Comm. Net.*, vol. 13, no. 5, pp. 456-462, Oct. 2011.

[81] Asaduzzaman and H. Y. Kong, “Ergodic and Outage Capacity of Interference temperature-Limited Cognitive Radio Multi-Input Multi-Output Channel”. *IET Commun.*, vol. 5, no. 5, pp. 652-659, 2011.

[82] Federal Communications Commission (FCC), “In the Matter of Establishment of an Interference Temperature Metric to Quantify and Manage Interference and to Expand Available Unlicensed Operation in Certain Fixed, Mobile and Satellite Frequency Bands”. ET Docket no. 03-237, FCC 07-78, May 2007.

[83] ECMA-392 Standard “MAC and PHY for Operation in TV White Space,” accessible at http://www.ecma-international.org/publications/files/ECMA-ST/ECMA-392.pdf, accessed March 2012.

[84] IEEE 802.22 Working Group on Wireless Regional Area Networks, http://www.ieee802.org/22, accessed March 2012.

[85] IEEE 802.11 Task Group af (TGaf) “Wireless LAN in the TV White Space”, http://www.ieee802.org/11/Reports/tgaf_update.htm, accessed March 2012.

[86] IEEE 802.15 Task Group 4m (TG4m) “TV White Space Amendment to 802.15.4”, http://www.ieee802.org/15/pub/TG4m.html, accessed March 2012.

[87] IEEE 1900.7 White Space Radio Working Group, http://grouper.ieee.org/groups/dyspan/7/index.htm, accessed March 2012.

[88] Ofcom, “Implementing geolocation,” consultation, November 2010. Available at: http://stakeholders.ofcom.org.uk/binaries/consultations/geolocation/summary/geolocation.pdf, accessed March 2012.

[89] Ofcom, "Implementing geolocation: Summary of consultation responses and next steps," September 2011. Available at: http://stakeholders.ofcom.org.uk/binaries/consultations/geolocation/statement/statement.pdf, accessed March 2012.

[90] Ofcom, "Draft regulatory requirements for white space devices in the UHF TV band," Ofcom discussion document, February 2012. Submitted to CEPT SE43 and elsewhere; accessible at: https://www.google.co.uk/url?sa=t&rct=j&q=&esrc=s&source=web&cd=1&cad=rja&ved=0CDIQFjAA&url=http%3A%2F%2Fwww.cept.org%2FDocuments%2Fse-43%2F6161%2F&ei=6vj1UKj2OI6U0QXz5YHQBQ&usg=AFQjCNGrLUcILAld_zP86sIGbbGKBdorFQ&bvm=bv.41018144,d.d2k.

[91] G. Hardin, "The Tragedy of the Commons," Science, vol. 162, pp. 1243–48, 1968.

[92] N. Abramson, "The Throughput of Packet Broadcasting Channels". *IEEE Trans. on Information Theory*, vol. 25, no.1, pp. 117–128.

[93] L. Kleinrock & F. A. Tobagi, "Packet Switching in Radio Channels: Part I-Carrier Sense Multiple-Access Models and Their Throughput-Delay Characteristics". *IEEE Trans. on Commun.*, vol. 23, no. 12, pp. 1400–1416.

[94] B. Hajek, A. Krishna and R. O. LaMaire, "On the Capture Probability for a Large Number of Stations". *IEEE Trans. on Commun.*, vol. 45, no. 2, Feb. 1997.

[95] R. Nelson and L. Kleinrock, "The Spatial capacity of a Slotted ALOHA Multihop Packet Radio Network with Capture". *IEEE Tran. on Commun.*, vol. COM-32, no. 6, June 1984.

[96] L. Kleinrock and J. Silvester, "Spatial reuse in Multihop packet radio Networks", *Proc. of the IEEE*, vol. 75, no.1, pp. 156-167, Jan. 1987.

[97] M. Zorzi and S. Pupolin, "Optimum Transmission Ranges in Multihop Packet radio Networks in the Presence of Fading". *IEEE Tran. on Commun.*, vol. 43, no.7, July 1995.

[98] [81] E. S. Sousa and J. A. Silvester, "Optimum Transmission Ranges in a Direct-Sequence Spread-Spectrum Multihop Packet Radio Network". *IEEE J. Sel. Areas in Commun.*, vol. SAC-8, pp. 762-771, June 1990.

[99] H. Zhou and R. H. Deng, "Capture Model for Mobile Radio Slotted Aloha Systems". *IEEE Proc. of Commun.*, vol. 145, no. 2, pp. 91-97, Apr. 1998.

[100] K. Zhang and K. Pahlavan, "Relation Between Transmission and Throughput of Slotted ALOHA Local Packet Radio network". *IEEE Trans. on Commun.*, vol. 40. No. 3, pp. 577-583, March 1992.

[101] G. Giancola, M.-G. Di Benedetto, "A Novel Approach for Estimating Multi-User Interference in Impulse Radio UWB Networks: The pulse Collision Model". *ELSEVIER Sig. Proc. Journal*, vol. 86, pp. 2185-2197, 2005.

[102] G. Durisi and G. Romano, "On the validity of Gaussian Approximation to Characterize the Multiuser capacity of UWB TH PPM*". IEEE Conf. on Ultra Wideband Syst. and Tech.*, pp. 157-161, 2002.

[103] B. Hu and N. C. Beaulieu, "Exact Bit Error Rate Analysis of TH-PPM UWB Systems in the Presence of Multiple-Access Interference". *IEEE Commun. Letters*, vol. 7, no. 12, pp. 572-574, Dec. 2003.

[104] M. Haenggi, J. G. Andrews, F. Baccelli, O. Dousse and M. Franceschetti, "Stochastic geometry and random Graphs for the Analysis and Design of Wireless Networks". *IEEE J. on Sel. Areas in Commun.*, vol. 27, no. 7, Sept. 2009.

[105] S. Srinivasa and M. Haenggi, “Modeling Interference in Finite Uniformly Random Networks”. *Proc. International Workshop on Information Theory for Sensor Networks (WITS-07)*, 2007.

[106] J. Riihijarvi and P. Mahonen, “A Model Based Approach for Estimating Aggregate Interference in Wireless Networks”. *Proc. of CrownCom* 2012, June 2012.

[107] J. P. Nolan, “Stable Distributions: Models for Heavy-Tailed Data”. Springer Verlag, 2009.

[108] J. Ilow and D. Hatzinakos, “Analytic Alpha-Stable Noise Modelling in a Poisson Field of Interferers or Scatterers”. *IEEE Trans. Wireless Commun.* Vol. 46, no. 6, pp. 1601-1611,June 1998.

[109] H. R. Thompson, “Distribution of Distance to Nth Neighbour in a Population of Randomly distributed Individuals”. *J. of Ecology*, vol. 37, no. 2, pp. 391-394, April 1956.

[110] M. Haenggi, “On Routing in random Rayleigh Fading Networks”. *IEEE Trans on Wireless Commun.*, col. 4, no. 4, July 2005.

[111] S. Srinivasa and M. Haenggi, “Distance Distributions in Finite Uniformly Random Networks: Theory and Applications”. *IEEE Trans. on Veh. Tech.*, vol. 59, no. 2, Feb. 2010.

[112] D. Stoyan, W. S. Kendall and J. Mecke, “Stochastic Geometry and its Applications”. Second Edition, Wiley, 2008.

[113] STG: SEAMCAT Technical Group. http://www.cept.org/ecc/groups/ecc/wg-se/stg.

[114] J.-P. Kermoal, “Introduction to SEAMCAT”. Available at http://www.cept.org.

[115] I. Sakal and D. Simunic, “Simulation of Interference between Bluetooth and 802.11b Systems”. *Int. Symp. On Elect. Comp.* (EMC’03), 2003.

[116] S. Lyubchenko, J.-P. Kermoal and M. Le Devendec, ”Implementation of Cognitive Radio in SEAMCAT*”, Proc. of 20th Int. Wroclaw symp. on Elect. comp.*, pp. 17 – 21, Sept. 13 – 17, 2010.

[117] S. Lyubchenko, J.-P. Kermoal and M. Le Devendec, “Spectrum Sensing Capabilities in SEAMCAT”. *Proc. of the 10th Int. Symposium on Elect. Comp. (EMC)*, Sept. 26-30, 2011.

[118] C. K. Huynh and W. C. lee, “Researching BEM in Interference Analysis of TV-Band Whitespace”. *Proc. of the Fourth Int. Conf. on Commun. and Elect. (ICCE)*, 2012.

[119] IEEE 802.19 “Wireless Coexistence” Working Group, http://ieee802.org/19/, accessed January 2013.

[120] IEEE 802.19.1 “Wireless Coexistence in the TV White Space” Task Group, http://ieee802.org/19/pub/TG1.html, accessed January 2013.

[121] FCC, “Second Report and Order and Memorandum Opinion and Order”, *FCC 08-260*, Nov. 2008.

[122] Ofcom,“ Implementing Geolocation” http://stakeolders.ofcom.org.uk/consultations/geolocation, 2010

[123] Infocomm Development Authority of Singapore, “Trial of White Space Technology Accessing VHF and UHF Bands in Singapore”, *Tech. Report*, 2010.

[124] M. Mishra and A. Sahai, “How Much White Space Is There?”, Technical Report UCB/EECS-2009-3, Electrical Eng. And Computer Sciences Dept., Univ. of California, Berkeley, http://wwweecs.berkeley.edu/Pubs/TechRpts/2009/EECS-2009-3.html, Jan. 2009.

[125] K. Harrison, S. Mishra and A. Sahai, “How Much White-Space Capacity Is There?”, *Proc. IEEE Symp. New Frontiers in Dynamic Spectrum Access Networks (DySPAN’10), 2010*.

[126] J. v. d. Beek, J. Riihijarvi, A. Achtzehn and P. Mahonen, "TV White Space in Europe", IEEE *Trans. On Mobile Comp., Vol. 11, no. 2*, Feb. 2012.

[127] CEPT-ECC, "Report from CEPT to the European Commission in Response to the Mandate on: Technical Considerations Regarding Harmonization Options for the Digital Dividend", *Tech. Report*, June 2008.

[128] CEPT-ECC, "Technical and Operational Requirements for the Possible Operation of Cognitive Radio Systems in the 'White Spaces' of the Frequency Band 470-790 MHz", ECC Report 159, January 2011.

[129] Cambridge White Spaces Consortium, "Cambridge TV White Spaces Trial: A Summary of the Technical Findings", 2012.

[130] M. Waddell et al, "Initial Considerations for Protection of PMSE", BBC Research and Development White Paper, WHP 224, April 2012.

[131] CSR, "Cambridge TV White Spaces Trial – PMSE Trials Report", Cambridge Silicon Radio Limited, Report CS-223198-RP, 2102.

[132] M. Waddell and T. Harold, "Measured DVB-T Protection Ratios in the presence of Interference from White Space Devices", BBC Research and Development White Paper, WHP 226, April 2012.

[133] A. Palaios, J. Riihijärvi, O. Holland, A. Achtzehn, P. Mähönen, "Measurements of Spectrum Use in London: Exploratory Data Analysis and Study of Temporal, Spatial and Frequency-Domain Dynamics," IEEE DySPAN 2012, Bellevue, WA, USA, October 2012.

[134] A. Palaios, J. Riihijarvi, O. Holland, P. Mahonen, "A week in London: Spectrum usage in metropolitan London," IEEE PIMRC 2013, London, UK, September 2013.

[135] ACROPOLIS Deliverable 9.3, "Report on Interference Awareness in Prospective Spectrum Usages", December 2013.

Glossary and Definitions

Acronym	Meaning
AP	Access Point
ASA	Authorized Shared Access
BPP	Binomial Point Process
BS	Base Station
CCDF	Complementary Cumulative Distribution Function
CDF	Cumulative Distribution Function
CDMA	Code Division Multiple Access
CEPT	European Conference of Postal and Telecommunications Administrators
CF	Characteristic Function
CLT	Central Limit Theorem
CR	Cognitive radio
DAA	Detect and avoid
DTVB	Digital TV broadcast
ECC	European Electronics Committee
ERO	European Radio Office
ERP	Effective Radiated Power
FAP	Femto Access Point
FCC	Federal Communications Commission
GPS	Global Positioning System
ISM	Industrial Scientific and Medical
IT	Interference Temperature
ITU	International Telecommunication Union
LDPC	Low Density Parity Check Codes
LTE	Long Term Evolution
LTE-A	Long Term Evolution - Advanced
MAC	Medium Access Control
MB	Multi-Band
MIMO	Multiple Input Multiple Output
MISO	Multiple Input Single Output
MUI	Multi User Interference
OFDMA	Orthogonal Frequency Division Multiple Access
pdf	Probability Density Function
PHY	Physical Layer

PMSE	Program Making and Special Event
PP	Point Process
PPP	Poisson Point Process
PU	Primary User
QoS	Quality of Service
RAT	Radio Access Technology
RV	Random Variable
SS	Spherically Symmetric
SU	Secondary User
TG	Technical Group
UE	User Equipment
UMTS	Universal Mobile Telecommunications System
UWB	Ultra Wideband
WGSE	Working Group Spectrum Engineering
WSD	White Space Device